THE JOURNAL
OF
CHEMICAL PHYSICS

VOLUME 6 NOVEMBER, 1938 NUMBER 11

The Atomic Distribution in the Allotropic Forms of Phosphorus at Different Temperatures*

C. D. THOMAS† AND NEWELL S. GINGRICH
University of Missouri, Columbia, Missouri

(Received July 25, 1938)

Monochromatic x-ray diffraction patterns of liquid yellow phosphorus, amorphous red phosphorus and amorphous black phosphorus were obtained, using Mo $K\alpha$ radiation. The effect of temperature upon these patterns was investigated for the first two forms. Analysis of these patterns led to the determination of the atomic distribution curves in each case. The number of nearest neighbors is three for all forms. This is taken as direct proof of the existence of P_4 molecules in liquid yellow phosphorus. Comparisons are made of the atomic distribution curves of each form and at the different temperatures for liquid yellow and amorphous red phosphorus.

INTRODUCTION

X-RAY diffraction methods, together with the theories of Zernike and Prins[1] and of Debye and Menke,[2] make possible the most quantitative determination of the so-called "structure" of a liquid. Such determinations have been made for liquid elements in the cases of mercury,[2] gallium,[3] sodium[4] and potassium.[5] Liquid yellow phosphorus is a convenient ele ment to study, and it is of special interest because phosphorus occurs in several allotropic forms. Furthermore, this method has been of use in certain crystal structure determinations,[6] and it is possible that work of this sort on liquid yellow phosphorus will serve to confirm the reported crystal structure[7] of yellow phosphorus, or to assist in arriving at a more complete determination of it.

Phosphorus exists in at least three allotropic forms, yellow (or white), red and black. Yellow phosphorus melts at 44.1°C, is highly inflammable, and has a density of 1.82 g/cc; red phosphorus melts at 593°C, is inflammable, and has a density of 2.20 g/cc; black phosphorus does not burn readily, and has a density of 2.70 g/cc. Red or black phosphorus may be made by subjecting yellow phosphorus to high hydrostatic pressures, and both forms may exist as crystalline or as amorphous material. Red may be formed from yellow through the application of heat alone. The vapor from each form consists of P_4 molecules. In both crystalline and amorphous forms of red and black phosphorus, there are three nearest neighbors about any one atom[6] in accord with the coordination to be expected

* Presented to the American Physical Society at the Washington meeting, April 30, 1938.

† On leave of absence from the School of Mines and Metallurgy, University of Missouri, Rolla, Missouri.

[1] Zernike and Prins, Zeits. f. Physik **41**, 184 (1927).

[2] Debye and Menke, Erg. d. Tech. Röntgenkunde, II (1931).

[3] Menke, Physik. Zeits. **33**, 593 (1932).

[4] Trimble and Gingrich, Phys. Rev. **53**, 278 (1938).

[5] Thomas and Gingrich, J. Chem. Phys. **6**, 411 (1938).

[6] Hultgren, Gingrich and Warren, J. Chem. Phys. **3**, 351 (1935).

[7] Natta and Passerini, Nature **125**, 707 (1930).

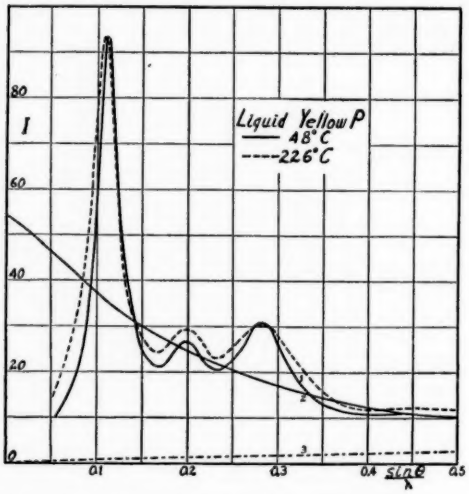

FIG. 1. Curve 1, corrected experimental intensity curve for liquid yellow phosphorus at 48°C; curve 2, independent unmodified scattering; curve 3, incoherent scattering; dashed curve, corrected experimental intensity curve for liquid yellow phosphorus at 226°C.

from covalent bonding of phosphorus. No x-ray diffraction work on liquid yellow phosphorus has been reported, and the reported work on crystalline yellow phosphorus is meager.

In the present work liquid yellow phosphorus was studied at several temperatures. One diffraction pattern was obtained at a temperature considerably above the temperature at which transition to red phosphorus takes place. This pattern showed it was practically identical to that previously obtained except that there was a peak more intense than all the others, at an angle so small as to be completely missed in the previous work.[6] Investigation showed that the most intense peak in the black pattern had also been missed. Complete determinations of the atomic distribution curves were made in these two cases, on the basis of the new patterns.

EXPERIMENTAL

Mo $K\alpha$ x-rays monochromated by reflection from a rocksalt crystal were diffracted by a cylindrical sample, centrallized in a cylindrical camera of 8.85 cm radius. Features of the camera included provision for heating the sample, cooling the film, measuring the temperature next to the sample, and adequate protection of the film against stray radiation. In all cases but one, the sample was contained in a thin-walled Pyrex glass capillary. In the one case (black phosphorus)[8] the sample was extruded from a capillary so that no container material was in the x-ray beam. Liquid yellow phosphorus was distilled over into the capillary, and it appeared perfectly clear and colorless. In one case, the sample remained liquid at a temperature of more than 50°C below the melting point. An exposure was made using this sample, but sometime during the exposure, it solidified, and a conglomerate picture was obtained. Normally, the sample was heated to the desired temperature, and an exposure of 40 hours was made. At 48°C, the phosphorus remained clear except for a very slight tinge of orange at the point where x-rays passed through the sample. At 226°C, the sample emerged from the exposure with a brilliant red color, with a slightly deeper red at the point where the x-rays penetrated. However, the pattern was wholly characteristic of yellow phosphorus, with no indication whatsoever of the red pattern. Temperatures intermediate between 48°C and 226°C produced intermediate effects. At a temperature of 271°C, the patterns of red and of yellow phosphorus were superimposed in roughly equal intensities. The sample was then heated to 350°C for seven hours and cooled to 50°C for an exposure. This produced the characteristic red amorphous pattern. Another exposure, with red phosphorus at

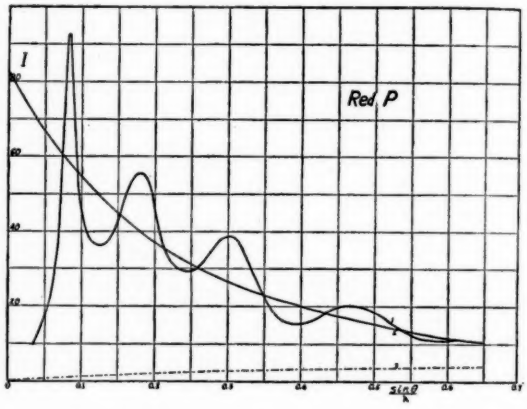

FIG. 2. Curve 1, corrected experimental intensity curve for amorphous red phosphorus at 50°C; curve 2, independent unmodified scattering; curve 3, incoherent scattering.

[8] We are indebted to Professor P. W. Bridgman of Harvard University for supplying us with a sample of amorphous black phosphorus.

325°C, showed so little difference in the diffraction pattern, from that taken at 50°C, that no further analysis was made. The slight difference that did occur was much less than that in the case of liquid yellow phosphorus taken over a smaller temperature range. Powdered black phosphorus was extruded from a capillary, and no effect of temperature was investigated.

Photographic densities in the various films were obtained by means of a microphotometer. The intensity of x-rays (proportional to the photographic densities here used) is shown in Figs. 1–3 as a function of $\sin\theta/\lambda$, where θ is half the total angle of scattering and $\lambda = 0.710$A. Fig. 1 shows the intensity curve for liquid yellow phosphorus at 48°C and at 226°C; Fig. 2 shows the intensity curve for amorphous red phosphorus; Fig. 3 shows the intensity curve for amorphous black phosphorus. Certain corrections have been made in these curves. The nature of the corrections will be given in the next section. Table I lists the values of $\sin\theta/\lambda$ for the intensity maxima in the various patterns.

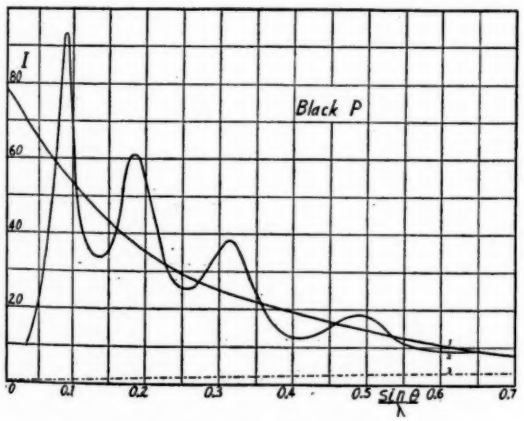

FIG. 3. Curve 1, corrected experimental intensity curve for amorphous black phosphorus at 20°C; curve 2, independent unmodified scattering; curve 3, incoherent scattering.

APPLICATION OF THE FOURIER METHOD

The theory behind this method is outlined elsewhere,[9] and it leads to the equation

$$4\pi r^2\rho(r) = 4\pi r^2\rho_0 + \frac{2r}{\pi}\int_0^\infty si(s)\sin rs\,ds. \quad (1)$$

In this equation, r is the distance in angstroms from any arbitrary atom, $\rho(r)$ is the actual density of atoms in atoms per cubic angstrom, ρ_0 is the average density of the material in atoms per cubic angstrom, and $s = (4\pi\sin\theta)/\lambda$. The function $i(s)$ contains the experimentally determined intensity (with corrections). It is defined as $i(s) = ((I/N) - f^2)/f^2$ where I/N is the intensity of coherent scattered radiation per atom from a sample having no absorption, and with corrections for the polarization of the x-ray beam; f is the structure factor of the atom.

The experimentally determined intensity is corrected for absorption in the sample, reducing the intensity curve to what it would be if there were no absorption. This is facilitated through the use of a graph[10] for this purpose. Correction for polarization due both to reflection from the crystal and from the sample reduces the intensity curve to the values it would have if there were no polarization of the x-rays at reflection. This correction is described elsewhere.[11] Correction is also made for the incoherent radiation. The ratio of coherent to incoherent radiation may be calculated[12] at any scattering angle. By assuming that at large angles, where no further interferences appear, the total radiation is the sum of the independent coherent and the incoherent radiation, the intensity curves may be placed on an absolute basis. The incoherent radiation at any angle may then be drawn in, and subtracted from the intensity curve. In addition to these corrections, it is sometimes necessary to correct for the x-rays scattered by the glass capillary. Capillaries for phosphorus could be made large enough in diameter and thin enough so that this correction was wholly negligible.

From the fully corrected intensity curve, the function $i(s)$ was determined. The values of the

TABLE I. *Peak positions in terms of* $\sin\theta/\lambda$.

	First Peak	Second Peak	Third Peak	Fourth Peak
Liquid yellow 48°C	0.111	0.198	~0.28	none
Liquid yellow 226°C	0.108	0.194	~0.28	none
Amorphous red 50°C	0.083	0.180	0.302	~0.47
Amorphous black 20°C	0.090	0.185	0.314	~0.49

[9] Warren, J. App. Phys. **8**, 645 (1937).

[10] Blake, Rev. Mod. Phys. **5**, 169 (1933).
[11] Katzoff, J. Chem. Phys. **2**, 841 (1934).
[12] Compton and Allison, *X-Rays in Theory and Experiment* (D. Van Nostrand, 1935), p. 781.

integral of Eq. (1) for various values of r were obtained graphically. The quantity $4\pi r^2 \rho(r)$ was then obtained, and it was plotted as a function of r. These atomic distribution curves are shown in Figs. 4–7. Fig. 4 shows this curve for liquid yellow phosphorus at 48°C; Fig. 5 shows this curve for liquid yellow phosphorus at 226°C; Fig. 6 shows this curve for amorphous red phosphorus at 50°C; Fig. 7 shows this curve for amorphous black phosphorus at 20°C. Table II lists the positions of the peaks in the atomic distribution curves for the various cases.

Discussion of Results

The diffraction pattern of yellow phosphorus (Fig. 1) shows a strong first peak, a weak second peak and a fairly strong third peak. In all other liquid elements so far studied, the intensity of the peaks decreases progressively. Several exposures were taken at each temperature, and the relative intensities of the peaks remained the same in the duplicate pictures taken at a given temperature. Thus, the experimental reality of this anomalous progression of intensities seems to be well established.

The effect of x-rays upon yellow phosphorus was noted qualitatively. At 48°C, several 40-hour exposures using Mo $K\alpha$ radiation produced faint orange coloring in the part of the sample which was irradiated. Exposure to Cu $K\alpha$ radiation for 40 hours produced considerably more coloring of the sample. Whether exposed to x-rays or not, and otherwise exposed only to relatively weak artificial illumination, the perfectly clear liquid samples very slowly acquired a turbid appearance. Successive melting and freezing hastened the appearance of this slightly yellow turbid condition.

A few attempts were made to obtain a diffraction pattern of crystalline yellow phosphorus. The material was melted, and suddenly cooled in some cases, and in other cases, it was cooled slowly. When solidified by cooling slowly, the yellow phosphorus solidified suddenly, producing an audible click. In none of the cases was a satisfactory pattern obtained. One of the patterns showed three distinct lines grouped in the region where the main liquid peak appeared, but generally, only radial asterism lines appeared.

The effect of temperature upon the yellow phosphorus samples was quite marked. A clear

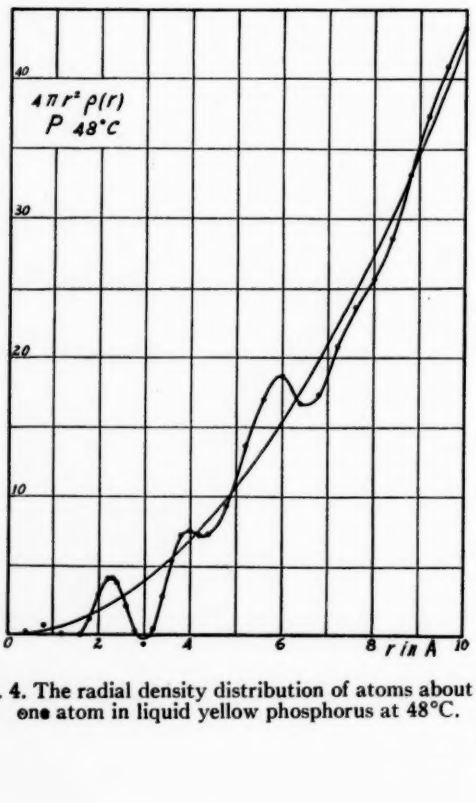

Fig. 4. The radial density distribution of atoms about any one atom in liquid yellow phosphorus at 48°C.

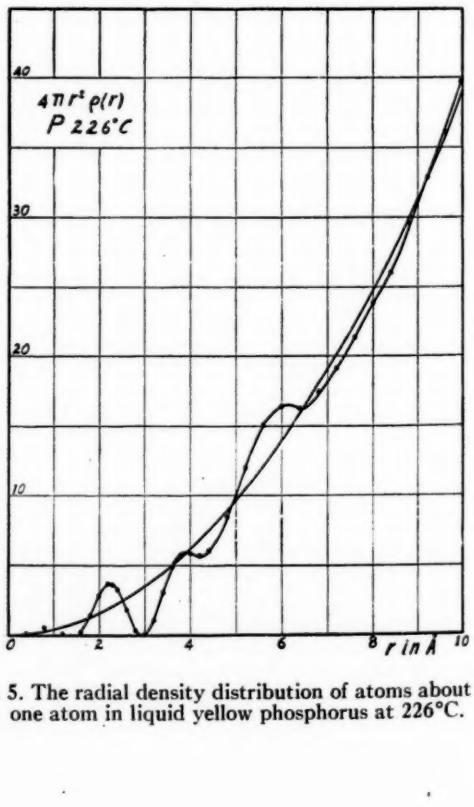

Fig. 5. The radial density distribution of atoms about any one atom in liquid yellow phosphorus at 226°C.

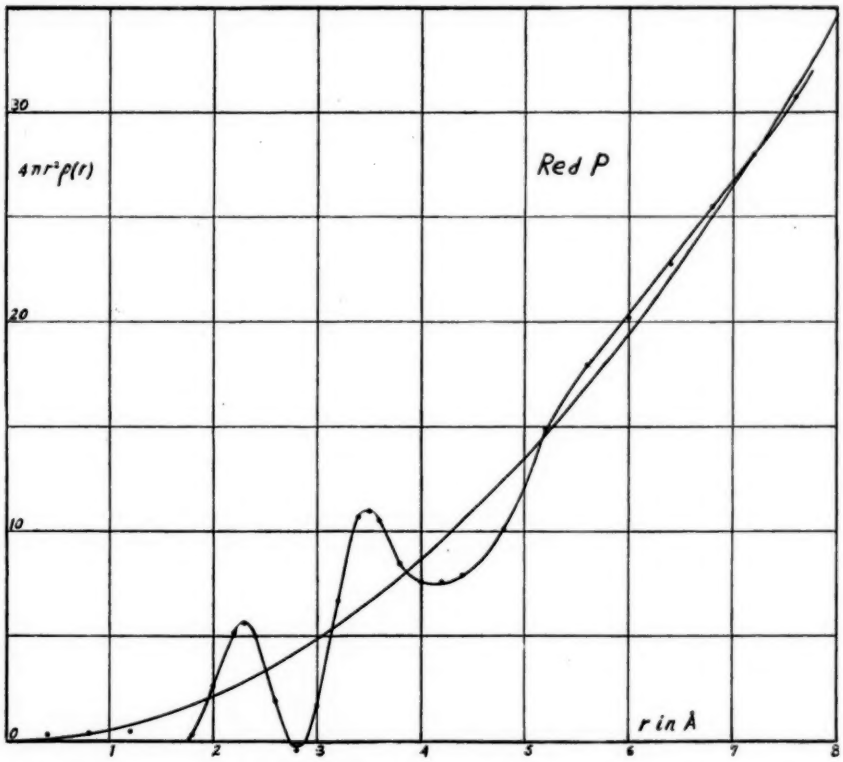

FIG. 6. The radial density distribution of atoms about any one atom in amorphous red phosphorus at 50°C.

sample exposed for 40 hours to a temperature of 226°C was changed to an opaque, deep red liquid. The region where x-rays penetrated was slightly deeper red in color. When these capillaries were broken open at room temperature, the red colored phosphorus burned much the same as yellow phosphorus.

The diffraction pattern of yellow phosphorus at 226°C (Fig. 1) shows typical temperature modification, but no great change over that at 48°C in spite of the fact that the liquid was deep red. The relative intensity of the background radiation was increased, i.e., for given main peak intensities at 48°C and 226°C, the background in the 226°C case was higher.

The pattern obtained at 271°C showed two distinct patterns superimposed in roughly equal intensities. This may mean that the transition from yellow to red phosphorus took place slowly during the exposure, or that it took place suddenly, half-way through the exposure. The former interpretation is in better accord with other observations[13] on the transition of phosphorus from yellow to red.

Yellow phosphorus heated at 350°C for seven hours, and cooled to 50°C for an exposure gave a diffraction pattern identical to that previously observed [6] except that a peak stronger than all others was found at a smaller angle than was included in the previous work. Because of this, a complete redetermination of the atomic distribution was made. In addition, a pattern was obtained for red amorphous phosphorus at 325°C. Although there was a definite and typical difference, the difference was considered too small to make an analysis of this worth while.

The atomic distribution curve for yellow phosphorus at 48°C is shown in Fig. 4. The first peak is discrete, it has its maximum at 2.25Å, and it covers an area of slightly over 2.9 units. This indicates that there are three permanent nearest

[13] Mellor, *A Comprehensive Treatise on Inorganic and Theoretical Chemistry*, Vol. VIII (Longmans, Green and Co., 1928), p. 745.

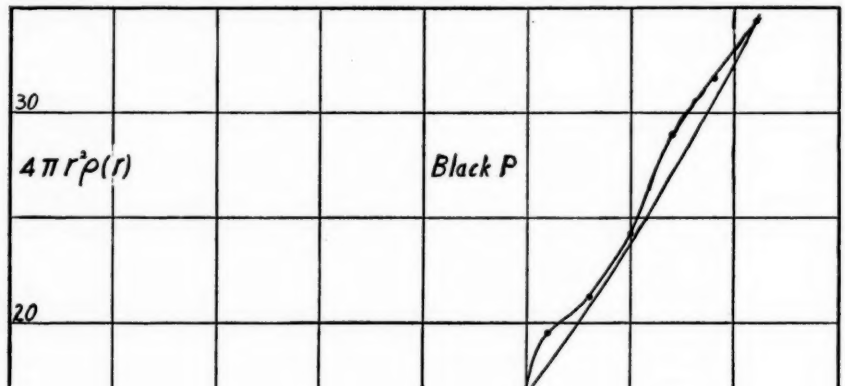

FIG. 7. The radial density distribution of atoms about any one atom in amorphous black phosphorus at 20°C.

neighbors at a distance of 2.25A from a given atom. The first peak for other liquid elements does not extend to the axis on the large "r" side of the maximum, and this is interpreted as being due to a constant interchange of nearest neighbors. Discrete neighbors have heretofore been characteristic of solids. This arrangement of three permanent nearest neighbors is in accord with the assignment of P_4 molecules in the yellow phosphorus liquid. From the symmetrical shape of the first peak, it may be inferred that all P atoms are equivalent, or very nearly so. This equivalence gives the P_4 molecule in liquid yellow phosphorus the same or very nearly the same tetrahedral symmetry that was found for P_4 vapor by electron diffraction.[14] The interatomic distance 2.25A in the present work compares favorably with that of 2.21A for P_4 vapor. The small peak at 3.9A is interpreted as being due to the closest distance of approach of P atoms not in the same P_4 molecule. This interpretation appears reasonable in the light of what is known concerning crystalline orthorhombic sulphur.[15] For this, the ratio of the distance between nearest neighbors within a molecule to that between sulphur atoms not in the same molecule is 2.12/3.3. In the present case, this ratio is 2.25/3.9. The area under the peak at 3.9A cannot be determined with much certainty, but it represents roughly 6 or 8 atoms. The large peak at 5.9A is interpreted as representing the average number of next nearest neighbors of P atoms not in the same P_4 molecule. The area under a reconstructed, isolated, symmetrical peak with its maximum at 5.9A is roughly 32, indicating that on the average, there are about 32 atoms at this distance.

The atomic distribution curve for yellow phosphorus at 226°C is shown in Fig. 5. The first peak is again discrete, it has its maximum at

[14] Maxwell, Hendricks and Mosley, J. Chem. Phys. **3**, 699 (1935).

[15] Warren and Burwell, J. Chem. Phys. **3**, 6 (1935).

2.25A, and it covers an area of slightly over 2.7. This indicates that an atom has three permanent nearest neighbors at a distance of 2.25A. Whereas in the case of other liquid elements, the position of this first peak changed with temperature, in this case no change can be detected. Thus, the molecule appears to remain as a rigid unit under these conditions. The weak second peak has about the same position as before, but in this case, measurement of its position is made difficult by its diffuse character. The third peak, however, shows a slight shift from 5.9A at 48°C to 6.1A at 226°C. This is taken as supporting evidence for the interpretation that the third peak represents in part the average and temporary grouping of molecules about the one in question. If one takes one-third the volume coefficient of expansion[16] for liquid yellow phosphorus and calculates the linear expansion for the experimental temperature change, the 5.9A peak at 48°C would be expected at 6.08A at 226°C. This is to be compared with the observed position of about 6.1A. The area under a reconstructed, isolated, symmetrical peak at 6.1A is roughly 33.

The atomic distribution curve for red amorphous phosphorus is shown in Fig. 6. The first peak is discrete, it occurs at a distance of 2.29A and it covers an area of 3 units. The second peak is sharp, but not isolated, and it occurs at 3.48A. The area to be associated with this peak is roughly 6.7 units. Beyond this distance, the distribution becomes random almost immediately. The number of nearest neighbors is again 3, due to the covalent bonding of P atoms. In the case of liquid yellow phosphorus, the assignment of P_4 molecules is reasonable because of its low melting point as well as other properties.[13] However, in amorphous red and amorphous black phosphorus their high melting points indicate that in these cases there are no simple P_4 molecules. It is possible that in the case of red amorphous phosphorus there is a puckered network somewhat similar to that found in crystalline black phosphorus.[6] If this is true, the number of next nearest neighbors should be 6, and the peak at 3.48A covers an area of slightly over 6. The bond angle is 99° as compared to 102° in crystalline black P.

TABLE II. *Interatomic distances in angstroms.*

		First Peak	Second Peak	Third Peak
Liquid yellow	48°C	2.25	~3.9	~5.9
Liquid yellow	226°C	2.25	~3.9	~6.1
Amorphous red	50°C	2.29	3.48	—
Amorphous black	20°C	2.27	3.34	—

[16] *International Critical Tables*, Vol. I (McGraw-Hill Book Co., 1926), p. 102.

The atomic distribution curve for black amorphous phosphorus is shown in Fig. 7. This is very similar to that for red phosphorus, except that the distances to the nearest and to the next nearest neighbors are 2.27A and 3.34A, respectively. If one assumes the atoms to be arranged in a puckered network as in crystalline black P, the bond angle is found to be 95.6°.

In the cases of red and black amorphous samples, the introduction of the first and strongest peaks in the intensity curves made relatively minor alterations in the distribution curves. This is an excellent illustration of the fact that the diffraction pattern at large angles is relatively of much greater importance than that at small angles.

It is a pleasure to acknowledge grants in aid of this research made to one of us (N. S. G.) by the Rumford Fund Committee of the American Academy of Sciences, and by the American Association for the Advancement of Science. We are indebted to Professor B. E. Warren and Dr. L. K. Frevel for suggestions regarding the interpretation of the distribution curves.

X-Ray Analysis of the Structure of Water

J. MORGAN AND B. E. WARREN
Eastman Laboratory of Physics, Massachusetts Institute of Technology, Cambridge, Massachusetts

(Received July 27, 1938)

X-ray diffraction patterns of water were obtained at five temperatures: 1.5°, 13°, 30°, 62°, and 83°C. The radiation was Cu $K\alpha$ and Mo $K\alpha$, monochromated by reflection from a rocksalt crystal. Radial distribution curves for water at the five temperatures were obtained by a Fourier analysis of the x-ray intensity curves. The first peak is only partially resolved, and it is not possible to interpret the distribution curves uniquely in terms of a definite number of neighbors at definite distances. The results can be interpreted in terms of a structure in which the tendency of a water molecule to bond itself tetrahedrally to 4 neighboring molecules is only partially satisfied.

INTRODUCTION

X-RAY diffraction studies of water have been carried out by Stewart,[1] Amaldi,[2] Meyer,[3] and Katzoff.[4] A quantitative interpretation of the experimental data has been given by Bernal and Fowler[5] and Katzoff.[4] Most of the subsequent work on the structure of water has been inspired and influenced by the pioneer work of Bernal and Fowler. Their method consisted of building up various molecular structures for water and finding the structure which gave the best agreement between the calculated and observed x-ray diffraction patterns. In this way they were able to verify the essentially tetrahedral structure of water, in which each water molecule has approximately four nearest neighboring molecules.

Katzoff was the first to apply to water the more straightforward method of Fourier analysis. With this method, one starts with the experimental intensity curve, and by a direct calculation obtains a radial distribution curve giving the number of water molecules to be found at any distance from a given molecule. Katzoff has given the distribution curves for two temperatures: 3° and 90°C. At both temperatures the area of the first peak indicated that each water molecule had roughly four nearest neighboring molecules.

The interest in the structure of water is so great, that it has seemed worth while to carry through the x-ray analysis for five different temperatures. In this way one can hope to follow any significant temperature changes in the structure. Although our results are in essential agreement with those of Bernal and Fowler, and Katzoff, the more extensive data have allowed more precise conclusions to be drawn.

EXPERIMENTAL

X-ray diffraction patterns of water were obtained for five temperatures: 1.5°, 13°, 30°, 62°, and 83°C. The usual sources of inaccuracy were eliminated in the following ways: (*a*) The patterns were obtained in a large-sized brass camera of 5.57 cm radius, and in an atmosphere of hydrogen to minimize gas scattering. (*b*) The sample was in the form of a free stream of liquid of diameter 1.7 mm. (*c*) The radiation employed was Cu $K\alpha$ and Mo $K\alpha$ monochromated by reflection from a rocksalt crystal. (*d*) The apparatus was constructed so as to eliminate the vapor scattering at the higher temperatures.

The essential features of the camera are shown in Fig. 1. The stream of liquid emerging from the nozzle N is supplied from the reservoir R, where it is held at a constant height, and either warmed or cooled to the desired temperature. The reservoir is thermally insulated from the camera, so that the film is kept at room temperature. The monochromating rocksalt crystal is mounted on the table T and adjusted so that the reflected $K\alpha$ line passes through the collimator C. The transmitted main beam passes into the exit tube B. At the higher temperatures, the exit tube was extended nearly to the water stream to

[1] G. W. Stewart, Phys. Rev. **37**, 9 (1931).
[2] E. Amaldi, Physik. Zeits. **32**, 914 (1931).
[3] H. H. Meyer, Ann. d. Physik **5**, 701 (1930).
[4] S. Katzoff, J. Chem. Phys. **2**, 841 (1934).
[5] J. D. Bernal and R. H. Fowler, J. Chem. Phys. **1**, 515 (1933).

minimize the scattering of the main beam by water vapor. The liquid stream falls into the receiving cup D, and is then pumped back to the reservoir. Hydrogen is circulated through the camera to eliminate air scattering.

The film was placed on the outside of the brass cylinder, and received the diffracted x-rays through a horizontal slot cut around the midsection of the camera. To prevent wet hydrogen from reaching the film, this slot was covered with aluminum foil. A lead jacket which surrounded the camera, protected the film from stray radiation from outside.

For each temperature three patterns were made: a normal exposure with Cu radiation, a normal exposure with Mo radiation, and a very long exposure with Mo radiation. The latter was used to bring out the weak part of the pattern at large values of $\sin\theta/\lambda$. The Cu patterns gave better detail at small values of $\sin\theta/\lambda$, and the Mo patterns gave the best results at the high values. The final intensity curve was obtained by combining the results from the three films. Exposures were of the order of 50 hours.

Results

A set of diffraction patterns taken with Mo radiation is shown in Fig. 2. All patterns were microphotometered along the equator, and the microphotometer record changed to an intensity curve in the usual way. Each intensity curve was then corrected for polarization[6] and absorption.[7] For each temperature, the three corrected intensity curves were combined to give the final curve. Fig. 3 shows the x-ray intensity curves for the five temperatures, the intensity being in arbitrary units.

A Fourier analysis of each of the intensity curves was made in the usual way. For a material containing only one kind of atom, the radial distribution function is given by the equation[8]

$$4\pi r^2\rho(r)=4\pi r^2\rho_0+\frac{2r}{\pi}\int_0^\infty si(s)\sin rs\,ds. \quad (1)$$

Since the scattering by hydrogen is almost completely Compton modified radiation, it is justifiable to treat water as a one atom substance. In Eq. (1) as applied to water:

r = distance from the center of any oxygen.

$4\pi r^2\rho(r)dr$ = number of oxygens (or H_2O molecules) between distances r and $r+dr$ from the center of any given oxygen atom.

ρ_0 = density of water expressed in molecules per cubic angstrom.

$s=(4\pi\sin\theta)/\lambda$.

$i(s)=(I/Nf^2-1)$.

f = atomic scattering factor.

I/N = experimental intensity of unmodified scattering in electron units per molecule.

The intensity scale of the experimental curves in Fig. 3 is put upon an absolute basis (electron units per molecule) by adjusting the scale of

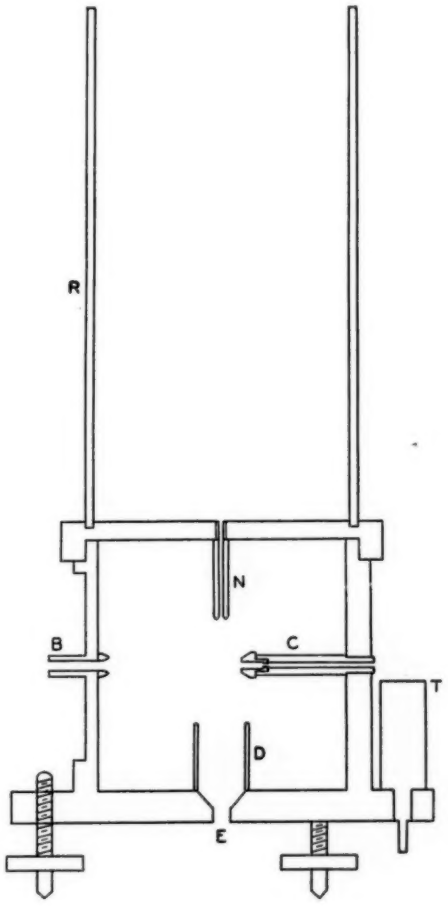

FIG. 1. Camera for x-ray diffraction study of water.

[6] Using a rocksalt crystal as monochromator, the polarization factor is:
$\frac{1}{2}(1+0.937\cos^2 2\theta)$ for Mo $K\alpha$,
$\frac{1}{2}(1+0.723\cos^2 2\theta)$ for Cu $K\alpha$.

[7] *International Tables for the Determination of Crystal Structures*, Vol. II (Gebrüder Borntraeger, Berlin 1935), p. 584.

[8] For a derivation of this equation see B. E. Warren, J. App. Phys. **8**, 645 (1937).

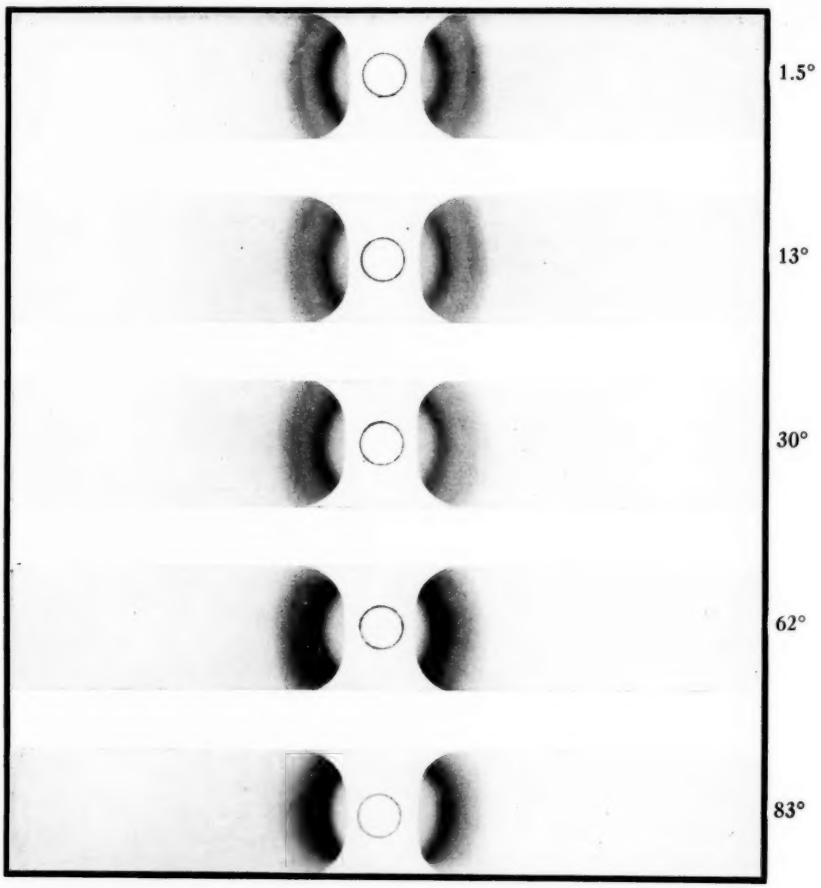

FIG. 2. X-ray diffraction patterns of water at temperatures 1.5°, 13°, 30°, 62°, and 83°C.

ordinates so that at large values of sin θ/λ the experimental curve approaches the sum of the modified and independent unmodified scattering per molecule. The independent unmodified scattering was taken as that of oxygen alone (f_0^2). The modified scattering was taken as the sum of the modified scattering of one oxygen and two hydrogens. These quantities are available in tabulated form.[9]

Having put the experimental intensity curves upon an absolute basis, the curve $si(s)$ is plotted for each temperature, and the integration in Eq. (1) carried out with a harmonic analyzer. For each $si(s)$ curve the integral is evaluated for about thirty values of r. The resulting values of $4\pi r^2\rho(r)$ plotted against r give the radial distribution curves shown in Fig. 4.

[9] Compton and Allison, *X-Rays in Theory and Experiment* (D. Van Nostrand Co., Inc., New York 1935), pp. 781–782.

DISCUSSION OF RESULTS

The change in the diffraction pattern of water with rise in temperature is clearly shown in Fig. 3. At 1.5°C the first peak is at sin $\theta/\lambda = 0.155\text{A}^{-1}$, and the second peak at 0.23A^{-1}. With rising temperature the second peak becomes less sharply resolved from the first peak. At 83°C the two peaks have practically merged into a single peak. About the only conclusion that can be drawn from the intensity curves of Fig. 3 is that there is a change in the structure of water with rise in temperature.

The radial distribution curves of Fig. 4 give directly as much information about the structure of water as can be obtained by x-ray diffraction study. It should be emphasized that these curves are obtained directly from the experimental intensity curves, and are therefore completely independent of any *a priori* assumptions as to

structure. The curves give the average distribution of neighboring molecules as a function of the distance from the center of any water molecule. The area under the curve between any two distances gives the number of neighboring water molecules in that range of distance.

The first peak in the distribution curves represents the nearest neighboring molecules, and the position of the peak gives the average distance of separation of closest neighbors. In ice the distance between neighboring water molecules is 2.76A. From the distribution curves it is seen that in water the distance between closest neighbors is 2.90A at 1.5°C increasing to about 3.05A at 83°C. The intermolecular distance is therefore slightly greater in water and increases with temperature. The area under the first peak is rather indefinite since the peak is not well resolved on the right-hand side. However, by taking the maximum of the peak as the mid-position, and

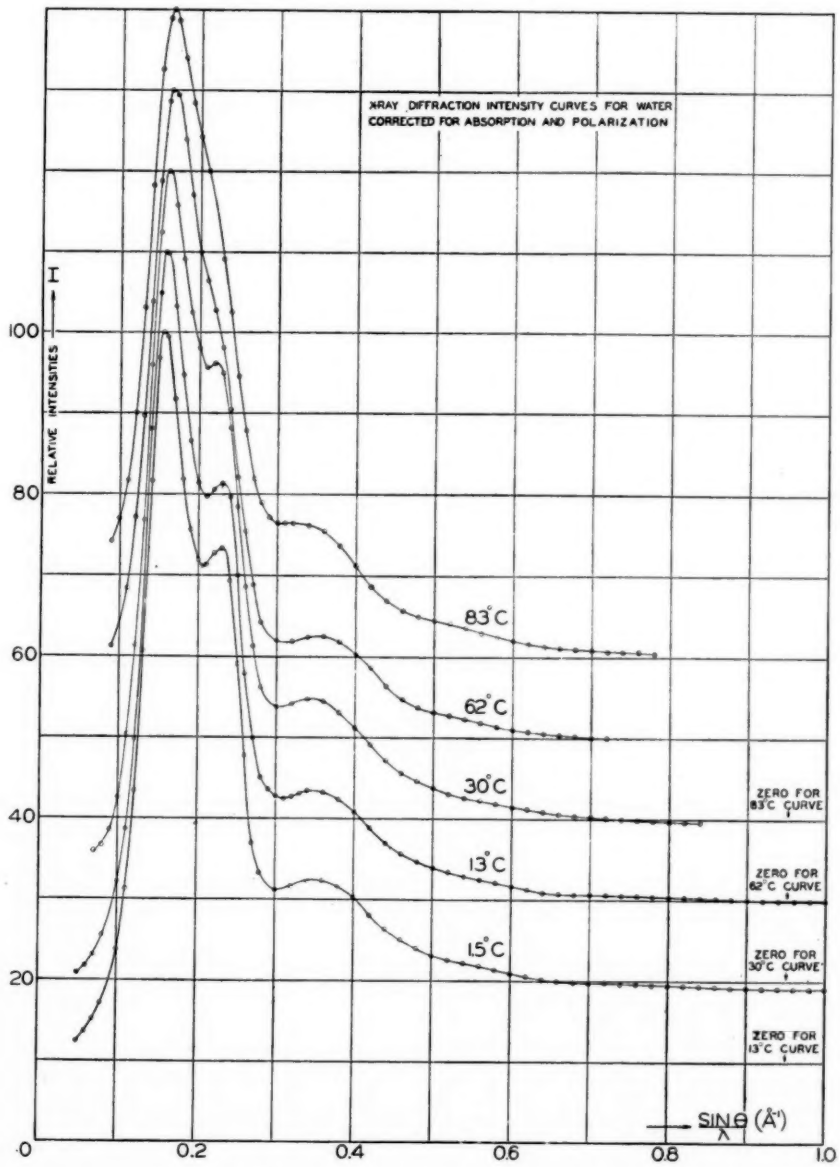

FIG. 3. X-ray intensity curves for water, corrected for absorption and polarization. The intensity is in arbitrary units.

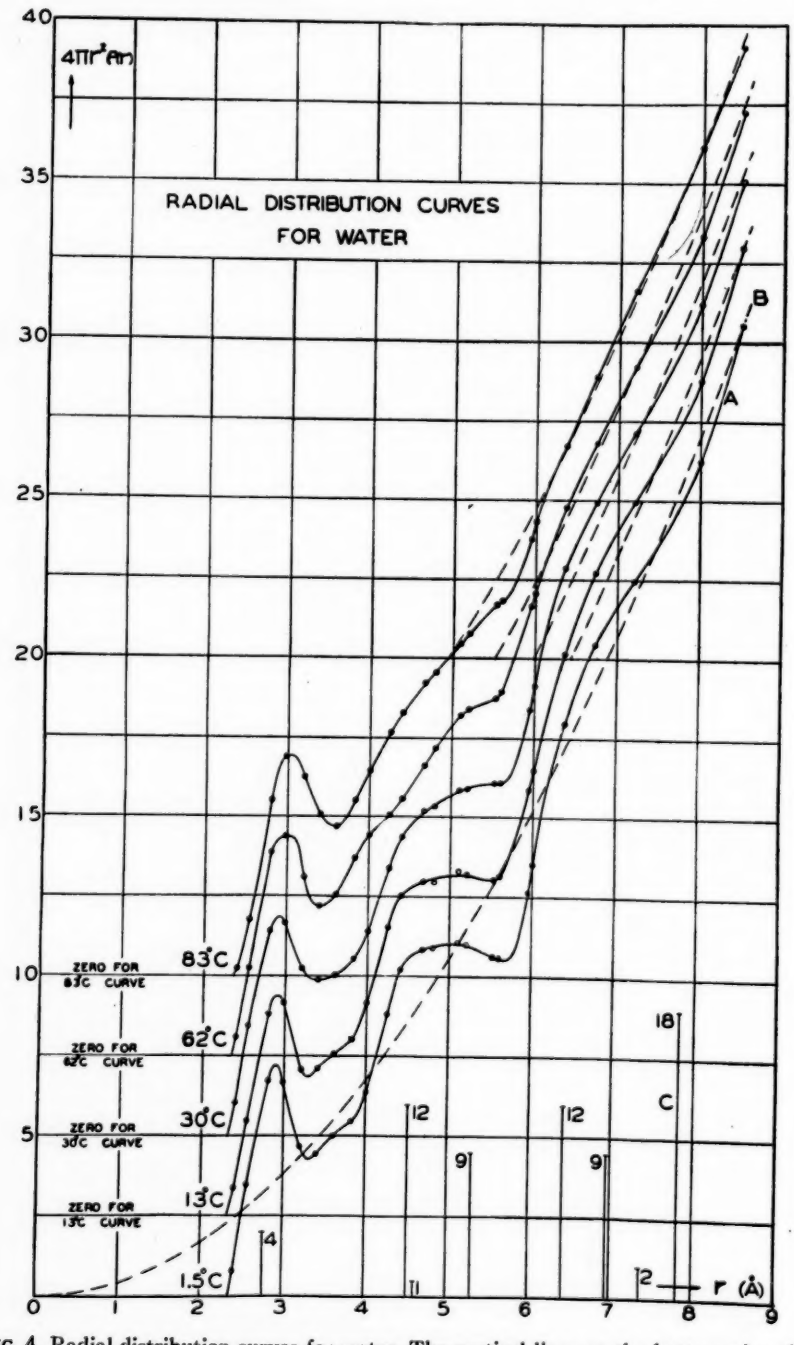

FIG. 4. Radial distribution curves for water. The vertical lines at the bottom give the number and position of the neighbors in ice.

drawing in the right-hand side symmetrical with the left-hand side, one gets what seems to be a fair assignment of peak area. The numbers of nearest neighbors as calculated from the peak areas are given in Table I.

In a close packing of spheres each sphere is in contact with 12 neighboring spheres. In an approximately close packed liquid, made up of essentially spherical molecules, we would expect to find a number of nearest neighbors slightly less

than 12. For example, in liquid sodium[10] the number of neighboring sodium atoms is roughly 10. The conclusion is therefore definite that water is not even approximately a close-packed liquid. In the crystalline structure of ice, each water molecule is tetrahedrally surrounded by 4 neighboring molecules. From the values in Table I it is evident that the water structure approximates more closely to the open tetrahedral type of structure in ice, than to a close-packed structure. Once we have determined that the intermolecular distances are roughly the same in ice and water, it follows immediately that the number of neighboring molecules must be roughly the same since the densities are not very different in ice and water.

If each water molecule were tetrahedrally surrounded by 4 water molecules, and each of these by 4, and so on, as in the crystalline structure of ice, each molecule would have a set of second nearest neighbors at a distance

$$r=2.76(8/3)^{\frac{1}{2}}=4.51\text{A}.$$

A marked concentration of neighbors at a distance of about 4.5A is clearly seen on the distribution curves for 1.5°, 13°, and 30°C. At the higher temperatures this concentration is much less marked. The concentration at 4.5A in the experimental curves is in good agreement with the existence of tetrahedral bonding in water. The disappearance of this concentration in the distribution curves indicates that the tetrahedral bonding becomes less sharply defined or less prevalent with rise in temperature. It should also be noted that the first peak becomes broader and more poorly defined with rise in temperature. This indicates that the nearest neighbors become less definitely defined as to number and distance of separation.

It is of interest to see how far we can go in giving a specific interpretation to the distribution curves of Fig. 4, and to see to what extent we can describe the structure of water in terms of a definite number of neighbors at definite distances. It is evident at the start that this will not be very successful, since the first peak is not well resolved on the right-hand side. In a glass such as vitreous silica, each silicon is tetrahedrally surrounded by four oxygens. The silicon has a definite number of permanent neighbors at a definite distance, and the first peak of the distribution curve is completely resolved.[8] All glasses so far studied show a first peak completely resolved, whereas for all liquids the first peak to represent an intermolecular distance is never more than partially resolved. This important difference has considerable bearing on the structure of liquids. It indicates that in a liquid we do not have a definite number of neighbors existing only at certain definite distances.

To illustrate the point that there is no simple unique interpretation of the distribution curves, we will consider a number of different ways of interpreting the 1.5°C curve. In Fig. 5 the distribution curve has been arbitrarily split up to indicate each molecule surrounded by 3 definite neighbors at a distance 2.8A and an indefinite number of neighbors at a continuous variety of larger distances. This could be interpreted in terms of a structure in which each water molecule is bonded on the average to 3 other molecules rather than to 4 as in ice. In addition to the bonded neighbors, there are an indefinite number of neighbors at a variety of distances.

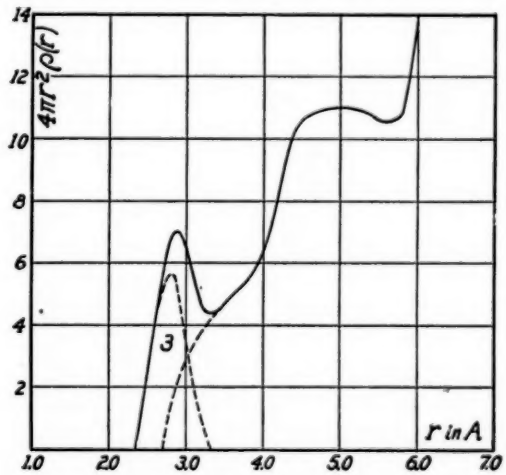

FIG. 5. Interpretation of 1.5°C distribution curve in terms of 3 nearest neighbors and others at a continuous variety of distances.

TABLE I. *Number of nearest neighbors.*

Temp. °C	1.5	13	30	62	83
Number	4.4	4.4	4.6	4.9	4.9

[10] L. P. Tarasov and B. E. Warren, J. Chem. Phys. **4**, 236 (1936). F. H. Trimble and N. S. Gingrich, Phys. Rev. **53**, 278 (1938).

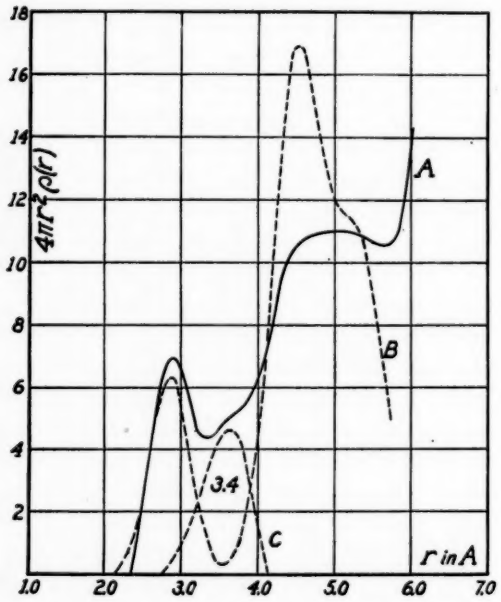

FIG. 6. Comparison of 1.5°C water distribution curve with an ice-like distribution. *A*, water distribution; *B*, calculated distribution; *C*, difference.

Another method of interpretation involves making a direct comparison with the distribution function of ice. Following Prins and Petersen[11] one can approximate the distribution in a liquid by smoothing out the distribution curve of the crystal by means of an error function

$$4\pi r^2\rho(r)=\sum_k \frac{N_k a}{(\pi r_k)^{\frac{1}{2}}}\exp\left[-(a^2/r_k)(r-r_k)^2\right], \quad (2)$$

where N_k is the number of neighbors at a distance r_k. Fig. 6 shows this applied to the first three sets of neighbors in ice. The curve is calculated for 4 neighbors at 2.85A, 13 at 4.50A, and 9 at 5.30A. The first neighbor distance is taken as 2.85 rather than 2.76A to correspond more closely to the experimental curve. The constant a in Eq. (2) is chosen arbitrarily to give a first peak comparable in width to the distribution curve. As seen from Fig. 6, this method of representation fails to account for about 3.4 neighbors at a distance around 3.6A and gives too great a concentration at about 4.5A.

If one smooths out the distribution more drastically by applying the equation

$$4\pi r^2\rho(r)=\sum_k \frac{N_k a}{(\pi r_k^3)^{\frac{1}{2}}}\exp\left[-(a^2/r_k^3)(r-r_k)^2\right] \quad (3)$$

to the structure of ice the curve of Fig. 7 is obtained. There is still a deficit of about 2.0 neighbors to be accounted for at distances between the nearest and next nearest neighbors. We conclude that an ideal 4 coordinated tetrahedral structure does not account for the neighbors which occur in water at distances between those of the first and second neighbors in ice. A structure involving partial tetrahedral bonding with continually changing neighbors seems to be the simplest interpretation of the x-ray distribution curves.

Following Bernal and Fowler's[5] picture of the tetrahedral water molecule, we would expect that in water each molecule is continually striving to bond itself tetrahedrally to 4 neighboring molecules. The peak in the experimental curve at about 4.5A indicates that the desire for tetrahedral bonding is at least partially realized. At any instant a molecule might be bonded to 2 or 3 neighboring molecules, and have other neighbors moving toward it or away from it and therefore occurring at a continuous variety of distances. A picture such as this involving partial tetrahedral bonding is in agreement with results obtained by other methods. Raman spectrum studies[12] indicate that water is slightly more than 2 co-

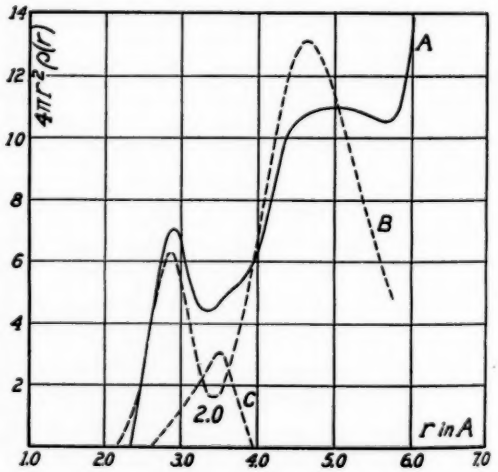

FIG. 7. Comparison of 1.5°C water distribution curve with a smoothed out ice-like distribution. *A*, water distribution; *B*, calculated distribution; *C*, difference.

[11] Prins and Petersen, Physica **3**, 147 (1936).

[12] Cross, Burnham and Leighton, J. Am. Chem. Soc. **59**, 1134 (1937).

ordinated in the range 25° to 90°. Viscosity studies[13] indicate that the average coordination in water is $2\frac{1}{2}$ at 0°, $1\frac{1}{2}$ at 50°, and 1 at 100°C.

We could attempt to explain the latent heat of fusion of ice in at least two ways. If we assumed that in water at 0°C each molecule is tetrahedrally bonded to 4 others exactly as in ice, the x-ray distribution curves show that the average intermolecular separation is about 2.90A rather than 2.76A as in ice. On the other hand, if we assume that each molecule is bonded to less than 4 neighboring molecules, the latent heat will be partly due to the work of breaking some of the bonds in the ice structure. From either point of view there is a definite difference between the ice and the liquid.

When ice melts, the volume decreases by 9 percent, in spite of the fact that the distribution curves show that the intermolecular distance actually increases from 2.76 to 2.90A. This is not as anomalous as it might seem, if we remember that the density of a substance depends upon the interatomic distances and also upon the scheme of packing or coordination number. Ice is an unusually open structure with a coordination number of four. In water the tetrahedral scheme of structure is partly broken down, and neighbors can occur at a variety of distances. As seen from Figs. 6 and 7, this effectively increases the number of approximate neighbors, and the increase in density due to this "filling in" effect more than compensates for the decrease in density due to the larger intermolecular distance. In Fig. 8 this point is illustrated schematically. Fig. 8a represents a very open type of structure with each molecule bonded to 3 neighbors at a definite distance. In Fig. 8b we have a closer scheme of packing, each molecule has 2 nearest neighbors at the same distance as in 8a, and 2 next nearest neighbors at a distance 10 percent larger. The average intermolecular distance is therefore greater in 8b. Due to the closer scheme of packing the density of 8b is 27 percent larger than 8a.

As the temperature of water is raised above 0°C we can think of two opposite effects going on.

[13] Ewell and Eyring, J. Chem. Phys. **5**, 726 (1937).

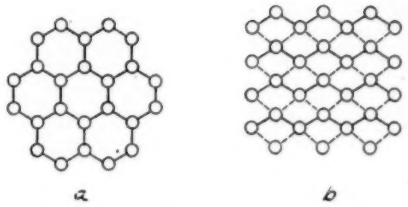

FIG. 8. Illustration of increase in density due to closer scheme of packing.

The progressive breaking down of the fourfold tetrahedral structure allows more neighboring molecules, and this "filling in" increases the density. The increase in intermolecular distance, as shown by the distribution curves for the different temperatures, tends to decrease the density. The minimum volume of water at 4°C is the result of these two opposing effects.

The higher density of water has been treated by Bernal and Fowler by calling water "quartz-like" and ice "tridymite-like." From the "quartz-like" point of view the higher density of water would be due to the next nearest neighbors moving in from 4.5 to about 4.2A. The second peak of the distribution curve, however, corresponds to a distance of 4.5A or slightly larger, rather than to 4.2A. The increased density of water is due not to closer next nearest neighbors, but rather to a "filling in" between the first and second neighbors of the ideal tetrahedral structure. The term "quartz-like" is therefore not a good description of the water structure.

The x-ray results show the essentially tetrahedral nature of the water structure, but cannot be interpreted uniquely in terms of a definite number of neighbors at certain definite distances. This is probably inherent in the nature of the liquid state. Water is well described by the term "broken down ice structure." By this we mean a structure in which each water molecule is striving to bond itself tetrahedrally to 4 neighboring molecules just as in ice, but in which bonds are continually breaking and reforming, so that at any instant a molecule will be bonded to less than 4 neighboring molecules, and have other neighbors at a continuous variety of distances.

Competition of Predissociation Processes in the Photolysis of Polyatomic Molecules

G. K. Rollefson and Milton Burton*
Department of Chemistry, University of California, Berkeley, California
(Received August 17, 1938)

It is shown that if a photoactivated polyatomic molecule may decompose in more than one way with different products for each path, certain generalizations govern the probability of an activated molecule decomposing by any given path. First, there is a tendency to form those products which require a minimum amount of the activation energy to appear as kinetic energy. This tendency increases with increase in energy of the molecule if the energies at which the different paths become possible are widely separated but the opposite effect is found if the separation is small. The effects of collisions in causing predissociation is shown to be interpretable partially as an alteration of the number of times that the molecule reaches a condition represented by the intersection of two hypersurfaces and partially as a disturbance of the restrictions existing at such crossings. These principles are applied in a discussion of the photolyses of acetone, acetaldehyde, acetic acid, formic acid, and normal butyraldehyde.

In a recent paper[1] we have defined simple rupture as a photodecomposition process which occurs at the locus of absorption in the molecule within one vibration period after the absorption act. All other photodecomposition processes were classified as types of predissociation. It was shown that in polyatomic molecules, provided only one bond is broken, a close correspondence is to be expected between the threshold of predissociation (spontaneous or induced) and the strength of that bond. In this paper it is our purpose to examine the factors which tend to determine the path of decomposition in the event of competition between two possible predissociation processes.

The Diatomic Molecule

Let us assume that the potential energy curves of an excited molecule RX are represented by the group of curves shown in Fig. 1. On absorption of light by the molecule in the normal state (not shown) a transition to curve a occurs. If the energy absorbed be sufficient, i.e., if the final potential energy level be at A or higher, the particles R*+X are formed within one vibration period. At levels lower than A, but higher than B or C (e.g. X) the nature of the products is determined by well-known principles. If a transition may occur in a certain configuration (e.g. r_B), its probability increases with the time spent near that configuration. Thus, if both the transitions

$$a \rightarrow b \qquad (1)$$

and

$$a \rightarrow c \qquad (2)$$

are allowed by the selection rules, and if the angular relationships at the two intersections are equally favorable[2] the ratio of the probabilities of the two transitions will be in the ratio of the times spent near the two intersections, i.e.,

$$p_1/p_2 = t_B/t_C,$$

where p_1 and p_2 are the respective probabilities of

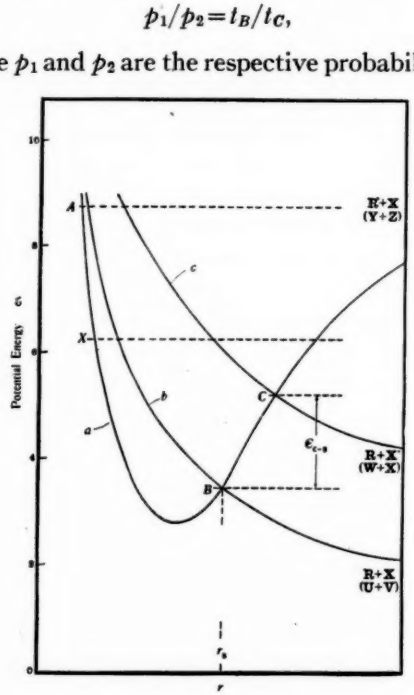

Fig. 1.

* Present address: Department of Chemistry, New York University, New York, N. Y.

[1] Burton and Rollefson, J. Chem. Phys. **6**, 416 (1938).

[2] Cf. Zener, Proc. Roy. Soc. **A137**, 696 (1932); **A140**, 661 (1933).

transitions 1 and 2 and t_B and t_C are the respective times spent in the neighborhoods of the two intersections. Since the kinetic energy of the molecule is zero at the extremity of its oscillations, it is evident that the molecule spends a large fraction of its time in a range of configurations corresponding closely to that condition. Thus, it is apparent that the most favorable condition for a transition is excitation to a level corresponding exactly to the intersection. As the energy increases beyond that level the probability of the transition decreases. In the case under consideration it may be shown that, on excitation to a level at C or higher, p_1/p_2 is a minimum at the excitation to level C.

It follows that, although the reaction

$$RX \xrightarrow{h\nu} R+X \qquad (3)$$

tends to be favored over the one in which the greater amount of energy is to be dissipated as kinetic energy,

$$RX \xrightarrow{h\nu} R+X, \qquad (4)$$

this tendency is a maximum at the absorbed wave-length corresponding to the upper intersection and decreases as the wave-length is decreased thereafter. Obviously, this conclusion holds irrespective of the nature of the curves b and c, which may possibly be weakly attractive instead of repulsive. It is not necessary that the selection rules be such as not to favor either transition. Even if one or the other is favored both by selection rules and angular relationship of the potential curves, the *tendencies* will be as already discussed.

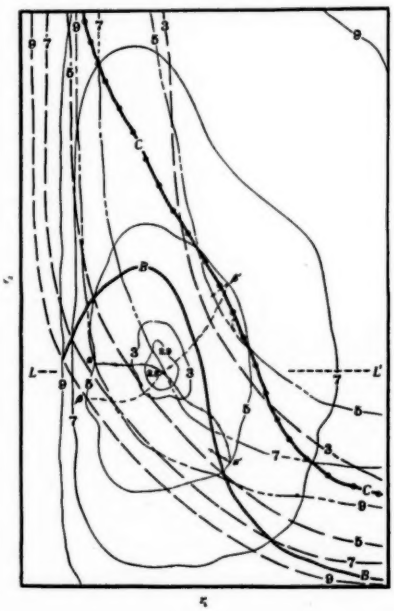

FIG. 2. Three-dimensional potential energy diagram. Key to contour lines: —— surface a, — — surface b, – – – surface c. The heavy lines represent intersections of surfaces.

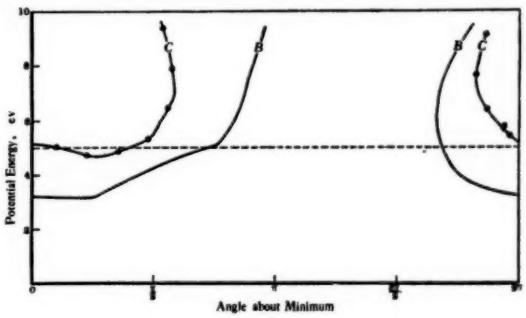

FIG. 3.

POLYATOMIC MOLECULES

It is not obvious whether the previous discussion can be applied unequivocally to *polyatomic molecules*, whose energy states can, in general, be represented only by potential hypersurfaces. For a polyatomic molecule, the potential energy curves of Fig. 1, for example, might represent a two-dimensional cut through the hyperspace in which the potential energies of the excited states are properly plotted. In a three-dimensional cut, it would be necessary to show the potential energy relationships by contour lines. Such a hypothetical cut is shown in Fig. 2. The cut in Fig. 1 is taken along the line LL' in Fig. 2. In this polyatomic case we will assume that the products of decomposition along b, c and a are U+V, W+X, and Y+Z, respectively.

In Fig. 2 the intersections B and C are represented by lines instead of by points. It may be seen also that they are not at one potential energy level but that they vary considerably. In Fig. 3 the potential energies of lines B and C are plotted as functions of the angle (in Fig. 2) about the potential energy minimum at 2.8 ev. Immediately after a molecule absorbs energy in the ground level it may *possibly* be represented by any of a number of points in the cut of Fig. 2,

depending on the wave-length of the light absorbed and the phase of the oscillation in the normal state at the moment of excitation. If the excitation be to point α on the 5 ev contour the molecule will execute a swing[3] along the dashed line to α', also on the 5 ev contour.[4] In executing this swing the intersection B is crossed; there is thus a certain probability that the transition $a \rightarrow b$ may occur and if the "angular relationship" between the potential hypersurfaces is favorable this probability may be high. Since b is the lowest repulsive potential energy hypersurface the products may be formed with high kinetic energy. On the other hand, there is also a possibility of fluorescence or collisional deactivation occurring before the transition $a \rightarrow b$ can occur. Such a reaction reduces the quantum yield.

If the normal state happens to be in a slightly different phase at the moment of absorption, the excitation may be, for example, to point β on the 5 ev contour. The molecule now executes a swing along the dotted line to β' also on 5 ev contour. In executing such a swing the molecular state crosses both the intersections B and C. Angular factors being equal, it is evident that the transition $a \rightarrow c$ will be favored over $a \rightarrow b$ and in this case the products with the lowest kinetic energy will be formed. The interesting point, however, is that although there is a wide range of swings which may result in a crossing of the B intersections at 5 ev only a very limited range of swings results in a crossing of the C intersection. It is evident that this difference results principally from two factors: the way we have drawn the contour lines and the large energy difference, ϵ_{C-B} (see Fig. 1), between the crossings. The smaller the value of ϵ_{C-B} the more nearly would the two ranges approach each other.

For large values of ϵ_{C-B}, it may be seen from Fig. 3 that when the excitation is to sufficiently high potential energy levels (i.e., sufficiently short wave-length absorption), the chance of cutting the C intersection (as indicated by the total length of C below a given energy level) is greatly increased and approaches the chance of cutting the B intersection. Thus, the effect of absorption at shorter wave-lengths is a tendency to favor the reaction producing products of minimum kinetic energy. As will appear below (see acetaldehyde and acetic acid) this is the governing tendency in predissociation[1] decompositions which take place via competitive processes involving as products of the primary acts free radicals on the one hand (transition at C) and ultimate molecules on the other (transition at B).

For small values of ϵ_{C-B}, the ranges of crossings are so nearly alike that approximately the same considerations govern as for the diatomic case. Decrease of wave-length does not (to any marked degree) enhance the probability of the crossing C as compared with the crossing B but it does increase the value t_B/t_C and therefore the value of p_1/p_2. If the selection rules which govern transitions 1 and 2 and the angular relationships of the hypersurfaces involved are equally favorable, it is evident that p_1/p_2 approaches unity as an upper limit as the wave-length is decreased. An increase beyond unity is an indication that some factor (selection rule or angular relationship) favors the lower transition. It will appear below that formic acid may be an illustration of such a case.

The effect of increased temperature must in any case be similar to that of decreased wave-length. Since increased temperature raises both the initial and excited energy level, considerations the same as already discussed must apply.

Classes of Induced Predissociation

Class 1a.—Under special circumstances (e.g. if the energy hypersurface corresponds to an elliptical bowl and the intersections are at the sides) it is possible that if an oscillation starts in an unfavorable locus (e.g. along the length of the bowl), decomposition will not normally occur no matter how long the oscillation is continued. Under such circumstances fluorescence, collisional deactivation, or induced predissociation may ensue. The way the latter occurs is by the disturbing effect of a momentary local intense field. The shapes of the contour lines of the a surface are momentarily altered and the direction of the swing (which is at all times precisely

[3] We define a *swing* as a portion of an oscillation beginning on the highest contour (hyper-) surface reached and ending on the same contour. An oscillation when complete ends at the starting point. One oscillation contains many *swings*.

[4] It must be remembered that this is but a limited representation of the facts. Since the true potential energy diagram is much more complicated than can be represented in two dimensions, the statement of what happens has to be telescoped.

determined by the contour lines) is thus diverted. The new direction may be such as to result in crossing of one or the other intersection.

Class 1b.—The case just cited is exaggerated. A variant case is the one in which the oscillation eventually would cross the intersection of itself but in which the crossing is so long delayed that the yield is cut down by fluorescence. For example, consider a molecule in which fluorescence occurs 10^{-9} sec. after activation and in which the first crossing (after a particular starting configuration) occurs in 10^{-8} sec. Obviously, the amount of decomposition would be small compared to the fluorescence. If, however, the pressure is increased or a foreign gas introduced, the first collision may be made to occur in 10^{-10} sec. Let us assume that this collision so deforms the contours that the direction of the swing is changed and that in half those cases the result is such as to further delay the crossing but that in the other half the subsequent crossing occurs in less than 10^{-10} sec. (i.e., before another collision occurs). Evidently, since the quantum yield is already quite low the first effect will not be detectable; only an increased quantum yield traceable to the second effect will be observed.

Class 1c.—In our previous paper we made the suggestion that slow spontaneous predissociation processes occur by rearrangement within the same potential hypersurface. Another possible model according to the view presented here considers that decomposition occurs as a result of a transition from one surface to another but the region in which such a transition may occur is so restricted that it is seldom reached. The distinction between the two cases is that in the former the decomposition corresponds to the passage of the system through a low "saddle" region whereas in the latter the system passes through a region in which a transfer from one state to another may occur but with a probability considerably less than unity. In such a case fluorescence or deactivation by collisions will usually reduce the quantum yield to some value less than unity. The effect of collisions will be to alter the swings of the molecule so as to cause an oscillation which will cover a larger area of the hypersurface. If the original swings did not cross the intersection of the two hypersurfaces the collisions will tend to cause a crossing whereas if the initial conditions favored a crossing collisions will tend to reduce the number of crossings. Two limiting conditions appear. At low pressures there is competition between fluorescence and decomposition. The fraction of the activated molecules decomposing is a constant determined by the types of swings which occur, without perturbation, in the molecule raised to the excited state by the absorption of light. According to this point of view it is possible for a reaction showing induced predissociation to exhibit a limiting quantum yield greater than zero at extremely low pressures. At high pressures fluorescence does not enter and the competition is between decomposition and deactivation by collisions. Under these conditions we have a maximum perturbation of the swings and the number of molecules decomposing will be proportional to the fraction of all possible swings, of a given total energy, which cross the intersection. In this case, therefore, the quantum yield of the decomposition deviates from that at low pressure. Whether it appears to approach a limit or drops toward zero will depend on whether the life of the activated state with great perturbation of the swings is short or long relative to the time required for deactivation by collision.

Class 2.—It has been mentioned that a necessary condition for a transition at an intersection is that the angular relationship of the hypersurfaces at the intersection be favorable. Another way in which induced predissociation may occur is immediately apparent. The effect of the external field may be to promote a more favorable relationship of the hypersurfaces at the intersection. The time of a collision process is $\sim 10^{-13}$ sec., which is of the order of the time required for a swing. Thus, there is a good probability that when two molecules collide such an effect may occur at a time favorable to a transition.

Class 3.—We have hitherto neglected the possibility that selection rules may restrict the probability of transitions between potential hypersurfaces. In general, predissociation may be induced by collision through a breakdown in the the selection rules which govern the transition involved.

Comment.—Classes *2* and *3* have been included merely for the sake of completeness. Class *1*, it will be seen, is adequate to explain the various

phenomena discussed in this paper; the present discussion is devoted to a consideration of predissociation processes other than types 1*a*ii (*x* and *y*), according to the classification of our earlier paper.

Acetaldehyde

Acetaldehyde decomposes by the predissociation processes[1, 5]

$$CH_3CHO+h\nu\rightarrow CH_3+CHO \qquad (1)$$

$$CH_3CHO+h\nu\rightarrow CH_4+CO. \qquad (2)$$

The heats of formation of CH_3 and CHO relative to CH_4 and CO may be estimated from the following considerations. We will assume that approximately as much energy is gained from the reaction $CH_3+H\rightarrow CH_4$ as is required for the reaction $CHO\rightarrow CO+H$. However, the CO formed is in an activated state and quickly rearranges to give normal CO with the emission of $\sim$100 kcal.[6] Thus, the heat of formation of the products of reaction 1 is *considerably* less than for those of reaction 2 and it is reasonable to infer that the considerations for large values of ϵ_{C-B} must apply. Thus, the effect of decreased wave-length would be to increase the probability of crossing intersection *C* before crossing *B*. The evidence presented by Blacet and Roof indicates[5b,c] that although the relative decomposition via reaction 1 is slight, it does increase with decrease of wave-length just as would be expected on the basis of the views here set forth.

Acetone

The absorption spectrum of acetone consists in part of a discrete region extending from 3340 to 2945A and a continuum beginning at 3000A.[7a] The evidence[7b] indicates that in the discrete region decomposition is exclusively via the rearrangement mechanism

$$(CH_3)_2CO\rightarrow C_2H_6+CO, \qquad (1)$$

whereas in the continuum only the reaction occurs to a measurable extent. It may be seen that this result is in agreement with the finding[7c, d] that increased pressure increases the quantum yield in the discrete region and that the yield in that region decreases toward a minimum of $\sim$0.04 at low pressures. This last result indicates a relationship of potential energy surfaces such as described in class *1b*. While the transition at *B* might eventually occur as a spontaneous process (or as an induced one) at longer wave-lengths, it is evident that a decrease in wave-length would favor the transition at *C* to such an extent as to decrease the probability of reaction 1 to a negligible factor in the continuum.

$$(CH_3)_2CO\rightarrow CH_3+CH_3CO \qquad (2)$$

Acetic Acid

Acetic acid likewise decomposes by two predissociation processes.[1] The evidence indicates that most of the decomposition of the monomer proceeds via the reaction

$$CH_3COOH+h\nu\rightarrow CH_4+CO_2. \qquad (1)^{8a}$$

A small part of the decomposition proceeds via the reaction

$$CH_3COOH+h\nu\rightarrow CH_3COO+H \qquad (2)^{8b,c}$$

and, according to one of us,[8b] the relative amount of that reaction increases with decrease in wave-length. Considerations similar to those in the case of acetaldehyde indicate that here also ϵ_{C-B} is high and that this result is to be expected. The only evidence[8a] available indicates a quantum yield $\backsimeq$1.0. However, it is apparent that the precise magnitude of the quantum yield is not essential to these considerations for whenever a competition between two predissociation processes occurs, one yielding free radicals and the other ultimate molecules in the primary step, ϵ_{C-B} must be high and the free radical decomposition will be favored by decrease in wave-length.

Formic Acid

The monomer of formic acid may decompose by either of the reactions[9a]

[5] (*a*) Blacet and Roof, J. Am. Chem. Soc. **58**, 278 (1936). Cf. (*b*) Rollefson, J. Phys. Chem. **41**, 259 (1937); (*c*) Burton, ibid. **41**, 322 (1937).

[6] Cf. Norrish, Trans. Faraday Soc. **30**, 103 (1934).

[7] (*a*) Noyes, Duncan and Manning, J. Chem. Phys. **2**, 717 (1934); (*b*) Spence and Wild, J. Chem. Soc. 352 (1937); (*c*) Norrish, Crone and Saltmarsh, ibid. 1456 (1934); (*d*) Damon and Daniels, J. Am. Chem. Soc. **55**, 2363 (1933).

[8] (*a*) Farkas and Wansbrough-Jones, Zeits. f. physik. Chemie **B18**, 124 (1932); (*b*) Burton, J. Am. Chem. Soc. **58**, 1645 (1936); (*c*) Cf. Henkin and Burton, ibid. **60**, 831 (1938).

[9] (*a*) E. Gorin and H. S. Taylor, J. Am. Chem. Soc. **56**, 2042 (1934); (*b*) Burton, ibid. **58**, 1655 (1936).

TABLE I. *Effect of wave-length and temperature on the photolysis of* HCOOH.

WAVE-LENGTH A	TEMP. °C	RATIO REACTION 1 : REACTION 2
2540	40	0.32
	100	0.45
2100 } 1900 }		1.38

$$\text{HCOOH}+h\nu \begin{cases} \nearrow \text{CO}_2+\text{H}_2 & (1) \\ \searrow \text{CO}+\text{H}_2\text{O}. & (2) \end{cases}$$

Free radicals or atoms are not involved.[9] The heats of formation[10] of the products from the atoms (except that for carbon we consider it in the form of graphite) are

$$\begin{aligned} &\text{CO}_2 \quad + \quad \text{H}_2 \\ &211.75^{11}+102.8^{12}=314.55 \text{ kcal.} \end{aligned}$$

and

$$\begin{aligned} &\text{CO} \quad + \quad \text{H}_2\text{O} \\ &85.49^{13}+219.251^{14}=304.741 \text{ kcal.} \end{aligned}$$

The difference of ~10 kcal. between the heats of formation of the products is so small as to indicate that ϵ_{C-B} is small. In that case we would expect that decrease in wave-length of absorbed light should favor the reaction corresponding to the lower transition, i.e., reaction 1. This is the result reported by Gorin and Taylor who give the data from which Table I is compiled. The table also shows the parallelism between the effect of decreased wave-length and the effect of increased temperature which has already been discussed. The ratio of 1.38 for reaction 1 : reaction 2 at 2100 and 1900A indicates that there is at least one factor which favors reaction 1. Since the value seems to tend toward this not very high limit at low wave-lengths, the most plausible explanation appears to be a steric one.

n-BUTYRALDEHYDE

n-Butyraldehyde decomposes according to all three of the reactions

$$\text{C}_3\text{H}_7\text{CHO}+h\nu \begin{cases} \nearrow \text{C}_3\text{H}_8+\text{CO} & (1) \\ \rightarrow \text{C}_3\text{H}_7+\text{HCO} & (2) \\ \searrow \text{C}_2\text{H}_4+\text{CH}_3\text{CHO}. & (3)^{15} \end{cases}$$

As might be expected from the discussions of acetaldehyde, acetone and acetic acid, reaction 2 is favored by decrease in wave-length. As for the other reactions, the heats of formation of the products are

$$\begin{aligned} &\text{C}_3\text{H}_8 \quad + \quad \text{CO} \\ &399.45^{16}+85.49^{13}=484.94 \text{ kcal.} \end{aligned}$$

and

$$\begin{aligned} &\text{C}_2\text{H}_4{}^{17}+\text{CH}_3\text{CHO}^{18} \\ &19.46 + \quad 308.25 \quad =502.85 \text{ kcal.} \end{aligned}$$

The difference of ~18 kcal. between the heats of formation of the products of the two reactions is such as to indicate that they may be classed for purposes of comparison in the case where ϵ_{C-B} is small. This assumption is insufficient for a complete explanation of the interpretation of their own data on the photolysis of *n*-butyraldehyde advanced by Leighton, Levanas, Blacet and Rowe. They concluded that the rate o reaction 3 fell off more rapidly than that of 1 as the wave-length is decreased. It may be possible to explain such a result on the basis of special assumptions. However, it would seem worth while first to establish this conclusion unequivocally, since it is based largely on observations concerning the volatility of a mixture of unsaturated hydrocarbons at liquid-air temperatures.

[9] Bichowsky and Rossini, *Thermochemistry of Chemical Substances* (Reinhold Publishing Corp., New York, 1936).

[11] This is calculated from the value of 94.45 kcal. for the heat of formation of CO_2 from its elements in the standard state (ref. 10) plus the heat of formation of O_2 from its atoms, 117.3 kcal. (Frerichs, Phys. Rev. **36**, 839 (1930); Johnston and Walker, J. Am. Chem. Soc. **55**, 172 (1933). No allowance has been made for the heat of sublimation of graphite or for the heat of dissociation of C_2.

[12] Giauque, J. Am. Chem. Soc. **52**, 4816 (1930).

[13] Calculated from the value of 26.84 kcal. for the heat of formation of CO from its elements in the standard state and from the heat of formation of O_2 from its atoms.

[14] Calculated from the value of 57.801 kcal. for the heat of formation of H_2O from its elements in the standard state (ref. 10) and from the heats of formation of H_2 and O_2 from their atoms.

[15] Leighton, Levanas, Blacet and Rowe, J. Am. Chem. Soc. **59**, 1843 (1937).

[16] Calculated from the value of 526.3 kcal. for the heat of combustion of C_3H_8 (ref. 10) and other data already given in the manner described in footnotes 11, 13 and 14.

[17] Calculated from the value of −11.0 kcal. for the heat of formation of C_2H_4 from its elements in the standard state (ref. 10), in the manner already indicated.

[18] Calculated from the value of 44.0 kcal. for the heat of formation of CH_3CHO from its elements in the standard state.

The Mechanism of the Photolysis of Deutero-Ammonia

MILTON BURTON*
Department of Chemistry, University of California, Berkeley, California
(Received August 26, 1938)

In order to avoid theoretical objections to the mechanism previously suggested for the photolysis of ND_3, a new mechanism is proposed involving competition between two spontaneous predissociation processes in the discrete region. The relative amounts dissociating by the two paths, one yielding atomic hydrogen and the other molecular hydrogen, are shown to be in the approximate ratio 19 : 1 in the primary act. In the diffuse region, the time of decomposition is so short that the reaction is exclusively by the first path.

ACCORDING to Wiig,[1] the photolysis of deutero-ammonia is distinguished in a rather unusual way. The quantum yield in the discrete region at λ2138A is greater than that in the diffuse region at λ2100A. Although the quantum yields in the two regions vary with pressure, their difference remains constant. A mechanism, of which the following are essential parts, was suggested to explain these results,

$$ND_3+h\nu\rightarrow ND_3^* \tag{1}$$

$$ND_3^*+ND_3 \begin{cases} \nearrow ND_2+D+ND_3 & (2) \\ \searrow N_2+3D_2 & (3) \end{cases}$$

Reaction 2 may be recognized as an induced predissociation reaction; this part of the mechanism can be subjected to simple tests such as a search for variation in fluorescence with pressure.[2] Reaction 3 is particularly interesting. If true it is one of the few cases in which there is still reason to believe in a photoactivated molecule entering into a reaction with a nonactivated molecule. One by one such cases (e.g. in the photolysis of hydrogen iodide) have been eliminated. Furthermore, there is theoretical objection to reaction 3. On the basis of the principle of microscopic reversibility, any reaction involving four product molecules seems extremely improbable. It is worth while, therefore, to determine whether the results obtained by Wiig can be explained in some simpler way.

In the first place, it must be emphasized that the discrete absorption at λ2138A is no indication that an induced predissociation process is occurring. Just as in the case of ammonia, whose absorption bands all appear diffuse, a spontaneous process may be involved. However, whereas the spontaneous process in NH_3 (and in ND_3 in the blurred region at 2100A) is rapid, in ND_3 at 2138A it is slow.[3] The slowness of the predissociation process introduces possibilities which might not otherwise occur.

In a determination of the mechanism of the photolysis of NH_3 it is necessary to consider two possible primary processes

$$NH_3^*\rightarrow NH_2+H \tag{4}$$

$$NH_3^*\rightarrow NH+H_2. \tag{5}$$

In that case only reaction 4 occurs.[4] The diffuseness of the bands indicates that it takes place in less than 10^{-11} sec. Reaction 5, which is a predissociation by rearrangement, takes a longer time (say 10^{-10} to 10^{-9} sec.) and consequently does not occur. In deutero-ammonia, however, there seem to be conditions (whose nature we need not examine) which make the reaction analogous to 4

$$ND_3^*\rightarrow ND_2+D \tag{6}$$

a slow process, requiring, say 10^{-10} to 10^{-9} sec. Since the reaction

$$ND_3^*\rightarrow ND+D_2 \tag{7}$$

* Present address: Department of Chemistry, Columbia University, New York, N. Y.

[1] Wiig, J. Am. Chem. Soc. **59**, 955 (1937).

[2] Cf. Burton and Rollefson, J. Chem. Phys. **6**, 416 (1938).

[3] In this respect the behavior of ammonia is analogous to that of formaldehyde in the discrete region above 2750A. See ref. 2.

[4] Wiig, J. Am. Chem. Soc. **59**, 827 (1937).

actually requires less energy than reaction 6,[5] it will proceed whenever the proper configuration is attained and there will in many molecules be time for the attainment of that configuration before reaction 6 can occur.

The next step suggested is

$$ND+ND\rightarrow N_2+D_2. \qquad (8)$$

The assumption is made that ND does not react readily with any of the other substances present, i.e., ND_3, N_2, D_2 and the assumed intermediates.[6] It follows that the quantum yield in that fraction of the ND_3 molecules in which decomposition occurs via reaction 7 is unity and independent of the pressure. In the portion decomposing via reaction 6 the quantum yield is low due to the various possible back reactions and varies with the pressure. However, the fraction entering into step 6 is unaffected by the pressure.

The fraction of ND_3 molecules decomposing via step 7 may be presumed equal to the difference between the quantum yields at λ2138 and λ2100A, i.e., ∼0.05. The total yield at λ2138A is then

$$\gamma_{2138}=0.05+0.95\phi(p), \qquad 1$$

where $\phi(p)$ is a function which indicates the effect of pressure on quantum yield via reaction 6. If it be assumed that there is no loss either by fluorescence or collisional deactivation at either λ2100 or λ2138A, $\phi(p)$ will have the same form at both wave-lengths and will be no greater than ∼0.27, the value for the maximum quantum yield at λ2100A. But

$$\gamma_{2100}=1.0\phi(p), \qquad 2$$

which value therefore differs from the second term of Eq. 1 by only 0.05×0.27 or ∼0.01 at a maximum, well within the experimental error of the method. The constancy of the difference between the quantum yields is thus accounted for.

It may also be seen from Eq. 1 that the rates of the two primary reactions 6 and 7 are in the ratio 19 : 1 at λ2138A. At λ2100A, of course, reaction 7 occurs not at all or in negligible amount.

Discussion

It has been shown by Rollefson and Burton[7] that in those cases where there is competition between decomposition into free radicals and into ultimate molecules in the primary act, the former is favored by decrease in wave-length. In acetone,[7] for example, only the former takes place at shorter wave-lengths.[8] In NH (as contrasted with NH_2) all the electrons are paired.[9] In the parallel case of CH_2, Pearson, Purcell and Saigh[10] have concluded, on the basis of mirror experiments, that methylene behaves more like a very reactive molecule than like a free radical. It consequently appears justifiable to treat NH as a molecule and to say that reaction 7 involves a decomposition into ultimate molecules in the primary act. It may be seen that this case of deutero-ammonia is but another illustration of the general behavior to be expected in the case of polyatomic molecules.[7]

[5] The reaction $NH_3\rightarrow NH_2+H$ requires ≥101 kcal. (cf. Ellis, Phys. Rev. **33**, 27 (1929)). The reaction $NH_3\rightarrow NH+H_2$ requires 45–57 kcal. (cf. Bates, Zeits. f. physik. Chemie. Bodenstein-Festband, 329 (1931)). The latter values are estimated on the basis of 249.85 kcal. as the heat of formation for NH_3 from its atoms (Bichowsky and Rossini, *The Thermochemistry of the Chemical Substances* (Reinhold Publishing Corp., New York, 1936)).

[6] It should, however, be noted that in explaining the Hg-photosensitized synthesis of NH_3 from its elements at high pressures, Noyes, J. Am. Chem. Soc. **52**, 2418 (1930) suggested such reactions as $NH+H_2\rightarrow NH_2+H$.

[7] Rollefson and Burton, J. Chem. Phys. **6**, 674 (1938).

[8] Cf. Spence and Wild, J. Chem. Soc. 352 (1937).

[9] Cf. Kronig, *The Optical Basis of the Theory of Valency* (Cambridge University Press, 1935), p. 134.

[10] Pearson, Purcell and Saigh, J. Chem. Soc. 409 (1938).

Infra-Red and Raman Spectra of Polyatomic Molecules. III. Ethane

BRYCE L. CRAWFORD, JR.,* WILLIAM H. AVERY AND J. W. LINNETT
Mallinckrodt Chemical Laboratory, Harvard University, Cambridge, Massachusetts

(Received August 22, 1938)

The Raman and infra-red spectra of ethane have been re-examined. The 993, 2900, and 2955 cm^{-1} Raman lines are polarized; there were indications of very faint lines appearing at 620 and 820 cm^{-1}. The strong infra-red peak at 1480 cm^{-1} is found to be a *single* minimum; the weak band at 1740 cm^{-1} is confirmed.

The available Raman and infra-red data are evaluated, and possible assignments discussed. It is shown that the observed frequencies do not require a 740 cm^{-1} fundamental, but are consistent with an "uncertain frequency" of about 1100 cm^{-1} and a high restricting potential.

RECENT work[1] on the problem of internal rotation in ethane has focussed considerable interest on the vibrational frequencies of this molecule. Although the magnitudes of most of the fundamental frequencies are known sufficiently well for thermodynamic calculations, two widely different values have been proposed for the so-called "uncertain frequency." Heat capacity data,[2] including that at low temperatures, seem unequivocally to indicate a value of about 1100 cm^{-1} for this frequency; on the other hand, Bartholomé and Karweil[3] have studied the overtone region carefully and find spectral evidence for a value of 740 cm^{-1}. In connection with this question, we have considered it worth while to re-examine the Raman and infra-red spectra of ethane, and have also considered possible assignments for the observed frequencies.

EXPERIMENTAL

The ethane used was especially prepared from pure hydrogen and ethylene. Both materials were obtained from the Ohio Chemical Co.; the hydrogen was rated 99.9 percent, and the ethylene 99.5 percent. Catalytic combination took place on reduced copper oxide at temperatures not exceeding 120°C. The Raman spectrum showed no traces of the strong lines of the probable impurities.

The Raman spectrograph has been previously described;[4] during exposures, the Raman tube containing the liquid ethane was kept at a temperature of about −60°C by a stream of cold air. Polarization measurements[5] on the four principal lines showed the 993, 2900, and 2955 cm^{-1} lines to be polarized, and the 1460 cm^{-1} line, depolarized. Microphotometer records of comparable plates made with polarized and unpolarized light are given in Fig. 1. It will be noted that the 2900 cm^{-1} line appears to be slightly more polarized than the 2955 cm^{-1} line.

The Raman spectrum of ethane has been examined several times with instruments of higher dispersion;[6] it does not seem worth while to report our frequencies for the lines previously found, which checked within experimental error.

On several plates, indications were found of two faint lines, difficult to measure, displaced from the Hg 4358A line by about 620 and 820 cm^{-1}. Professor George Glockler has informed us that these lines had appeared on his plates also,[7] and were measured at 617 and 813 cm^{-1}. These lines are extremely faint, and moreover the corresponding shifts excited by Hg 4047A were not observed; nevertheless, the appearance of these lines in two independent investigations seems to provide some evidence for their reality.

* National Research Fellow in Chemistry.

[1] G. B. Kistiakowsky and E. B. Wilson, Jr., J. Am. Chem. Soc. **60**, 494 (1938); K. S. Pitzer and J. D. Kemp, ibid. **60**, 1515 (1938); and references given therein.

[2] W. Hunsmann, Zeits. f. physik. Chemie **B39**, 23 (1938); G. B. Kistiakowsky, J. R. Lacher, and F. Stitt, J. Chem. Phys. **6**, 407 (1938); E. B. Wilson, Jr., ibid. **6**, 408 (1938).

[3] E. Bartholomé and J. Karweil, Zeits. f. physik. Chemie **B39**, 1 (1938).

[4] H. Gershinowitz and E. B. Wilson, Jr., J. Chem. Phys. **6**, 247 (1938).

[5] J. T. Edsall and E. B. Wilson, Jr., J. Chem. Phys. **6**, 124 (1938).

[6] P. Daure, Ann. de physique **12**, 375 (1929); S. Bhagavantam, Ind. J. Phys. **6**, 596 (1931); C. M. Lewis and W. V. Houston, Phys. Rev. **44**, 903 (1933); G. Glockler and M. M. Renfrew, J. Chem. Phys. **6**, 295 (1938).

[7] We are indebted to Professor Glockler for sending us these data; he had not reported them because on his plates, as on ours, these shifts excited by the Hg 4047A line did not appear.

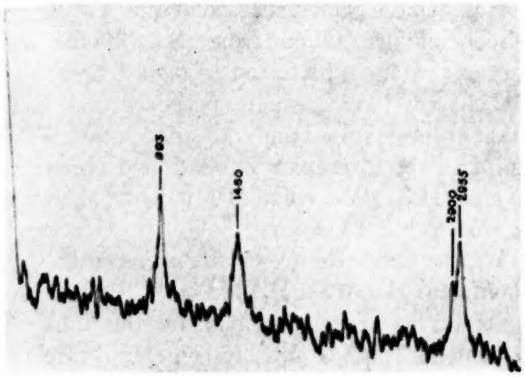

FIG. 1 (a). Microphotometer records of plates made with polarized light, showing the shifts at 993 (*P*), 1460 (*D*), 2900 (*P*), and 2955 (*P*) cm^{-1}. To conform with Table I the lines are labeled with the corresponding gas-phase frequencies instead of the actual liquid-phase frequencies.

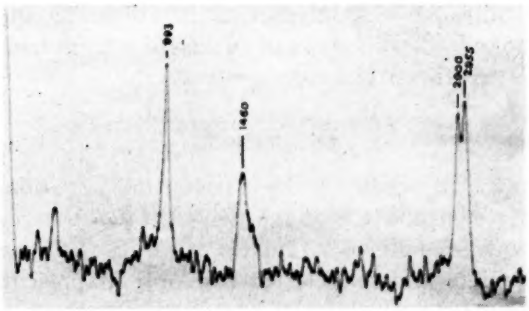

FIG. 1 (b). Microphotometer records of plates made with unpolarized light, showing the shifts at 993 (*P*), 1460 (*D*), 2900 (*P*), and 2955 (*P*) cm^{-1}. To conform with Table I the lines are labeled with the corresponding gas-phase frequencies instead of the actual liquid-phase frequencies.

The infra-red absorption of gaseous ethane was studied with the spectrometer previously described;[8] a fluorite prism was used for the region from 3 to 9μ, and a rocksalt prism from 9 to 15μ. Transmission curves of the absorption regions beyond 5μ are given in Fig. 2.

The infra-red spectrum has been studied by several investigators.[9] The band at 827 cm^{-1} is well established. The 1740 cm^{-1} band was reported by Benedict, Morikawa, Barnes and Taylor as lying at 1770 cm^{-1}; we believe our value of the frequency to be more reliable than theirs, since they used a rocksalt prism, which gives lower resolution.

Our results for the 7μ region are of particular interest. This region was examined under high resolution by Levin and Meyer; their measurements show a peak at 1379 cm^{-1}, a region of weak absorption between 1390 and 1430 cm^{-1}, and a strong band with center about 1480 cm^{-1} which shows regular rotational spacing from 1442 to 1515 cm^{-1}, and gives every appearance of a single band of the perpendicular type. Bartholomé and Sachsse, using a fluorite prism, found a single weak minimum at 1365 cm^{-1}, and found the strong peak to be double, with minima at 1465 and 1495 cm^{-1}. Our curve (Fig. 2) shows a *single* strong minimum at 1477 cm^{-1}, and two weaker minima at 1380 and 1414 cm^{-1}. The resolution of our spectrometer in this region is more than adequate; in studies of cyclopropane, two minima at 1425 and 1445 cm^{-1} are clearly resolved. It is difficult to explain the double minimum found by Bartholomé and Sachsse; it is possible that they did not properly correct for the strong atmospheric water bands which overlie this region. Considering our own data and those of Levin and Meyer, we believe that the evidence is strongly in favor of a single strong band at 1480 cm^{-1}, with weaker bands at 1380 and 1415 cm^{-1}, as shown in our curve.

Our results above 2000 cm^{-1} are consistent with the grating measurements of Bartholomé and Karweil in this region, except for one very large discrepancy. Their curves show a band at 2303 cm^{-1}, while we find this band at 2353 cm^{-1}, as shown in Fig. 2. While our resolution was con-

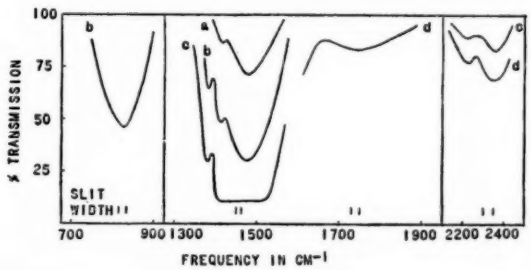

FIG. 2. Infra-red transmission of ethane gas. Path length, 30 cm; pressures, (a) 60 mm, (b) 125 mm, (c) 355 mm, (d) 760 mm.

[8] H. Gershinowitz and E. B. Wilson, Jr., J. Chem. Phys. **6**, 197 (1938).

[9] A. Levin and C. F. Meyer, J. Opt. Soc. Am. **16**, 137 (1928); E. Bartholomé and H. Sachsse, Zeits. f. physik. Chemie **B30**, 40 (1935); W. S. Benedict, K. Morikawa, R. B. Barnes, and H. S. Taylor, J. Chem. Phys. **5**, 1 (1937); E. Bartholomé and J. Karweil, Zeits. f. physik. Chemie **B39**, 1 (1938).

siderably less than that of Bartholomé and Karweil, this difference of 50 cm^{-1} lies far outside the experimental error.

Discussion

After a study of the various investigations referred to above, we have arrived at the observed frequencies given in Table I as being the most complete and reliable list available at present. The Raman frequencies are principally the gas-phase values of Lewis and Houston; we have rejected the weak 1344 cm^{-1} line, which is almost certainly due to ethylene present as an impurity, and have added the 620 and 820 cm^{-1} lines discussed above, the 1463 and 2963 cm^{-1} shifts observed in the liquid by Glockler and Renfrew, and the 975 cm^{-1} shift found by Bhagavantam. Of the infra-red frequencies, those lying below 2000 cm^{-1} have been discussed above. The higher frequencies are taken from Bartholomé and Karweil; we have preferred to regard their peak at 2230 cm^{-1} as a single perpendicular band rather than as two bands 15 cm^{-1} apart. With regard to the discrepancy mentioned above, we have included their value of 2303 cm^{-1} as well as our own value, 2350 cm^{-1}.

Glockler and Renfrew[10] have recently suggested that the 813 and 1463 cm^{-1} Raman lines found in liquid ethane may be the infra-red fundamentals at 827 and 1480 cm^{-1}, appearing in the Raman effect through a breakdown of the selection rules due to intermolecular forces active in the liquid. These frequencies would actually be permitted in the Raman effect if the selection

[10] G. Glockler and M. M. Renfrew, J. Chem. Phys. **6**, 409 (1938).

Table I. *Observed frequencies of ethane, with a possible assignment.**

Freq. cm^{-1}	Int'y.; Type	Ass.	Calc. Freq.	Symmetry D_{3h}	Symmetry D_{3d}
Infra-Red:					
827	⊥s	Fund.	(827)	E'	E_u
1380	∥w	Fund.	(1380)	A_2''	A_{2u}
1414	⊥w	1120+300	1420	E'	E_u
1480	⊥s	Fund.	(1480)	E'	E_u
1740	?w	1460+300	1760	E'	E_u
2230	?⊥w	1120^2	2240	$A_1'+A_2'+E'$	—
		1375+827	2202	—	E_u
2303	?∥w	827+1480	2307	$A_1'+A_2'+E'$	—
		827+1460	2287	—	$A_{1u}+A_{2u}+E_u$
2350	?∥w	993+1380	2373	A_2''	A_{2u}
2660	⊥w	2970−300	2670	E'	E_u
2755	∥m	1380+1375	2755	A_2''	A_{2u}
2895	∥m	Fund.	2926	A_2''	A_{2u}
2955	∥s	1480+1460	2940	$A_1''+A_2''+E''$	$A_{1u}+A_{2u}+E_u$ resonance
3007	∥m	993+827+1120	2940	$A_1''+A_2''+E''$	$A_{1u}+A_{2u}+E_u$ triplet
2950–3000	⊥w	Fund.	2980	E'	E_u
3100–3150	⊥w	827^2+1480	3134	$A_1'+A_2'+2E'$	$A_{1u}+A_{2u}+2E_u$
3186	∥w	1460^2+300	3220	$A_1''+A_2''+E''$	$A_{1u}+A_{2u}+E_u$ resonance
3223	∥w	1120+1480+300^2	3200	$A_1''+A_2''+E''$	$A_{1u}+A_{2u}+E_u$ doublet
Raman:					
(620)?	v.w.	300^2	600	A_1'	A_{1g}
(813)	v.w.	Fund.	(827)	E'	E_u†
975	w	$C^{12}-C^{13}$ Fund.	—	A_1'	A_{1g}
993	s, P	Fund.	(993)	A_1'	A_{1g}
(1463)	m, D	Fund.	(1460)	E''	E_g
			1480	E'	E_u†
2744	w	1375^2	2750	A_1'	A_{1g} resonance
2778	w	1380^2	2760	A_1'	A_{1g} doublet
2900	s, P	Fund.	2927	A_1'	A_{1g} resonance
2955	s, P	1460^2	2920	A_1'	A_{1g} doublet
2940	w	1480+1460	2940	$A_1''+A_2''+E''$	—
		1480^2	2960	—	$A_{1g}+A_{2g}+E_g$ resonance
(2963)	w	Fund.	2970	E''	E_g doublet in D_{3d} case

* Liquid-phase frequencies in parentheses: s = strong, m = medium, w = weak, v.w. = very weak, P = polarized, D = depolarized.
† Breakdown of D_{3d} selection rules.

rules appropriate to the D_{3h} configuration apply to ethane.[11]

If the 620 cm^{-1} line is real, there is the interesting possibility that it is the first overtone of the internal torsional motion associated with a high potential barrier. The selection rules permit the appearance of this overtone in the Raman effect. Professor E. B. Wilson, Jr., has calculated certain levels of this motion;[12] for a restricting potential of 3000 cal./mole magnitude and the usually assumed cosine shape, the two lowest excited levels lie at about 300 and 565 cm^{-1}. While this value for the overtone is too low to fit the 620 cm^{-1} Raman line, it is quite possible that the actual potential barrier has a different shape which would give a somewhat higher second excited level when adjusted to fit the thermodynamic data, an idea which is confirmed by a study of a square potential barrier. Another possible assignment for the 620 cm^{-1} line would be the difference tone 1463–813 (liquid-phase frequencies); this calculated value lies 30 cm^{-1} too high.

Since a study of the infra-red and Raman spectra of heavy ethane, C_2D_6, is now in progress in this laboratory, it seems best to postpone any final vibrational analysis until data for the two isotopic molecules may be considered together. However, it may be well to point out that the overtone region, studied by Bartholomé and Karweil,[3] does not afford conclusive evidence on the magnitude of the "uncertain frequency." These authors account for their observed frequencies with the use of a 740 cm^{-1} fundamental and the selection rules appropriate to the D_{3h} configuration. The double minimum, 1465 and 1495 cm^{-1}, reported by Bartholomé and Sachsse, would suggest a 740 cm^{-1} fundamental; as discussed above, however, the evidence seems to be in favor of a *single* peak at 1480 cm^{-1}. When we accept this single peak, it is possible to account for the observed frequencies without the use of a 740 cm^{-1} frequency. To illustrate this, we give in Table I possible assignments of the observed frequencies, using the fundamentals listed in Table II. These fundamentals are consistent with the existence of a 3000 cal./mole restricting potential, an "uncertain frequency" of about 1100 cm^{-1}, and an internal torsional oscillation of about 300 cm^{-1}. We have given assignments satisfying the selection rules for both the D_{3h} and the D_{3d} equilibrium configurations; the D_{3h} assignment is slightly more satisfactory in the three cases where different assignments are required. It is to be emphasized that this assignment is not to be regarded as a final one, but is given merely to show that the observed overtones do not require a 740 cm^{-1} fundamental.

TABLE II. *A possible set of fundamental frequencies for ethane.*

(SYMMETRY SYMBOLS ARE GIVEN FOR POINT GROUPS D_{3h}',[11] D_{3h}, AND D_{3d}, IN THAT ORDER.)

A_1, A_1', A_{1g}:	993	E, E', E_u:	827
	1375		1480
	2927		2980
$\bar{A}_2, A_2'', A_{2u}$:	1380	$\bar{E}, E'', E_g$:	1120
	2926		1460
$\bar{A}_1, A_1'', A_{1u}$:	300		2970

In concluding, we should like to express our gratitude to Professor E. B. Wilson, Jr., who suggested this project and has constantly contributed to its progress.*

[11] J. B. Howard, J. Chem. Phys. **5**, 442 (1937).
[12] E. B. Wilson, Jr., J. Chem. Phys. **6**, 408 (1938).

* *Note added in proof:* Since this paper was submitted, two papers of the same series as that of Bartholomé and Karweil[3] have been received, one by Goubeau and Karweil (Zeits. f. physik. Chemie **B40**, 376 (1938)) on the Raman effect, and one by Karweil and Schäfer (ibid., **B40**, 382) on the assignment.

The Raman work of Goubeau and Karweil shows four shifts differing significantly from previous work—786, 1335, 1491, and 2791 cm^{-1}. The values 786 and 2791 cm^{-1} deviate from the measurements of Glockler and Renfrew further than one would expect. The evidence that the 1335 cm^{-1} line arises from ethane seems insufficient. The 1491 cm^{-1} line may well be the second degenerate fundamental of this magnitude (see Table I).

The analysis now given by Karweil and Schäfer, which differs from the former analysis of Bartholomé and Karweil, is based on essentially the same set of fundamentals as ours. However, we feel that the available evidence is insufficient to exclude the D_{3d} equilibrium configuration, contrary to the conclusion of Karweil and Schäfer.

Infra-Red and Raman Spectra of Polyatomic Molecules. IV. Allene

J. W. LINNETT AND W. H. AVERY
Mallinckrodt Chemical Laboratory, Harvard University, Cambridge, Massachusetts

(Received August 22, 1938)

The infra-red absorption spectrum and the Raman spectrum of allene were examined. In the infra-red nine bands were observed at 4200, 2960, 2420, 1980, 1700, 1389, 1165, 1031 and 852 cm^{-1} and in the Raman effect there were ten individual shifts of 3062, 2992, 2858, 1956, 1684, 1430, 1069, 838, 705 and 353 cm^{-1}. With the aid of heat capacity data it was possible to assign values to the frequencies of all the eleven fundamental modes of vibration of allene. The assignment accounted for all the features of the Raman and infra-red spectra. Calculations were made of the free energy, the entropy and the heat capacity and expressions for the first two, as functions of temperature, derived.

BECAUSE of the simple atomic arrangement in the allene molecule and of its close relation structurally to ethylene the determination of the vibration frequencies of this molecule is of some interest. The Raman spectrum of allene has been studied by Bourguel and Piaux[1] and by Kopper and Pongratz.[2] The frequencies found by the former authors were 1073, 1438, 3000 and 3072 and by the latter 1074, 1435, 2995 and 3060 cm^{-1}. Both describe the 1073 and 3000 cm^{-1} lines as intense and the other two as of medium intensity. The infra-red spectrum has been studied by Bonner and Hofstadter.* The results summarized by them seem to agree well with those described here particularly as regards the bands with frequencies below 3000 cm^{-1}.

RAMAN SPECTRUM

The Raman spectrum of allene was investigated using the apparatus which has been described in Part II.[3] The sample of allene used in these experiments was kindly supplied to us by Professor G. B. Kistiakowsky, it being a part of that which had been employed in the determination of the heat of hydrogenation.[4] The allene, in the liquid state, was contained in a cylindrical tube, the volume of which was *ca.* 50 cc, closed at one end by a plane Pyrex window. The allene was illuminated through the sides of the tube by four mercury vapor lamps. The light filter solutions were those previously described. The Raman tube was kept at temperatures from −40°C to −50°C by means of a current of air which had been cooled by passage through a copper spiral immersed in a mixture of alcohol and dry ice.

The results are summarized in Table I. In the first column are listed the frequencies (in vacuum) of the lines observed. The second column gives the suggested interpretation of these lines, the accompanying letter indicating the exciting mercury line. Measurements were made on four plates. The line at 24011 cm^{-1} was observed on one plate only and on this was so faint as to be measurable only with difficulty. Microphotometer records were made of each plate and all lines were identified on these in addition to being observed directly on the plates. A microphotometer record of one of the plates is shown in Fig. 1.

There appear, therefore, to be ten individual Raman frequencies. These are summarized in

TABLE I. *Observed frequencies* (cm^{-1} *in vacuum*) *with displacements from mercury lines: 22938* (*e*), *22995* (*f*), *23039* (*g*), *24516* (*i*) *and 24705* cm^{-1} (*k*).

ν IN cm^{-1}	$\Delta\nu$ IN cm^{-1}	ν IN cm^{-1}	$\Delta\nu$ IN cm^{-1}
(24011)	694 (*k*)	21868	1070 (*e*)
23865	840 (*k*)	21713	2992 (*k*)
23636	1069 (*k*)	21643	3062 (*k*)
23447	1069 (*i*)	21508	1430 (*e*)
23274	1431 (*k*)	21254	1684 (*e*)
22585	353 (*e*)	20982	1956 (*e*)
22233	705 (*e*)	20080	2858 (*e*)
22102	836 (*e*)	19946	2992 (*e*)
21970	1069 (*g*)	19876	3062 (*e*)
21927	1068 (*f*)		

[1] Bourguel and Piaux, Bull. Soc. Chim. **51**, 1041 (1932).
[2] Kopper and Pongratz, Wien Ber. **141 IIb**, 840 (1932).
* Bonner and Hofstadter, Phys. Rev. **52**, 249 (1937).
[3] Gershinowitz and Wilson, J. Chem. Phys. **6**, 247 (1938).
[4] Kistiakowsky, Ruhoff, Smith and Vaughan, J. Am. Chem. Soc. **58**, 146 (1936).

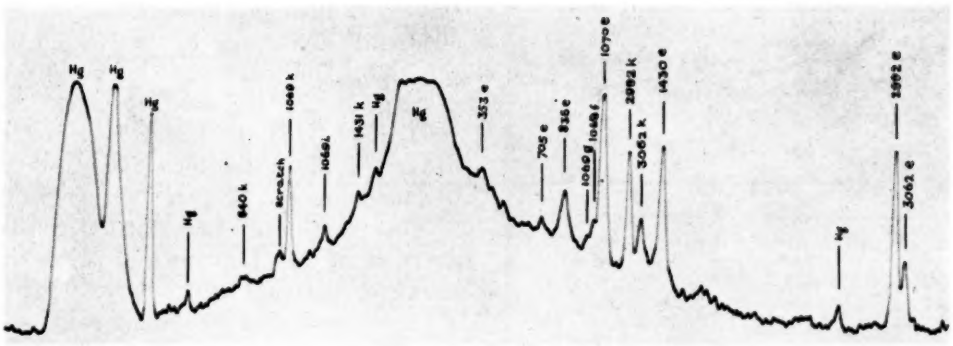

FIG. 1. A microphotometer record of the Raman spectrum of allene.

Table II together with the estimated relative intensities with which these appear.

THE INFRA-RED SPECTRUM

The apparatus used to measure the infra-red absorption of this compound was that described in Part I.[5] The gaseous allene was contained in cylindrical cells closed by windows of rocksalt or KBr, the material of the windows depending on the region of the spectrum that was under investigation. The cells were 20 cm long and pressures of allene ranging from 30 mm to 760 mm were used.

Figure 2 shows the transmission curve that was obtained experimentally. It will be seen that there are six relatively intense absorption bands, the centers of which were situated at the wavelengths: 3.38; 5.05; 5.88; 7.2; 9.7; and 11.73μ. The corresponding frequencies (in cm^{-1}) together with the relative intensities of the bands are 2960 (4); 1980 (10); 1700 (8); 1389 (12); 1031 (10) and 852 (30). In addition to these there were faint bands at 2.4 and 4.13μ, and the band at 9.7μ which appeared unsymmetrical at higher pressures showed a "shoulder" at lower pressures (see Fig. 2). The frequencies and intensities of the 2.4 and 4.13μ bands are 4200 (1) and 2420 cm^{-1} (2). It was difficult to estimate the position of the band which gave rise to the "shoulder" on the absorption curve of the 9.7μ band since the much greater intensity of the latter meant that under no conditions could a definite maximum of absorption be observed for the fainter nearby absorption band. Examination of the curves indicated that the maximum must be near 8.6μ. The frequencies and relative intensities of the infra-red bands are included in Table II with the Raman frequencies, the correspondence between the two sets being indicated.

TABLE II. *Observed frequencies in infra-red and Raman spectra together with the relative intensities.*

INFRA-RED	RAMAN
4200 (1)	
	3062 (10)
2960 (4)	2992 (20)
	2858 (2)
2420 (2)	
1980 (10)	1956 (1)
1700 (8)	1684 (2)
	1430 (12)
1389 (12)	
[1165 (1)]	
	1069 (20)
1031 (8)	
852 (30)	838 (5)
	705 (2)
	353 (4)

[5] Gershinowitz and Wilson, J. Chem. Phys. **6**, 197 (1938).

SYMMETRY PROPERTIES

The allene molecule belongs to the symmetry point group V_d. It has seven nondegenerate and four doubly degenerate fundamental modes of vibration. These are divided among the four symmetry classes given in the first column of Table III in the manner shown in the second column. The third and fourth columns indicate the selection rules for the vibrations of these classes for the Raman and infra-red spectra. The last three columns list the symmetry of the vibrations in the various classes with respect to

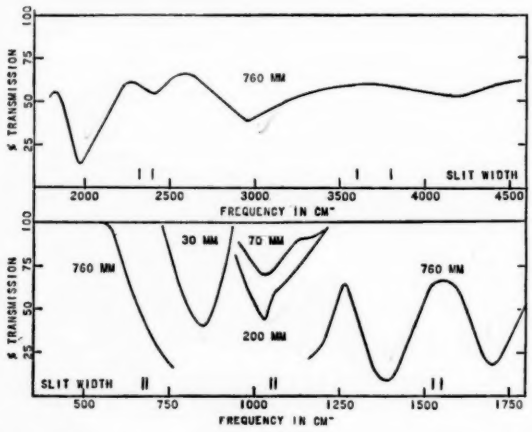

FIG. 2. Infra-red transmission of gaseous allene. Path length 20 cm.

the two planes, σ_1 and σ_2, and the alternating axis of symmetry S_4, S and A indicating symmetrical and anti-symmetrical, respectively. The symmetry of the degenerate vibrations cannot be given since the symmetry of the vibrations of the two complementary sets separately will depend on how the sets are chosen.

DISCUSSION OF THE OBSERVED FREQUENCIES

The observed vibration frequencies may be summarized from Table II as follows: 4200 (I.R.), 3062 (Ram. I.R. ?), 2992 (Ram. I.R. ?), 2859 (Ram.), 2420 (I.R.), 1968 (Ram. I.R.), 1692 (Ram. I.R.), 1430 (Ram.), 1389 (I.R.), 1165 (I.R.), 1069 (Ram.), 1031 (I.R.), 845 (Ram. I.R.), 705 (Ram.), 353 (Ram.). It is possible at once to make a partial assignment. It is often, though not always, found that the most symmetrical vibrations appear most intensely in the Raman effect. On these grounds we may assign to the three vibrations of class A_1 the values 2992, 1430 and 1069 cm^{-1}. In agreement with this selection these frequencies do not appear in the infra-red spectrum. The vibrations of the symmetry classes B_2 and E are active in both spectra. Each class will include one carbon-hydrogen valency vibration. That in B_2 may be expected to have a frequency similar to that of the carbon-hydrogen valency vibration in A_1 since both are symmetrical to the two symmetry planes of the molecule. It will therefore be *ca.* 3000 cm^{-1}. The carbon-hydrogen valency vibration in E then presumably has the frequency 3062 cm^{-1} giving rise to the Raman lines with this shift. The frequencies below 3000 cm^{-1} appearing in the infra-red spectrum are 1968, 1692, 1389, 1165, 1031 and 845 cm^{-1}. Of these 845 cm^{-1} is the most intense and must correspond to a fundamental. 1692 cm^{-1} is then probably the first overtone of this fundamental. Since the first overtone of a B_2 fundamental is inactive in the infra-red spectrum this indicates that 845 cm^{-1} is a fundamental of the symmetry class E. Of the remaining five bands that at 1165 cm^{-1} is quite faint and probably corresponds to an overtone or combination level. There are left, therefore, four infra-red bands with frequencies 1968, 1389, 1031 and 845 cm^{-1} for fundamentals in the classes B_2 and E. This still leaves one of the fundamentals in these two classes unaccounted for. There remains the 353 cm^{-1} Raman shift which may or may not appear also in the infra-red spectrum since our measurements could not be extended into this region. This might therefore be the seventh fundamental of the two classes B_2 and E or it might be the B_1 fundamental.

FREQUENCY CALCULATIONS

It has been pointed out by Thompson and Linnett[6] that if the values of the force constants found in ethylene are carried over for use in allene with a similar potential function the calculated frequencies agree remarkably well with those observed. For the totally symmetrical vibrations they calculated by this means the frequencies 3003, 1459 and 1069 cm^{-1}. This indicates that the values assumed above for the A_1 fundamentals were correct since the calculated frequencies differ by only 0.3, 2.0 and 0.0 percent, respectively, from the observed figures.

TABLE III.

Symmetry Class	Number of Fundamental Vibrations in Class	Permitted to Appear in		Symmetry with Respect to		
		Raman	Infra-Red	σ_1	σ_2	S_4
A_1	3	Yes	No	S	S	S
B_1	1	Yes	No	A	A	A
B_2	3	Yes	Yes	S	S	A
E	4	Yes	Yes	Degenerate		

[6] Thompson and Linnett, J. Chem. Soc. 1384 (1937).

Such agreement is as good as can be expected when the force constants employed for one molecule are transferred unaltered for use in another. The constants given by Thompson and Linnett[7] can be used also to calculate the frequencies of the B_2 fundamentals. The values obtained are 2998, 1415 and 2001 cm^{-1}. For these calculations the dimensions assumed for the allene molecule were: for the carbon-hydrogen bond length 1.08A, for the carbon-carbon bond length 1.33A and for the HCH angle 118°. These are the values suggested by Penney[8] for ethylene and are in agreement with the electron diffraction data of Wierl[9] who gave 1.31±0.05A and of Pauling and Brockway[10] who gave 1.34±0.02A. The above calculated frequencies indicate that the B_2 fundamentals below 3000 are in reality 1389 and 1968 cm^{-1}. The agreement in both cases is within 2 percent. It seems, therefore, that we may definitely make the assignments A_1: 2992, 1430, 1069; B_2: *ca.* 3000, 1968, 1389; E: 3062, 1031 and 845 cm^{-1}.

The Vibration Frequencies

From the above considerations, therefore, nine of the eleven frequencies have been determined and moreover, the magnitude of one of the remaining two is 353 cm^{-1}. Preliminary measurements on the heat capacity of gaseous allene have been made in this laboratory and we wish to thank Professor Kistiakowsky, Dr. Lacher and Mr. Rice for kindly giving us permission to make use of their results before publication. A study of the observed heat capacity between 150 and 330°K indicates that the 353 cm^{-1} frequency is to be assigned to the doubly degenerate class and that the B_1 fundamental has a frequency of about 820 cm^{-1}.* The knowledge of the heat capacity was invaluable in determining whether the low 353 cm^{-1} fundamental was doubly degenerate or not and after this in fixing the approximate value of the eleventh fundamental. The final assignment which accounts for all the features of the Raman and infra-red spectra and also for the heat capacity over a considerable temperature range is shown in Table IV. This table also summarizes the manner in which the fundamentals appear in the spectra. It will be seen that in no case is an infra-red active fundamental above 400 cm^{-1} not observed and in only two cases are Raman active fundamentals definitely absent. It seems likely that the 3000 cm^{-1} frequency in the class B_2 which should appear in the Raman spectrum is obscured by the intense line arising from the A_1 fundamental. The 838 cm^{-1} Raman line is probably caused by a superposition of lines from the 820 cm^{-1} B_1 vibration and the vibration in the degenerate class. For this reason the value for the degenerate frequency has been revised to 852 cm^{-1} which is the position of the infra-red band.

Table IV.

Symmetry Class	Frequency	Raman Effect	Infra-Red Spectrum
A_1	2992	2992	forbidden
	1430	1430	forbidden
	1069	1069	forbidden
B_1	820	(838)	forbidden
B_2	*ca.* 3000	(2993)	broad band over this region
	1968	1956	1980
	1389	not observed	1389
E	3062	3062	broad band over this region
	1031	not observed	1031
	852	(838)	852
	353	353	unobservable

Table V.

Observed Frequency	Spectrum	Suggested Combination	Symmetry of Level
705	Raman	2×353=706	A_1+E
1165	I.R.	353+820=1173	E
1684	Raman	2×852=1704	A_1+E
1700	I.R.		
2420	I.R.	1389+1031=2420	E
2858	Raman	2×1430=2860	A_1
4200	I.R.	3062+1069=4131	E
		3062+820+353=4235	$A_1+A_2+B_1+B_2$
		3062+852+353=4267	$4E$
		2992+852+353=4197	$A_1+A_2+B_1+B_2$
		3000+852+353=4205	$A_1+A_2+B_1+B_2$
		3×1389=4167	B_2
		1389+2×1430=4249	B_2

[7] Thompson and Linnett, J. Chem. Soc. 1376 (1937).
[8] Penney, Proc. Roy. Soc. **158A**, 306 (1937).
[9] Wierl, Ann. d. Physik **13**, 453 (1932).
[10] Pauling and Brockway, J. Am. Chem. Soc. **59**, 1223 (1937).

* The relation of this to the spectroscopic data will be discussed later.

Overtone and Combination Levels

The interpretation of the observed overtones in terms of the fundamental vibration frequencies listed in Table IV is summarized in Table V. The first column gives the observed frequency, the second where it is observed, the third the suggested combination together with the calculated frequency and the last the symmetry class to which the overtone or combination belongs. It will be observed that in the last column a fifth symmetry class A_2 is mentioned. This was not included in Table III since there are no fundamental vibrations of the allene molecule which fall into this class. Overtone levels in A_2 would appear in the Raman effect but not in the infra-red spectrum. It will be observed in Table V that the value of 820 cm^{-1} for the B_1 fundamental is required to account for the faint infra-red band of frequency 1165 cm^{-1}. Without this the best means of accounting for this band would be 353 $+852=1205$ cm^{-1} which is highly unsatisfactory. This therefore provides evidence for the value of 820 cm^{-1} in addition to that derived from the heat capacity. Further spectroscopic evidence is obtained from the fact that the infra-red frequency at 852 cm^{-1} does not correspond sufficiently closely with the Raman frequency at 838 cm^{-1}, this also being accounted for by the B_1 fundamental at 820 cm^{-1}.

All the levels below 3000 cm^{-1} are accounted for as fundamentals or as binary combinations. Only for the faint infra-red band at 4200 cm^{-1} are ternary combinations postulated and then it would appear that absorption is observed because there are so many superimposed bands. It is interesting that in ethylene the Raman frequency at 2880 cm^{-1} is ascribed to the first overtone of the fundamental frequency 1444 cm^{-1} in just the same manner that the 2858 cm^{-1} Raman shift in this instance is ascribed to the first overtone of the 1430 cm^{-1} fundamental.

The Twisting Frequency

The vibration in the class B_1 which is antisymmetrical to the two symmetry planes may best be described as a twisting vibration. The magnitude of the frequency of this vibration is of particular interest since the analogous vibration in ethylene is completely inactive and its frequency can only be obtained by indirect means. *A priori* it might be expected that the twisting frequency in ethylene would be higher than in allene since the two methylene groups are joined by one double bond in the former and by two through a central carbon atom in the latter. Since the distortion has two double bonds in which to dissipate itself in allene compared with one in ethylene it might be expected that the force constant for allene would be about half as great as that for ethylene. This means that the ratio of the frequencies would be $1:\sqrt{2}$ and on the basis of a value of 820 cm^{-1} for allene that the ethylene twisting frequency would be about 1150 cm^{-1}. This frequency has been given various values by different investigators. Bonner[11] gave 830 cm^{-1}; Eucken and Parts,[12] 747; and Teller and Topley,[13] 1110. The evidence here is extremely indirect but at least it indicates that such twisting frequencies may not be as low as has been supposed.

Calculation of Thermodynamic Quantities

Since all the fundamental frequencies of the allene molecule have been determined it is possible to calculate the free energy, entropy and heat capacity for the substance in the gaseous state. To compute the translational and rotational components of the free energy F and entropy S it is necessary to know the moments of inertia of the molecule. These have been calculated assuming that the molecular dimensions are as listed earlier in this paper. In Table VI the results of the calculation of the thermodynamic quantities are summarized. In the second and third columns are given the translational and rotational components of $-(F-E_0^0)/T$ and S at the temperatures, T, listed in the first column. The fourth and fifth columns give the vibrational parts of $-(F-E_0^0)/T$ and S and the sixth and seventh the total values. The last column gives the value of the heat capacity, C_p^0. The necessary constants were obtained from the *International Critical Tables* and the assumption made that the vibrations were harmonic.

---

[11] Bonner, J. Am. Chem. Soc. **58**, 34 (1936).
[12] Eucken and Parts, Zeits. f. physik. Chemie **B20**, 184 (1933).
[13] Teller and Topley, J. Chem. Soc. 885 (1935).

TABLE VI.*

T °K	TRANSLATIONAL AND ROTATIONAL $-\frac{(F-E_0^0)}{T}$	TRANSLATIONAL AND ROTATIONAL S	VIBRATIONAL $-\frac{(F-E_0^0)}{T}$	VIBRATIONAL S	TOTAL $-\frac{(F-E_0^0)}{T}$	TOTAL S	C_p^0
100	36.27	44.22	0.03	0.16	36.30	44.38	8.61
150	39.49	47.44	0.14	0.64	39.63	48.08	9.77
200	41.78	49.73	0.35	1.34	42.13	51.07	11.08
250	43.55	51.50	0.63	2.20	44.18	53.70	12.55
300	45.00	52.95	0.97	3.18	45.97	56.13	14.16
350	46.23	54.17	1.36	4.25	47.59	58.42	15.73
400	47.29	55.23	1.80	5.39	49.09	60.62	17.22
500	49.06	57.01	2.75	7.75	51.81	64.76	19.84
600	50.51	58.46	3.78	10.11	54.29	68.57	22.02
700	51.73	59.68	4.85	12.43	56.58	72.11	23.86
800	52.80	60.74	5.94	14.66	58.74	75.40	25.44
900	53.73	61.68	7.02	16.81	60.75	78.49	26.48
1000	54.57	62.52	8.10	18.85	62.67	81.37	28.02

* The units used in this table are calories per mole and degrees Absolute.

Murphy[14] has given analytical expressions for describing the free energy, entropy and heat capacity as functions of the temperature. He considered however only very simple molecules in which the contribution from the vibrational degrees of freedom was not as great as in the present case. It was found possible to extend Murphy's equation for $-(F-E_0^0)/T$ and S by introducing an extra term so that a good fit for the values listed in Table VI could be obtained. The expression derived for C_p^0 from this was not satisfactory. This presumably arose from two causes. Firstly because C_p^0 is related to S as a temperature derivative and hence errors in the expression for S are multiplied on passing to C_p^0 and secondly because the vibrational component of C_p^0 forms a much larger part of the whole than does the vibrational component of S. The equations for the translational and rotational parts of $-(F-E_0^0)/T$ and S are:

$$-(F-E_0^0)/T=18.300\log T-0.332$$

and

$$S=18.300\log T+7.616$$

and for the vibrational parts:

$$-\frac{(F-E_0^0)}{T}=44.920-\frac{9.936\times10^2\log T}{T}-18.608\log T+2.482\times10^{-2}T-0.379\times10^{-5}T^2+\frac{9.749\times10^2}{T},$$

$$S=36.838-18.608\log T+4.964\times10^{-2}T-1.138\times10^{-5}T^2-\frac{4.315\times10^2}{T}.$$

The equations for the total values of $-F/T$ and S are then:

$$-\frac{(F-E_0^0)}{T}=44.588-\frac{9.936\times10^2\log T}{T}-0.308\log T+2.482\times10^{-2}T-0.379\times10^{-5}T^2+\frac{9.749\times10^2}{T},$$

$$S=44.454-0.308\log T+4.964\times10^{-2}T-1.138\times10^{-5}T^2-\frac{4.315\times10^2}{T}.$$

The equations for the vibrational components of $-(F-E_0^0)/T$ and S give values within 0.02 and 0.04 units, respectively, over the range from 100° to 1000°K. The two analytical expressions for the full values of $-(F-E_0^0)/T$ and S give figures within 0.1 percent of those in Table VI.*

We wish to thank Professor E. Bright Wilson, Jr. for his encouragement and assistance during the course of this research.

[14] Murphy, J. Chem. Phys. **5**, 637 (1938).

* There are several effects which will lead to uncertainty in the calculated values of the thermodynamic quantities. The most important of these are: (a) uncertainties in the knowledge of the absolute frequencies arising both from errors in measurement and also because the Raman spectra was observed with the liquid, and (b) neglect of the anharmonicities of the various vibrations.

Infra-Red and Raman Spectra of Polyatomic Molecules. V. Cyclopropane and Ethylene Oxide

J. W. LINNETT
Mallinckrodt Chemical Laboratory, Harvard University, Cambridge, Massachusetts

(Received August 22, 1938)

The Raman and infra-red spectra of cyclopropane and ethylene oxide have been examined. The infra-red spectra were examined using a potassium bromide prism from 25 to 11μ, a rock-salt prism from 15 to 7μ and a fluorite prism from 8 to 1.5μ. Because of the greater dispersion of fluorite more bands than had previously been observed were resolved in the region in which this prism could be used. The nature, symmetry and selection rules of the vibrations of these two molecules are summarized. It was found possible to make a complete assignment of the fundamental frequencies of cyclopropane which accounts for all the features of the spectra. With ethylene oxide it was only possible to make a partial assignment. The frequencies of the corresponding fundamental modes of vibration of the two molecules are compared. On the basis of the frequency assignment described, values for the free energy, entropy and heat capacity of cyclopropane are calculated between 100° and 1000°K.

A COMPLETE knowledge of the vibration frequencies of cyclopropane and of ethylene oxide would be of considerable interest in relation to the theory of molecular vibrations. This necessitates a knowledge of the Raman and infra-red spectra and of the heat capacity at various temperatures. In this paper are described some measurements on the spectra and the results are discussed.

The Raman spectrum of cyclopropane has been examined by a number of workers,[1] the most complete investigations being those of Ananthakrishnan[2] and of Harris, Ashdown and Armstrong.[3] In the infra-red Bonner[4] examined the region 15−1.5μ using a rocksalt prism spectrograph and King, Armstrong and Harris[5] the region 10−0.8μ using both a rocksalt prism spectrograph and a quartz monochromator. Measurements on the Raman spectrum of ethylene oxide have been made by Lespiau and Bourguel,[6] by Timm and Mecke[7] and by Ananthakrishnan.[2] The infra-red spectrum has been studied by Bonner[4] from 15 to 1.5μ.

In this investigation photographs of the Raman spectra of both cyclopropane and ethylene oxide were taken. More particularly, however, the infra-red spectra of both compounds were studied in the region 25−1.5μ. For this a potassium bromide prism was used from 25 to 11μ, a rock-salt prism from 15 to 7μ and a fluorite prism from 8 to 1.5μ. The potassium bromide prism enabled the spectra beyond 15μ to be studied. Fluorite gives better dispersion than rocksalt for wavelengths shorter than 8μ and is particularly valuable therefore for studying the fundamentals and combination levels from 1200 to 3000 cm^{-1}. Above 3000 cm^{-1} a quartz prism is to be preferred.

CYCLOPROPANE

Experimental results

The Raman spectrum of liquid cyclopropane at −40°C was examined using the apparatus described by Gershinowitz and Wilson.[8] The spectrum was excited by the 4047A and 4358A mercury lines. The results confirm entirely those of Ananthakrishnan who used the same means of excitation. No evidence was found for the 382 cm^{-1} frequency observed by Harris, Ashdown and Armstrong using the 2537A mercury line, but this may arise because they employed more intense excitation.

The infra-red spectrum was studied using the apparatus described by Gershinowitz and Wilson[9]

[1] Lespiau, Bourguel and Wakeman, Bull. Soc. Chim. **4**, 51, 400 (1932). Kohlrausch and Köppl, Zeits. f. physik. Chemie **B26**, 209 (1934).
[2] Ananthakrishnan, Proc. Ind. Acad. Sci. **4**, 82 (1936).
[3] Harris, Ashdown and Armstrong, J. Am. Chem. Soc. **58**, 852 (1936).
[4] Bonner, J. Chem. Phys. **5**, 704 (1937).
[5] King, Armstrong and Harris, J. Am. Chem. Soc. **58**, 1580 (1936).
[6] Lespiau and Bourguel, Bull. Soc. Chim. **47**, 1365 (1930).
[7] Timm and Mecke, Zeits. f. Physik **97**, 221 (1935).
[8] Gershinowitz and Wilson, J. Chem. Phys. **6**, 247 (1938).
[9] Gershinowitz and Wilson, J. Chem. Phys. **6**, 197 (1938).

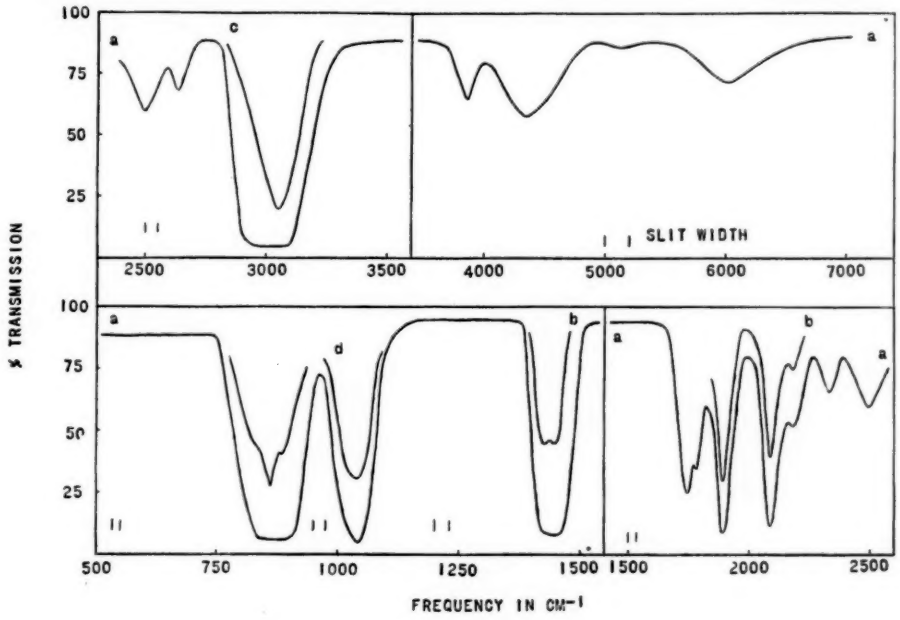

FIG. 1. Infra-red transmission of cyclopropane gas. Path length, 30 cm; pressures, (a) 750 mm, (b) 270 mm, (c) 120 mm, (d) 50 mm, (e) 30 mm.

only with the addition of a fluorite prism. The apparatus was calibrated by observing known bands of ethylene, benzene, acetylene and carbon dioxide. The gaseous cyclopropane was contained in cylindrical cells 20–30 cm in length and closed by windows of potassium bromide and rocksalt. Gas pressures from 30–750 mm were used.

Figure 1 shows the transmission curve that was obtained experimentally. The positions of the bands together with the estimated intensities are summarized in Table I. This table also summarizes the available Raman data. As regards the individual bands, that at 860 cm^{-1} appears to be unsymmetrical when plotted on a frequency scale and shows apparently a Q branch. The 10μ band showed maximum absorption at 1041 cm^{-1}. Bonner gave the center as 1020 cm^{-1}. The band seems to be somewhat unsymmetrical, the transmission curve rising more rapidly on the high frequency side. The fluorite prism resolved the band at 1435 cm^{-1} into two branches, the doublet separation being 20 cm^{-1}. The band at 1739 cm^{-1} was found to have a shoulder on the high frequency side, the position of this being 1779 cm^{-1}. Fairly intense bands were observed at 1890 and 2083 cm^{-1} in agreement with Bonner. In the region from here up to 3000 cm^{-1}, whereas Bonner observed only one band the fluorite prism was able to resolve four. The band at 3.3μ appeared at 3049 cm^{-1} compared with Bonner's value of 3086 cm^{-1}. The band at 3580 cm^{-1} described by King, Ashdown and Armstrong was not observed, but a band was found at 3846 cm^{-1}. The band observed at 4348 cm^{-1} (Bonner gives 4425 cm^{-1}) was separated by King, Ashdown and Armstrong into two bands at 4200 and 4450 cm^{-1} presumably because a quartz prism was used by them in this region. A very weak band was observed at 5128 cm^{-1} and faint broad band at about 6020 cm^{-1}. Despite repeated investigation no band could be found at 15μ where faint absorption was observed by Bonner. Except for the absence of the 15μ band and the resolution of more faint bands because of higher dispersion, the results described here agree closely with those of Bonner.

Symmetry properties

The cyclopropane molecule provides an example of the group D_{3h}. In Table II are summarized the number of vibrations in the various classes together with their symmetry and selection rules. In the first column are listed the symmetry classes forming the group D_{3h} and in the

second the number of vibrations of the cyclopropane molecule which belong to these various classes. Vibrations in the classes designated by the letter A are nondegenerate while those in the E classes are doubly-degenerate. In the third and fourth columns the selection rules for the Raman and infra-red spectra are given while the last two columns give the symmetry of the vibrations with respect to σ_h, the plane of the C_3 ring and $3\sigma_v$, the three symmetry planes perpendicular to σ_h. It will be seen from Table II that there are two completely inactive fundamental vibration frequencies, four frequencies that should be active in both the Raman and infra-red spectra, two that should be active in the infra-red only and six in the Raman only. Of these last six the three in A_1' should lead to polarized Raman lines.

Form of vibrations

There will be four distinct molecular vibrations which involve mainly changes in the carbon hydrogen bonds. These will belong to the classes A_1', E', A_2'' and E'' and will have frequencies in the neighborhood of 3000 cm^{-1}. Also there will be two vibrations which involve mainly distortions of the C_3 ring. One of these will be in the A_1' class and the other in E'. The other eight fundamental frequencies will depend on motions of the methylene groups. These may be divided into four types: (a) deformation of the methylene groups symmetrical to σ_h and σ_v involving a change in the HCH angle; (b) bending of the methylene group against the ring with the HCH angle remaining the same, this also being symmetrical to σ_h but antisymmetrical to σ_v; (c) rocking of the methylene groups, the HCH angle remaining constant and the motion being antisymmetrical to the σ_h plane but symmetrical to the σ_v plane; (d) twisting of the methylene groups, the motion being antisymmetrical to both σ_h and σ_v. The nature of these elementary motions is shown diagrammatically in Fig. 2. All actual motions of the methylene groups can be explained as combinations of these four elementary motions. The two methylene deformations will be in the classes A_1' and E', the bending motions in A_2' and E', the rocking motions in A_2'' and E'' and the twisting motions in A_1'' and E''. Any actual motions of the cyclopropane molecule will, of course, not be simple. For example one of the individual vibrations in E' will involve a combination of a methylene deformation, a methylene bending and ring deformation. However, though not rigidly applicable, this simplification may assist in fixing the order of magnitude of various frequencies and will also be of help in comparing the results for cyclopropane and ethylene oxide. In Table III are

TABLE I. *The observed wave-lengths and frequencies of the infra-red bands of cyclopropane and the Raman frequencies.*

Infra-red Spectrum			Raman Frequencies
Description	Wave-length (μ)	Frequency (cm^{-1})	
			382
			740
very strong P branch*	12.10	826	
very strong Q branch	11.63	860	863
very strong R branch	11.29	886	
strong	9.61	1041	1022
			1187 (P)†
medium P branch	7.02	1425	
medium strong Center	6.97	1435	1434
medium strong R branch	6.92	1445	
			1454
			1503 (P)
medium	5.75	1739	
weak	5.62	1779	
strong	5.29	1890	1873
medium strong	4.80	2083	
weak	4.59	2179	
weak	4.29	2331	
medium weak	4.01	2494	
weak	3.80	2632	
			2852 (P)
			2952 (P)
			3010 (P)
			3028 (P)
very strong	3.28	3049	3080
weak	2.60	3846	
medium weak	2.30	4348	
very weak	1.95	5130	
weak	1.66	6020	

* The notation P, Q, R is used for convenience and is not intended to indicate that the band is a parallel one.
† (P) indicates that the line is polarized.

TABLE II. *The symmetry and selection rules for the vibrations of the cyclopropane molecule.*

Symmetry Class	No. of Fundamental Vibrations in Class	Permitted to Appear in		Symmetry with Respect to	
		Raman	Infra-red	σ_h	$3\sigma_v$
A_1'	3	Yes	No	S	S
A_2'	1	No	No	S	A
E'	4	Yes	Yes	S	degenerate
A_1''	1	No	No	A	A
A_2''	2	No	Yes	A	S
E''	3	Yes	No	A	degenerate

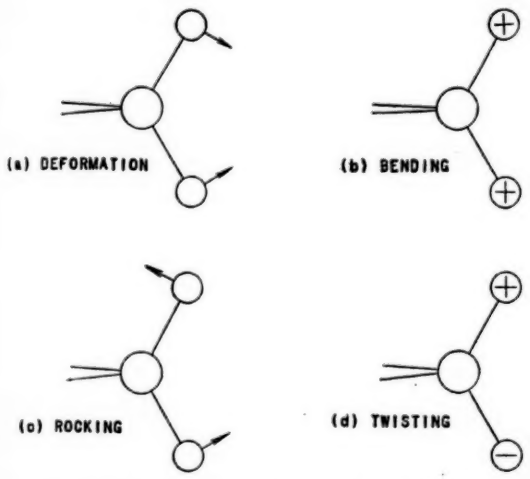

FIG. 2. Diagrammatic representation of the four elementary motions of the methylene group in cyclopropane, (a) Deformation, (b) bending, (c) rocking, (d) twisting.

given the types of distortions that will occur in the vibrations of the various classes.

The vibration frequencies

Ananthakrishnan observed in the Raman effect polarized lines at 1503 and 1187 in addition to those in the neighborhood of 3000 cm^{-1}. For the A_1' frequencies we should expect therefore, *ca.* 3000, 1503 and 1187 cm^{-1}. The 3000 cm^{-1} frequency corresponds, of course, to the carbon-hydrogen valency vibration and, by analogy with other molecules, the 1503 cm^{-1} frequency may be supposed to result from a vibration involving largely methylene deformation. 1187 cm^{-1} is then the ring frequency as has been postulated by Bonner.[10] The E' vibrations are active in both spectra. The carbon-hydrogen valency vibration frequency must be *ca.* 3000 and the methylene deformation frequency 1435 cm^{-1}. The latter appears in the Raman effect at 1434 cm^{-1} and in the infra-red at 1435 cm^{-1}. As has been suggested by Bonner, the ring frequency in this class must be 860 cm^{-1} (Raman effect 863, Infra-red 860). For the fourth frequency in this class 1022 cm^{-1} seems to be the most likely value since Harris, Ashdown and Armstrong observed a Raman shift of 1022 cm^{-1} and there is an infra-red band at 1041 cm^{-1}. This will be discussed in more detail later. For the remaining frequency symmetrical to σ_h there is the methylene bending vibration in A_2'. This is totally inactive but since the methylene bending frequency in E' has the value 1022 we should expect this to be at least of approximately the same order of magnitude.

As regards the vibrations antisymmetric to σ_h we may consider first those in A_2'' which are infra-red active. One of these will be in the neighborhood of 3050 cm^{-1}. For the other there are only two infra-red bands below 1400 cm^{-1}, *viz.*, 860 and 1041. It seems likely that by comparison with the frequencies of similar motions in ethylene and formaldehyde the methylene rocking frequency is not as low as 860 cm^{-1}. If the frequency is 1041 cm^{-1}, the 10μ band would appear to be really two superimposed bands. This is in agreement with the appearance of this band. The appearance is, moreover, quite in keeping with the existence of a band at 1041 cm^{-1} with a

TABLE III. *Distortions occurring in the vibrations of the various symmetry classes for cyclopropane.*

A_1'	A_2'	E'
CH valency CH_2 deformation ring deformation	CH_2 bending	CH valency CH_2 deformation CH_2 bending ring deformation
A_1''	A_2''	E''
CH_2 twisting	CH valency CH_2 rocking	CH valency CH_2 rocking CH_2 twisting

[10] Bonner, J. Chem. Phys. **5**, 293 (1937).

TABLE IV. *The magnitudes of the fundamental frequencies of cyclopropane with the corresponding Raman and infra-red frequencies.*

SYMMETRY CLASS	SUGGESTED FUNDAMENTAL FREQUENCIES	RAMAN FREQUENCIES	INFRA-RED FREQUENCIES
A_1'	3000 1485 1187	2952, 3010, 3028 1503, 1454 1187	forbidden forbidden forbidden
A_2'	1070	forbidden	forbidden
E'	3000 1435 1022 860	(3008) 1434 1022 863	(3049) 1435 (1041) 860
A_1''	1000	forbidden	forbidden
A_2''	3050 1041	forbidden forbidden	3050 1041
E''	3080 1250 740	3080 not observed 740	forbidden forbidden forbidden

less intense band at 1022 cm^{-1}. Another possibility is that this fundamental does not appear in the infra-red spectrum although it is allowed. Data on other molecules however seem to indicate that fundamentals allowed in the infra-red usually appear. The fundamentals in E'' should appear depolarized in the Raman effect. This indicates for the carbon-hydrogen valency vibrations 3080 cm^{-1} and for the methylene twisting vibration 740 cm^{-1}. The third fundamental in E'', the methylene rocking vibration, apparently does not appear. The remaining fundamental, which is in A_1'', is completely inactive.

By the above considerations, therefore, the values of eleven of the fourteen fundamental frequencies have been fixed. The others must be determined by a consideration of the overtone and combination levels. At this stage it may be mentioned that it seems probable that resonance would occur between the first overtone of 740 cm^{-1} and the methylene deformation fundamental in A_1'. This would indicate that this fundamental has the unperturbed frequency of *ca.* 1485 cm^{-1} rather than 1503 cm^{-1}, resonance giving rise to two neighboring levels leading to the Raman frequencies at 1503 and 1454 cm^{-1}. On this basis the Raman lines with $\Delta\nu = 1454$ cm^{-1} should be polarized as are those with $\Delta\nu = 1503$ cm^{-1}. The closeness of the 1434 cm^{-1} Raman line has prevented the determination of this. The fundamentals still to be determined are the two in A_2' and A_1'', and one of the E'' vibrations.

In Table IV is given an assignment of all the fundamentals together with the manner of their appearance in the spectra which seems to explain most satisfactorily all the observed overtones. In cases where the fundamental is the member of a resonance doublet or triplet the frequencies of all the components have been listed. Also where the fundamental may be obscured by another the value of the latter has been included in brackets. It will be seen that only one Raman line is definitely absent and there are no infra-red bands certainly missing.

TABLE V. *Suggested interpretation of overtone and combination levels of cyclopropane.*

Observed Frequency	Observed in:	Suggested Combination	Symmetry Class
382	Raman	1250 − 865 = 385	$[A_1''+A_2''+E'']$
1454 / 1503	Raman	2 × 740 = 1480 / 1485	$A_1'+E'$ / A_1'
1739	Infra-red	1000 + 740 = 1740	E'
1779	Infra-red	1041 + 740 = 1781	E'
1890 / 1873	Infra-red / Raman	1020 + 865 = 1885	$A_1'+A_2'+E'$
2083	Infra-red	1020 + 1070 = 2090	E'
2179	Infra-red	1435 + 740 = 2175	$A_1''+A_2''+E''$
2331	Infra-red	1485 + 865 = 2350	E'
2494	Infra-red	1485 + 1020 = 2505	E'
		1435 + 1070 = 2505	E'
2632	Infra-red	1435 + 1187 = 2622	E'
2856	Raman	2 × 1435 = 2870	A_1'
2952		4 × 740 = 2960	A_1'
3010	Raman	2 × 1485 = 2970	A_1'
3028		3000	A_1'
3846	Infra-red	3000 (A_1') + 865 = 3865	E'
		3000 (E') + 865 = 3865	$A_1'+E'$
4200*	Infra-red	3000 (E') + 1187 = 4187	E'
		3050 + 1187 = 4137	A_2''
		3000 (E') + 1250 = 4250	$A_1''+A_2''+E''$
4450*	Infra-red	3000 (A_1') + 1435 = 4435	E'
		3000 (E') + 1435 = 4435	$A_1'+A_2'+E'$
		3000 (E') + 1485 = 4485	E'
		3000 (A_1') + 2 × 740 = 4480	$A_1'+E'$
		3000 (E') + 2 × 740 = 4480	$A_1'+A_2'+2E'$
5128	Infra-red	3000 (E') + 2 × 1070 = 5140	E'
		3080 + 2 × 1022 = 5124	$A_1''+A_2''+2E''$
		3050 + 1041 + 1022 = 5113	E'
		3000 + 1250 + 860 = 5110	$A_1''+A_2''+E''$
6020	Infra-red	First overtones of E' and E'' 3000 fundamentals. Also combinations	

* Observed by King, Armstrong and Harris.[5]

Overtone and combination levels

Table V summarizes the suggested interpretation of the observed overtone levels. The first and second columns give the observed frequency and the spectrum in which it is detected. The third column gives the suggested combination together with the calculated frequency and the last the symmetry class to which the level belongs. In the large majority of cases only binary combinations of fundamental frequencies have been used in interpreting the observed levels and for the exceptions there are circumstances which render such postulates acceptable. In the first case one component of the resonance triplet 2952, 3010, 3028 cm^{-1} has been ascribed to 4 × 740, that is, the third overtone. The prominence of the overtone presumably is to be explained because of resonance with the first overtone of 1485 cm^{-1} and the A_1' fundamental, just as the first overtone appears because of resonance with the A_1' fundamental at 1485 cm^{-1}. In the second case certain overtones above 4000 cm^{-1} have been ascribed to ternary combinations but only when a number of such overtones are coincident. This superposition may lead to a piling up of absorption and hence the appearance of an otherwise rather improbable band.

The above assignment therefore accounts in a

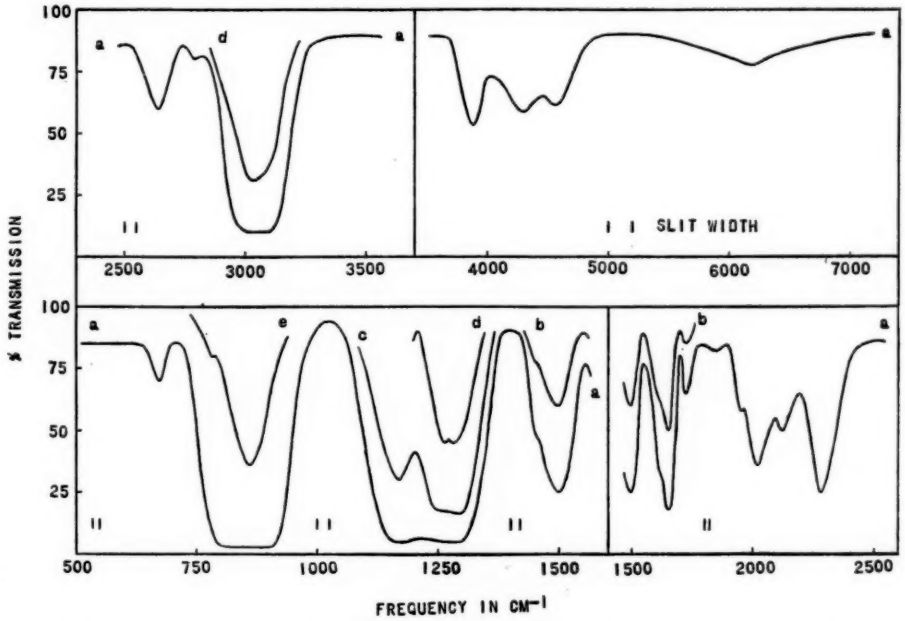

FIG. 3. Infra-red transmission of ethylene oxide gas. Path length 30 cm; pressures, (a) 750 mm, (b) 270 mm, (c) 220 mm, (d) 40 mm, (e) 10 mm.

completely satisfactory manner for the observed spectroscopic evidence. Moreover, added support is given for this assignment since heat capacities calculated from the above frequencies are in agreement with experimental values over the temperature range from 0°–70°. These have been determined in this laboratory and I wish to thank Professor Kistiakowsky for allowing me to use these results prior to their publication.

ETHYLENE OXIDE

Experimental results

The Raman spectrum of liquid ethylene oxide has been examined with results that are in agreement with those of Ananthakrishnan. The results for the infra-red spectrum agree in general with those obtained by Bonner. There are, however, minor differences some of which can be ascribed to the varying dispersion of the different prisms employed.

Figure 3 shows the transmission curve that was obtained experimentally. The positions and intensities of the bands are summarized in Table VI together with Ananthakrishnan's figures for the Raman frequency shifts. The band at 11.6μ, very intense as in cyclopropane, overlaps a

TABLE VI. *The observed wave-lengths and frequencies of the infra-red bands of ethylene oxide and the Raman frequencies.*

INFRA-RED SPECTRUM			RAMAN FREQUENCIES
DESCRIPTION	WAVE-LENGTH (μ)	FREQUENCY (cm^{-1})	
weak	14.86	673	
weak	12.33	811	807
very strong	11.54	867	869
			1122 (*P*)
strong	8.56	1168	1159
strong (*P* branch)	7.91	1264	
strong (Center)	7.87	1271	1270 (*P*)
strong (*R* branch)	7.81	1280	
weak	6.88	1453	
medium	6.68	1497	1492 (*P*?)
weak	6.19	1616	
medium	6.06	1650	
weak	5.81	1721	
very weak	5.42	1845	
weak	5.13	1949	
medium	4.95	2020	
weak	4.72	2119	
medium	4.39	2278	
medium weak	3.79	2639	
weak	3.59	2786	
			2917 (*P*)
			2952 (*P*)
			3028 (*P*)
very strong	3.30	3030	3080
medium weak	2.58	3876	
medium weak	2.33	4292	
weak	2.18	4587	
weak	1.62	6173	

(*P*) indicates that the line is polarized.

TABLE VII. *The symmetry and selection rules for the vibrations of the ethylene oxide molecule.*

Symmetry Class	Number of Fundamental Vibrations in Class	Permitted to Appear in		Symmetry with Respect to	
		Raman	Infra-red	σ_h	σ_v
A_1	5	Yes	Yes	S	S
B_1	4	Yes	Yes	S	A
B_2	3	Yes	Yes	A	S
A_2	3	Yes	No	A	A

fainter band, the position of which, as of all partially obscured bands, is difficult to determine. However, it seems to be at about 811 cm^{-1}. In the potassium bromide region only one faint band was observed, this being at 673 cm^{-1}. Bonner describes a faint band at 696 cm^{-1}. The discrepancy between the two figures is surprising. Bonner, using a rocksalt prism, was working towards the very limit available with this substance and this might lead to some inaccuracy in the determination of the position of the band. Towards higher frequencies a band was observed at 1168 cm^{-1}. Bonner gives 1134 cm^{-1} for the position of this band. The intense band at 7.9μ was observed both with the rocksalt and fluorite prisms. The measured values for the position of the center were 1275 and 1271 cm^{-1}, respectively, with the two prisms. This agreement is quite satisfactory. As the fluorite prism has the greater dispersion, the value of 1271 cm^{-1} is taken to be the better one. Bonner gave 1255 cm^{-1} but the existence of a Raman shift of 1270 cm^{-1} lends support to the value of 1271 cm^{-1}. Over the region from 1400 to 3100 cm^{-1} Bonner's observations agree as regards the main features with those described here, but whereas he observed only seven bands, this examination revealed thirteen as may be seen by reference to Fig. 3 and Table VI. Beyond 3100 cm^{-1} bands were observed at 3876, 4292, 4587 and 6173 cm^{-1}. Bonner observed three bands at 3891, 4310 and 6211 cm^{-1}, in satisfactory agreement.

Symmetry properties

The ethylene oxide molecule provides an example of the group C_{2v}. In Table VII are summarized the number of vibrations in the various symmetry classes together with their symmetry and selection rules. This is similar to Table II for cyclopropane. In the last two columns of the table the symmetries with respect to σ_h, the plane of the ring, and with respect to σ_v, the symmetry plane perpendicular to the ring, are listed. It will be seen from the above table that all the fifteen fundamental frequencies may appear in the Raman effect and all but three in the infra-red. This renders an assignment of the observed frequencies to individual vibrations more difficult than in cyclopropane, where the selection rules were of real assistance. The five vibrations in A_1 lead to polarized Raman lines.

TABLE VIII. *Distortions occurring in the vibrations of the various symmetry classes for ethylene oxide.*

A_1	B_1	B_2	A_2
CH valency CH_2 deformation CH_2 bending ring deformation ring deformation	CH valency CH_2 deformation CH_2 bending ring deformation	CH valency CH_2 rocking CH_2 twisting	CH valency CH_2 rocking CH_2 twisting

Form of vibrations

It is possible to make a table similar to Table III for cyclopropane in which the molecular distortions occurring in the vibrations of the different symmetry classes are summarized. This is done in Table VIII. These various distortions may be described in the same way with ethylene oxide as with cyclopropane. Since the two molecules are so similar it is to be expected that frequencies which depend largely on similar distortions will have approximately the same value in ethylene oxide and cyclopropane.

TABLE IX. *Suggested values for the fundamental frequencies of ethylene oxide with the corresponding Raman and infra-red frequencies.*

Symmetry Class	Suggested Fundamental Frequency	Raman Frequencies	Infra-red Frequencies
A_1	3000	3008, 2960	(3030)
	1494	1492	1497
	1122	1122	(1168)
	1270	1270	1271
	811	(807)	811
B_1	3000	(3008)	(3030)
	1453	not observed	1453
	1163	1159	1168
	868	869	867
B_2	3062	(3062)	(3030)
	1172	not observed	(1168)
	673	not observed	673
A_2	3062	(3062)	forbidden
	—	not observed	forbidden
	807	807	forbidden

The vibration frequencies

One of the A_1 vibrations will have a frequency *ca.* 3000 cm^{-1} and there will be four with frequencies lower than this. Below 2000 cm^{-1} Ananthakrishnan observed only three polarized lines.* These had shifts of 1492, 1270 and 1122 cm^{-1}. On this basis, therefore, the methylene deformation vibration has a frequency of 1492, the methylene bending 1122 and one of the ring frequencies 1270 cm^{-1}, the value of the other frequency in this class remaining in doubt. Bonner [10] assigned to it the value 807 cm^{-1}. If this were correct, however, it would be expected that lines with this shift would be polarized instead of being depolarized. The frequencies 1492 and 1270 appear also in the infra-red spectrum at 1497 and 1271. The band at 1168 cm^{-1} may obscure the band corresponding to 1122 cm^{-1} if the latter is faint.

One of the four vibrations in the class B_1 will have a value *ca.* 3000 cm^{-1} and there will be three vibrations with smaller frequencies. The methylene deformation frequency is presumably 1453 cm^{-1}, being observed in the infra-red spectrum; and the methylene bending frequency 1163 cm^{-1}, observed in the Raman spectrum at 1159 and in the infra-red at 1168 cm^{-1}. The fourth vibration in this class consists mainly of ring distortion and by analogy with the similar vibration in cyclopropane may be assigned the frequency 868 cm^{-1}. The infra-red band falls at 867 and the Raman shift at 869 cm^{-1}.

In the class B_2 there is one vibration which has a frequency around 3000 cm^{-1}. This may be assigned the value 3062 cm^{-1} observed in the Raman effect. There are also two smaller frequencies. The methylene twisting frequency is presumably 673 cm^{-1}. The value for the rocking frequency cannot be determined from the evidence available.

The carbon-hydrogen valency vibration in A_2 may be expected to have about the same frequency as that in B_2 since both are antisymmetrical to σ_h. The rocking frequency apparently does not appear. There is still the depolarized Raman line at 807 cm^{-1} which might be assigned to the twisting frequency in this class. However, there is an infra-red band at 811 cm^{-1} and an A_2 fundamental is inactive in the infra-red spectrum. It may be that the infra-red band corresponds to the A_1 fundamental and that the polarized Raman line expected to correspond to it is obscured by the line arising from the A_2 fundamental.

The values of thirteen of the fifteen fundamental frequencies have now been determined. Estimates can be made of the possible order of magnitude of the two remaining frequencies by comparison with cyclopropane. The methylene rocking frequency of cyclopropane in the symmetry class A_2'' had the frequency 1041 cm^{-1}. This vibration is similar to that of the missing frequency in B_2. However, it must be remembered that the methylene bending frequencies in cyclopropane of *ca.* 1050 cm^{-1} are raised in ethylene oxide to *ca.* 1150 cm^{-1}. If there is a similar increase in this case, a frequency between 1100 and 1200 would be expected for the missing B_2 fundamental. Moreover, if this frequency does lie in this region, its absence in the infra-red spectrum would be accounted for since the band at 1168 cm^{-1} which has been assigned to the B_1

TABLE X. *Suggested interpretation of overtone and combination levels of ethylene oxide.*

Observed Frequency	Observed in:	Suggested Combination	Symmetry Class
1616	Infra-red	$2\times807=1614$	A_1
		$2\times811=1622$	A_1
1650	Infra-red	$807+868=1675$	B_2
		$811+868=1678$	B_1
1721	Infra-red	$2\times868=1736$	A_1
1845	Infra-red	$1172+673=1845$	A_1
1949	Infra-red	$1270+673=1943$	B_2
2020	Infra-red	$1163+868=2031$	A_1
2119	Infra-red	$1270+868=2138$	B_1
2278	Infra-red	$1122+1163=2285$	B_1
2639	Infra-red	$1494+1163=2657$	B_1
2786	Infra-red	$1494+1270=2764$	A_1
2917	Raman	$2\times1453=2906$	A_1
2960	Raman	$2\times1494=2988$	A_1
3008		3000	A_1
3876	Infra-red	3000 (A_1)$+868=3868$	B_1
		3000 (B_1)$+868=3868$	A_1
		3062 (B_2)$+811=3873$	B_2
		3062 (B_2)$+807=3869$	B_1
		3062 (A_2)$+807=3869$	A_1
4292	Infra-red	3000 (A_1)$+1270=4270$	A_1
		3000 (B_1)$+1270=4270$	B_1
4587	Infra-red	3062 (B_2)$+1495=4557$	B_2
6173	Infra-red	Binary combinations of 3000 frequencies	—

* In Ananthakrishnan's paper[2] there is a discrepancy between the table for individual lines observed and the final table of Raman shifts. According to the first the 1492 cm^{-1} shift leads to polarized lines, but according to the second, to lines which are depolarized. The line has been taken to be polarized.

fundamental would perhaps obscure it. It is found that all the observed overtone and combination levels can be accounted for in terms of the thirteen determined fundamentals and a value of 1172 for the missing B_2 fundamental. The spectroscopic data do not, therefore, allow a determination of all the fifteen fundamental frequencies. In Table IX are summarized the figures for the fundamental frequencies, with the manner in which they appear in the spectra. It will be seen that according to this table there are only four of the allowed frequencies which are definitely absent. In the infra-red none of the allowed fundamentals are definitely absent. In Table X it is shown how the observed overtone and combination frequencies can be interpreted in terms of these fundamentals. All the observed infra-red bands and Raman frequency shifts have been accounted for by means of fundamentals or binary combinations.

The available data on ethylene oxide do not therefore allow a complete determination of the fundamental frequencies. Because of the nature of the selection rules for this molecule any assignment is of necessity only tentative since there are several assignments possible. Nevertheless with the facts at present at our disposal that described above seems to be the most probable. Further data that are required to determine the complete assignment must be obtained with a grating spectrograph so that bands which are not separated with a prism spectrograph may be resolved. A grating spectrograph would also allow a determination of the type of the individual bands and this might assist in the assignment. Heat capacity data would also be of great value.

TABLE XI. *A comparison of the vibration frequencies of cyclopropane and ethylene oxide.*

Cyclopropane			Ethylene Oxide		
Symmetry	Freq.	Vibration	Vibration	Freq.	Symmetry
$[S, S]\ A_1'$	3000	CH valency	CH valency	3000	$A_1\ [S, S]$
	1485	CH_2 deform.	CH_2 deform.	1494	
	1187	ring deform.	CH_2 bending	1122	
			ring deform.	1270	
$[S, A]\ A_2'$	1070	CH_2 bending	ring deform.	811	
$[S, —]\ E'$	3000	CH valency	CH valency	3000	$B_1\ [S, A]$
	1435	CH_2 deform.	CH_2 deform.	1453	
	1022	CH_2 bending	CH_2 bending	1163	
	860	ring deform.	ring deform.	868	
$[A, S]\ A_2''$	3050	CH valency	CH valency	3062	$B_2\ [A, S]$
	1041	CH_2 rocking	CH_2 rocking	1172	
$[A, S]\ A_1''$	1000	CH_2 twisting	CH_2 twisting	673	
$[A, —]\ E''$	3080	CH valency	CH valency	3062	$A_2\ [A, A]$
	1250	CH_2 rocking	CH_2 rocking	—	
	740	CH_2 twisting	CH_2 twisting	807	

TABLE XII. *Calculated values* for the free energy, entropy and heat capacity of cyclopropane.*

	TRANSLATIONAL AND ROTATIONAL		VIBRATIONAL		TOTAL		
T °K	$\frac{(F-E_0^0)}{T}$	S	$\frac{(F-E_0^0)}{T}$	S	$\frac{(F-E_0^0)}{T}$	S	C_p^0
100	38.71	46.66	0.00	0.00	38.71	46.66	7.96
150	41.93	49.88	0.00	0.04	41.93	49.92	8.25
200	44.22	52.17	0.03	0.25	44.25	52.42	9.26
250	45.99	53.94	0.12	0.73	46.11	54.67	11.03
300	47.44	55.39	0.28	1.48	47.72	56.87	13.27
350	48.67	56.62	0.52	2.48	49.19	59.10	15.66
400	49.73	57.68	0.84	3.67	50.57	61.35	18.07
500	51.50	59.45	1.67	6.40	53.17	65.85	22.34
600	52.95	60.90	2.70	9.35	55.65	70.25	25.88
700	54.18	62.13	3.87	12.34	58.05	74.47	28.81
800	55.24	63.19	5.11	15.29	60.35	78.48	31.25
900	56.18	64.13	6.39	18.17	62.57	82.30	33.39
1000	57.01	64.96	7.73	20.95	64.74	85.91	35.22

* The units used in this table are calories per mole and degrees absolute.

Comparison with cyclopropane

In Table XI the frequencies of the comparable modes of vibration of ethylene oxide and cyclopropane are compared. In this table the types of vibration together with the suggested values for the frequencies are described. The symmetry with respect to the symmetry planes is described by the bracketed letters. The first letter indicates the symmetry with respect to the plane of the ring, σ_h, and the second the symmetry with respect to the three σ_v planes in cyclopropane and the one σ_v plane in ethylene oxide. For the degenerate vibrations of cyclopropane the symmetry with respect to the three σ_v planes cannot be given. Because of this it cannot be stated whether the E' vibrations are related to those in A_1 or to those in B_1 in ethylene oxide or whether the E'' vibrations are related to those in B_2 or to those in A_2. In addition certain of the ethylene oxide vibrations are related to two cyclopropane frequencies since cyclopropane has six more vibrational degrees of freedom. The lines in the center of the table indicate the manner in which the vibrations are related.

The correspondence between the carbon-hydrogen valency and the methylene deformation vibrations is immediately apparent. As regards the ring vibrations it is to be noted that the frequency of 1187 cm^{-1} for cyclopropane increases to 1270 for ethylene oxide. Likewise, the methylene bending frequencies in ethylene oxide are about 100 cm^{-1} higher than in cyclopropane. The methylene twisting frequencies are a little lower in ethylene oxide than in cyclopropane. The evidence regarding the rocking frequencies is more indefinite though it appears that they may be higher in ethylene oxide than in cyclopropane. This comparison would lead us to expect for the methylene rocking frequency in A_2, missing in the Raman spectrum of ethylene oxide, a value in the neighborhood of 1300 cm^{-1}. It is unfortunate that no direct evidence can be obtained as to the magnitude of this frequency. In general, therefore, the fundamental frequencies deduced for cyclopropane and ethylene oxide agree in a most satisfactory manner, lending support to the individual assignments. These facts, in addition, indicate a greater rigidity in ethylene oxide compared with cyclopropane with reference to all distortions except that involving methylene twisting.

Calculation of thermodynamic quantities

Since a complete assignment of the vibration frequencies of cyclopropane has been made, it is possible to calculate the free energy, F, the entropy, S, and the heat capacity, C, of this substance. The inadequate knowledge for ethylene oxide does not warrant such a calculation in this case. The molecular dimensions of cyclopropane that have been used in the calculation of the translational and rotational contributions to the free energy and entropy are 1.53A for the carbon-carbon link, 1.09A for the carbon-hydrogen link and 116°56′ for the HCH angle. The figure for the carbon-carbon link is obtained from electron diffraction data,[11] that for the carbon-hydrogen distance is that in methane[12] which is likely to be close to the value here. The methylene angle has been chosen so that it and the four HCC angles round any single carbon atom are the same, thus dividing the strain between all the angles. This value for the angle cannot be far from the real one. Table XII summarizes the results of the calculations. In the second and third columns are given the translational and rotational contributions to $-(F-E_0^0)/T$ and S at the temperatures, T, in the first column. The fourth and fifth give the vibrational contributions to these quantities while the sixth and seventh give their total values. The last column gives the value of the heat capacity at constant pressure, C_p^0.*

[11] Pauling and Brockway, J. Am. Chem. Soc. **59**, 1223 (1937).

[12] Ginsburg and Barker, J. Chem. Phys. **3**, 668 (1935).

* The constants used in calculating the above quantities were obtained from the *International Critical Tables*. It was assumed that the vibrations were harmonic.

Murphy[13] has given analytical expressions for describing the free energy, entropy and heat capacity as functions of the temperature. The application of these to allene has been discussed by Linnett and Avery,[14] where it was found that the more complicated molecule necessitated the introduction of an extra term into the expressions for $-(F-E_0^0)/T$ and S and that the heat capacity required an even more complicated expression. Expressions similar to those for allene were used for cyclopropane. The equations for the translational and rotational parts of $-(F-E_0^0)/T$ and S are:

$$-(F-E_0^0)/T=18.300\log T+2.112,$$
$$S=18.300\log T+10.060$$

and for the vibrational parts:

$$-\frac{(F-E_0^0)}{T}=131.60-\frac{34.757\log T}{T}-51.386\log T+4.395T\times10^{-2}-0.686T^2\times10^{-5}+\frac{36.289\times10^2}{T},$$
$$S=109.28-51.386\log T+8.791T\times10^{-2}-2.058T^2\times10^{-5}-\frac{15.095\times10^2}{T}.$$

The equations for the complete values of $-(F-E_0^0)/T$ and S are then:

$$-\frac{(F-E_0^0)}{T}=133.71-\frac{34.757\log T}{T}-33.086\log T+4.395T\times10^{-2}-0.686T^2\times10^{-5}+\frac{36.289\times10^2}{T},$$
$$S=119.34-33.086\log T+8.791T\times10^{-2}-2.058T^2\times10^{-5}-\frac{15.095\times10^2}{T}.$$

The equations for the vibrational components of $-(F-E_0^0)/T$ and S reproduce the values in Table XII very well between 200 and 1000°K, but not so well between 100 and 200°. Nevertheless the equations for the total values of $-(F-E_0^0)/T$ and S reproduce the tabulated values within 0.2 percent over the whole range between 100° and 1000°.*

I wish to thank Professor E. Bright Wilson, Jr., who suggested my studying these compounds, for his advice during this work.

[13] Murphy, J. Chem. Phys. **5**, 637 (1937).
[14] Linnett and Avery, J. Chem. Phys. **6**, 686 (1938).

* Uncertainty in the calculated values of the thermodynamic quantities may arise from several causes. In the first place there is uncertainty in our knowledge of the frequencies both from experimental inexactitude and also because Raman measurements were made on the liquid. Another source of error comes from our lack of knowledge regarding the anharmonicities of vibrations in polyatomic molecules.

NOVEMBER, 1938 JOURNAL OF CHEMICAL PHYSICS VOLUME 6

A Partial Analysis of Some Infra-Red Absorption Spectra of Organic Molecules in Dilute Solution*

OLIVER R. WULF AND LOLA S. DEMING
Bureau of Chemistry and Soils, Washington, D. C.
(Received August 18, 1938)

An attempt is made to resolve into component parts a number of relatively complex infra-red absorption coefficient curves for several OH-containing organic molecules in the region of the first overtone absorption of the OH group. Such analyses suggest certain relations between the structure of the molecule and its effect upon the character of the absorption of the absorbing group.

IN dilute solution of a nonpolar solvent such as carbon tetrachloride, the absorption in the near infra-red characteristic of the presence of a single OH or NH group in an organic molecule is often relatively simple, the curve of the absorption coefficient consisting of one or two absorption peaks which are narrow and fre-

* Material presented at the Rochester meeting of the American Chemical Society, September 1937, and at the Indianapolis meeting of the American Association for the Advancement of Science, December 1937.

quently symmetrical. A considerable number of molecular absorption coefficient curves of this type, measured in the region of the first overtone, have been published in articles from this laboratory during the last few years. In the present article an attempt is made to resolve certain of the more complex absorption curves published in the above-mentioned work into simple component peaks and to relate the results to the structure of the absorbing molecules. Insofar as this can be accomplished the work seems to comprise an analysis of the vibrational spectra of such molecules. These infra-red spectra in solution seem to be devoid of structure that would suggest discrete rotational transitions, and appear to consist of material originating in the vibrational motions within the molecule. Frequently a characteristic vibration of a polyatomic molecule is such that appreciable amplitude of vibration occurs only within a single group, as the O−H or C=O group, and such a vibration is often spoken of as an OH vibration or a C=O vibration. This article is principally concerned with absorption spectra characteristic of the presence of the OH group in certain molecules.

The present work is based on the assumption that absorption coefficient curves, such as those mentioned above, are in reality the superposition of a number of single symmetrical peaks, each single group such as OH or NH in one particular position and orientation in the molecule giving rise to one of these peaks. That these component peaks should be symmetrical is not evident *a priori* but will be assumed here. Proceeding on this basis it is possible, in a rather natural way, to resolve several of the absorption coefficient curves in the above-mentioned papers into a small number of component curves. In some cases these analyses lead to suggestions regarding the structure of the absorbing molecules, and it is believed that they may afford an aid in the utilization of this type of spectra by the chemist. Moreover, in those cases where there is now reason for expecting two symmetrical peaks, such as in certain of the *ortho* substituted phenols, this process of decomposing the over-all curve into components seems to be a justifiable procedure.

It is experimentally difficult to measure such absorption coefficients with high accuracy and

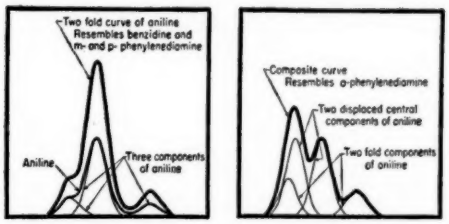

FIG. 1. Possible components of the absorption characteristic of the presence of NH_2 in *m*- and *p*-phenylenediamine and benzidine, and in *o*-phenylenediamine, using aniline as a basis.

in what follows the expression "symmetrical peak" is used to differentiate those peaks which appear single and at least nearly symmetrical from those which are evidently asymmetrical or which contain more than one actual maximum. There may, however, be present in what may at a cursory glance appear as a single symmetrical peak, a small amount of real asymmetry but which may lie within the rather wide limits of experimental error to which such quantitative measurements are often subject. In this paper the attempt will be made to discuss the structure of some absorption coefficient curves which are evidently complex in terms of certain of the more typical single peaks which are at least practically symmetrical. It seems necessary to neglect slight deviations from exact symmetry in the experimental results from whichever cause they may have arisen, in order to progress in the work of analyzing the more complicated curves.

Before discussing those cases in which a rather careful analysis has been attempted, it may be helpful to give a somewhat rough illustration of the reasonableness of breaking up complex curves in this way. Such an illustration is contained in the curves for the amino analogs of catechol, resorcinol, and hydroquinone, the curves for the latter group affording a relatively simple basis of reference.[1] The curves for *m*- and *p*-phenylenediamine, and indeed also for the substance benzidine, resemble the curve for aniline, whereas a considerable change occurs in passing to *o*-phenylenediamine.[2] To see the

[1] Wulf and Liddel, J. Am. Chem. Soc. **57**, 1464 (1935).

[2] In the discussion in reference 1 these cases were mentioned, pointing out that reference to the OH analogs indicated that it should be possible to resolve the curves for these amino compounds into component peaks, and that a certain parallelism existed between the behavior of the two sets of compounds.

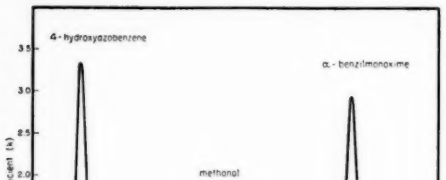

FIG. 2. A comparison of the form $(\cdots\cdot)$ $y=\frac{y_0}{1+(x^2/a^2)}$ and the form $(-\cdot-\cdot)$ $y=y_0e^{-a^2x^2}$ with experimental curves.

nature of this change, it is necessary to consider the character of the curve for aniline.[1]

The absorption characteristic of the NH_2 group in aniline in the region 6000–7000 cm^{-1} may be approximately resolved into three symmetrical component peaks, as indicated in Fig. 1. The two principal components are at roughly 6680 and 6880 cm^{-1}, respectively. These two peaks, while varying in intensity and also somewhat in separation from compound to compound, seem to characterize the presence of an NH_2 group. This suggests that they may represent two modes of vibration of the group which in analogy to water might be somewhat loosely termed the parallel valence vibration and the asymmetrical vibration. The third peak at roughly 6580 cm^{-1} differs considerably when the group appears in different molecules, giving indication that it arises from interaction with the rest of the molecule which varies with the structure. In certain molecules containing the NH_2 group, still further detail can be seen, indicating a more complicated interaction with the remainder of the molecule. Using this structure of the absorption of aniline, one may make the absorption curves for the three phenylenediamines and benzidine somewhat clearer by the process of resolution just described. The curves for *m*- and *p*-phenylenediamine and for benzidine, while differing somewhat from one another, may be approximately represented by a curve derived from the aniline curve itself multiplied by a factor of two, as shown in Fig. 1. This is not surprising when one recalls that the only striking difference between hydroquinone and resorcinol on the one hand and phenol on the other was the twofold greater intensity of the absorption of the former two, indicating that the two OH groups were practically independent of one another, that is, simply additive. In the case of catechol, however, two separate phenol-like peaks were found, the separation in this instance being about 100 cm^{-1}. Turning now to the absorption curve for *o*-phenylenediamine, which appears more complicated than those of the other three, it may be approximated, as shown in Fig. 1, by the simple addition of both the second and third peaks of aniline multiplied by a factor of two, and two peaks of the first frequency of aniline separated from one another by a spacing which happens here also to be about 100 cm^{-1}. This analysis of the *o*-phenylenediamine curve, which is suggested by the relatively simple result for catechol, affords an illustration of the basis for attempting to break up complex curves in this way.[3]

In the above, the only condition placed on the component curves was that they be symmetrical, their shapes being determined by choosing symmetrical curves which would best fit the complete observed curve. In proceeding now to discuss some observed curves which have been resolved with more care, the question of the shape of the individual peaks, postulated as characterizing any single OH or NH group in a particular position and orientation, becomes of importance. These curves are frequently surprisingly sharp as was discussed in reference 1. For the theory of their breadths, it is, of course, of particular interest to know whether the shape of such curves may be represented by any simple analytical expression. Two relatively simple forms suggest themselves as possibilities: (1) the curve for a damped oscillator, and (2) the Gauss error curve, both of these having at least a possible connection with the actual physical phenomenon. Inspection shows that there is considerable variation among the many measured curves. Some conform more nearly to the one type of curve and some more nearly to the other. In Fig. 2 three curves have been chosen

[3] In this connection see for example, Fox and Martin, Proc. Roy. Soc. **A162**, 422 (1937); and Rose, Nat. Bur. Stand. J. Research **20**, 129 (1938).

to illustrate this, showing, with the experimental curves which were measured in earlier work,[4] Gauss error and damped oscillator curves in dashed and dotted lines, respectively. The two types of curves have in each case been determined from the value of the ordinate at the maximum and the half-value width of the experimental curves. As can be seen, none of the three conforms closely to either type. However, α-benzilmonoxime and 4-hydroxyazobenzene approximate more nearly the Gauss curve, while methanol, flaring more broadly at the base, approximates more nearly the damped oscillator curve.[5]

In proceeding to break up the more complex curves into their component parts, somewhat less freedom in fitting and hence somewhat more significance in the result is had if one constant form of curve is adopted, this being a reasonable procedure if the breadth of the curve derives from one principal cause. Actually. with an expression which is the sum of the damped oscillator and Gauss error forms of the same half-value widths but with arbitrary values of the ordinates, a very close fit can be obtained with some of the experimental curves, as is perhaps to be expected from Fig. 2. However, it seems probable that the much greater freedom introduced by this procedure should make it possible to fit most symmetrical curves of this type within the limits of error of such experimental measurements and that to do this would sacrifice some of the significance of such analyses. In the work which follows the Gauss error form has been used, and component curves have been placed by trial, attempting in the final addition of the components to obtain as good a representation of the experimental curve as possible. In none of the cases is the representation exact, but in several it is sufficiently close to indicate that the actual curve is to be considered as made up of components at least similar to those employed.

In certain of the *ortho* substituted phenols two distinct peaks characterize the absorption of the OH group, despite the fact that there is only one OH group present. Pauling has suggested[6] an explanation for this, with which experimental results have proved to be in remarkable accord. The explanation attributes the two peaks to two forms of the molecule, isomers, in which the *orientation* of the OH group differs. It seems probable, as discussed by Pauling, that this is a rather general phenomenon, not restricted to the *ortho* substituted phenols. Certain of the latter, however, offer particularly clear illustrations of this composite form of complex absorption curves.

The absorption of tetrabromocatechol[7] seems evidently to be composed of at least two peaks. This curve may be fairly well represented by two Gauss curves of forms chosen with reference to the *cis* peak of *o*-bromophenol and the *cis* peak of catechol, since it is reasonable to suppose in a first approximation that if the complete curve is the sum of two components, the two curves just mentioned should indicate their form. This representation of the tetrabromocatechol curve is shown in Fig. 3, the two components being of the same half-value width, which is equal to the *cis* peak of catechol and slightly greater than the

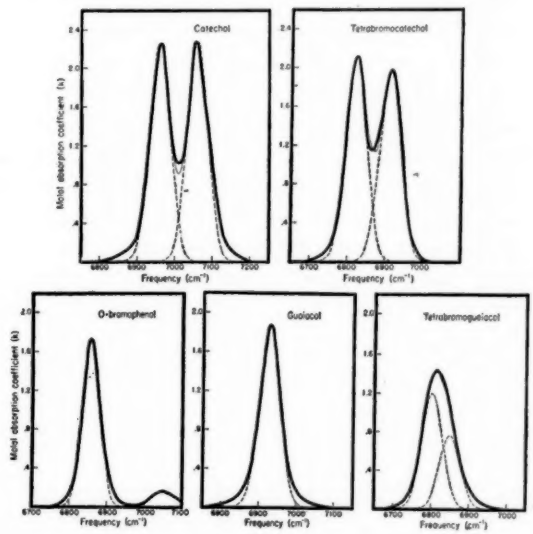

FIG. 3. Resolution of curves for tetrabromocatechol and tetrabromoguaiacol.

[4] Hilbert, Wulf, Hendricks, and Liddel, J. Am. Chem. Soc. **58**, 548 (1936); Hendricks, Wulf, Hilbert, and Liddel, *ibid.* **58**, 1991 (1936); and reference 1.

[5] In the work which follows the Gauss curve will be used. Fig. 2 illustrates a characteristic tendency of the measured curves to persist more strongly in intensity at greater distances from the maximum than does the Gauss curve of the same height and half-value width.

[6] J. Am. Chem. Soc. **58**, 94 (1936).

[7] Wulf, Liddel, and Hendricks, J. Am. Chem. Soc. **58**, 2287 (1936).

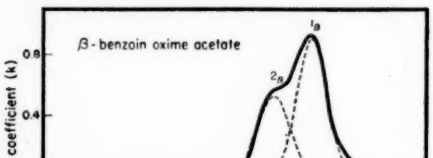

FIG. 4.

cis peak of *o*-bromophenol. The shifted position of a peak relative to the normal phenol position and the increase in the half-value width relative to that of phenol seem to depend on disturbing influences such as nearby polar or polarizable groups in the molecule. There is evidence in the experimental results that an increase in breadth is apt to accompany marked shift in the position of the peak. There are, however, cases where a greater broadening of a peak appears than would be expected from the apparent shift in position of that peak from its normal undisturbed position.

The curve for tetrabromoguaiacol[7] might be expected similarly to be composed of two peaks, though this is less evident on simple inspection of the curve. However, as was done in tetrabromocatechol, the absorption for tetrabromoguaiacol may be resolved into two components, using the peak for guaiacol and the *cis* peak of *o*-bromophenol as indicating approximately the character of the two component parts. This is shown also in Fig. 3. The half-value widths of the two Gauss curves used are the same, and slightly greater than either that for guaiacol or for the *cis* peak of *o*-bromophenol.

Such resolution of absorption curves into their component parts seems to take on particular significance when applied to certain ordinary geometric isomeric molecular forms. The benzoin oxime acetates illustrate this. By virtue of the

$$\diagdown \quad C{=}N- \quad \text{group, benzoin oxime acetate exists} \quad \diagup$$

in two isomeric forms similar to fumaric and maleic acids. In the β-form absorption is observed as shown in the upper portion of Fig. 4. That it consists of at least two peaks seems evident, and the figure illustrates the attempt to fit the observed absorption with two symmetrical curves of the Gauss form and of appropriate intensities and half-value widths. The resulting fit is good except at the right-hand end, this divergence illustrating the tendency mentioned in footnote 5. The curve for the α-form is of particular interest in that it appears to contain in part absorption such as is found in the β-form, reduced in intensity, however, because a portion of the molecules have taken up two other forms indicated by the two curves at the left, which from the point of view of the present work, arise from two new orientations which the OH group may assume in the molecule. These results at first sight might seem to raise the question as to whether the α-form is indeed a pure compound. Dr. A. H. Blatt, who very kindly supplied these compounds originally for measurement, informs us that the behavior of the two materials in characteristic reactions of hydrolysis and cleavage precludes the possibility that there is an appreciable amount of either substance as impurity in the other. We believe the situation should be described by saying that in the α-form, which differs from the β-form fundamentally because of the different orientation with respect to the carbon-nitrogen double bond, the OH group finds four positions, all of which are populated to an appreciable extent and two of which are practically identical with the two positions which the OH group may occupy in the β-form. Benzoin, the parent substance, seems to contain in its absorption[1] principally the two low frequency peaks of the α-form, and suggests that in this molecule the two additional positions of the OH group characterizing the β-oxime acetate and present also in the α-oxime acetate, are absent or but slightly populated.

The isomers of which the two common isomeric forms of benzoin oxime acetate are themselves composed, just as the isomers in *o*-chlorophenol, would seem to be of a rather subtle sort and such perhaps as to defy separation and isolation. However, in the results obtained for another compound which has been studied,[8] β-2,3,4,6-tetraacetyl-*d*-glucose, there is indication that such forms may yet prove separable. Certain

[8] Hendricks, Wulf, and Liddel, J. Am. Chem. Soc. **58**, 1997 (1936).

physical properties of the compound showed variations depending on the method of preparation and subsequent treatment. The results of the measurements of the infra-red absorption of this compound indicated similar behavior, the absorption undergoing change concomitant with the change in physical properties such as melting point and optical activity. At room temperature the change was very slow. A high temperature coefficient, however, permitted observing the change in a time of the order of hours in CCl_4 solution at 60°C. After the change was complete, or nearly so, the substance could be returned to its original form by crystallization from ether. A decided alteration in the infra-red OH absorption accompanied this change, the absorption reverting to that which the substance possessed at or near the beginning of the reaction. This OH absorption shows a similarity to that of the benzoin oxime acetates, and it may be represented as composed of nearly the same type of component curves as those of the benzoin oxime acetates. The absorption of two other related compounds, β-2,3,4,6-tetraacetyl-*d*-galactose and α-2,3,4-triacetyl-*d*-xylose, were measured in the same work[8] and their curves afford additional information concerning the character of the OH absorption in this type of molecule. In Fig. 5 an analysis has been made of the absorption curves for the high and low melting forms of the glucose compound as well as of the curves for the galactose and xylose compounds. The similarity between these absorptions and those of the benzoin oxime acetates can be seen by referring to Fig. 4 and it suggests certain structural features in commons. Past experience has shown that difference in the character of a molecule more than one or two atoms removed from the absorbing group is usually without much effect on the absorption of the group, except in cases where, through the structure of the molecule, an atom several removed in valence bonding has been brought into close proximity to the absorbing group.

The hypothesis of component symmetrical peaks requires that an absorption curve such as that for the high melting form of the glucose compound be composed of at least three peaks, and it seems probable, working by construction from the maximum peak to lower frequencies,

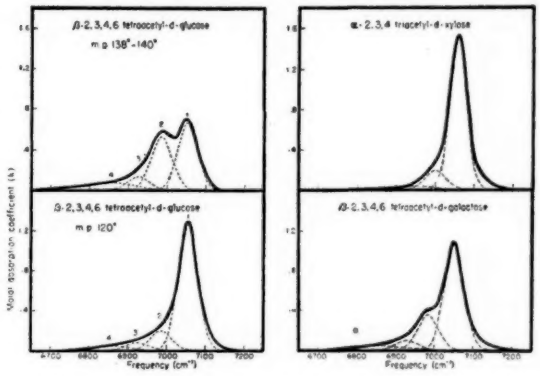

FIG. 5.

that four component peaks describe the absorption better. Thus it seems that in these molecules, also, there exist isomers of the kind composing the two isomeric forms of benzoin oxime acetate. In the spontaneous intramolecular change in which the melting point of the substance falls, the peak at approximately 7050 cm^{-1} increases at the expense of the other three. Thus the relative amounts of the several isomers undergo a change. This change occurs at a rate which increases with temperature, indicating that a potential maximum must be surmounted in each case in the transformation. The fractional change in the peak at about 6890 cm^{-1} is particularly marked.

Thus in β-2,3,4,6-tetraacetyl-*d*-glucose, owing to the slowness of the intramolecular change, what was essentially a partial separation of several forms was possible. This seems to argue for the reality of the picture implied in our primary assumption that an absorption curve such as that of this substance is not a complex absorption of many peaks due to one molecular form (there is, of course, only one OH group in the molecule), but rather is a composite of several simple peaks due to several molecular forms.

It is of particular interest that the spontaneous, that is the thermal, change which β-2,3,4,6-tetraacetyl-*d*-glucose undergoes leads to an increase in the normal OH peak (7050 cm^{-1}) at the expense (diminution) of the three shifted peaks. In accordance with the above interpretation, the shifted peaks should be due to forms of the molecule in which polar groups exist in positions such that the OH group lies in the

vicinity of one of these polar groups. Where an intramolecular change occurs spontaneously, one might expect that this would occur with a decrease in polarity brought about by the change in the orientations of polar groups in such a way as to mutually saturate one another. In accord with this the spontaneous change in the glucose compound is accompanied with a decrease in the melting point, as would be expected in passing from a more polar to a less polar compound. It is of interest in this connection to recall that the preparation of the more polar form (high melting form) of the molecule was effected at will by recrystallization of the compound from the polar solvent ether. Where a solute molecule possesses two or more isomeric forms which differ in polarity and which have but a slight difference in energy, one would expect the polar form to predominate in solution of a polar solvent, while the nonpolar form should predominate in a nonpolar solvent. In the process of crystallization from the polar solvent, the solvent molecules would, so to speak, control the crystallizing out process, putting molecules of the polar form into the growing crystal. For the nonpolar solvent, the reverse would be expected.

Resolution of complex absorption coefficient curves, such as has been illustrated above, could undoubtedly be carried out more successfully were the true form of the component peaks known. This, together with the fact that remarkable sharpness often characterizes single absorption maxima of this kind, makes it particularly desirable to formulate an explanation for the basic cause of the breadth of these absorptions. Important evidence relative to this is contained in the experimental results for the fundamental and first overtone of phenol in CCl_4 solution. Fox and Martin have measured the fundamental, which is shown in Fig. 2 of their article.[9] The concentration employed was sufficiently high that the association band shows prominently, but the half-value width of the normal OH peak can be seen to be about 25 cm^{-1}. In the work of reference 1, phenol was measured in the first overtone, and as can be seen in Fig. 2 of that article, the half-value width is about 50 cm^{-1}. This twofold increase seems to eliminate any cause of broadening which would act upon the two absorptions in the same way, such as collision broadening, and strongly suggests that the curves represent the absorption of a distribution of oscillators, in which the restoring force governing the vibration varies slightly about a mean value and in a roughly symmetrical manner, indeed in a manner bearing at least some resemblance to the distribution given by the Gauss curve for errors about the mean value. Each of the oscillators in the distribution behaves independently and produces its own fundamental and first overtone, leading thus to an increase in the breadth of the first overtone by a factor of two. On this hypothesis a cause should be sought which leads to such a symmetrical distribution of all the oscillators around a most probable value.

From the above it seems probable that, even in the cases of complex absorption curves, a single absorption peak characterizes a single OH group in a particular position *and orientation* in the molecule. There is indication that the same thing is true of single NH and CH groups. Where a single peak can be adequately studied, such as the absorption of the OH group in phenol, there seems to be, in sufficiently dilute solution, little or no indication of absorption to either side of the main peak that could be interpreted as the envelope of rotational absorption. Such absorption might be expected if the group were free to rotate, as around the O−C bond connecting the OH group to the ring in phenol. It may be worth while recalling here that the separation of the two rotational maxima for a free OH rotator would be about 150 cm^{-1}, a quantity much larger than the apparent half-value width of a peak such as phenol. As has furthermore been pointed out above, there seems to be good reason to believe that, in many if not most cases, single groups such as OH are constrained to remain in the close vicinity of a preferred position.[6] An explanation for the observation that single peaks characterize the absorption of single groups under such circumstances has been suggested to the authors by Professor E. Teller. The explanation is similar to that offered by West and Edwards[10] in their work on the absorption of hydrogen chloride in

[9] Proc. Roy. Soc. **A162**, 419 (1937).

[10] J. Chem. Phys. **5**, 14 (1937).

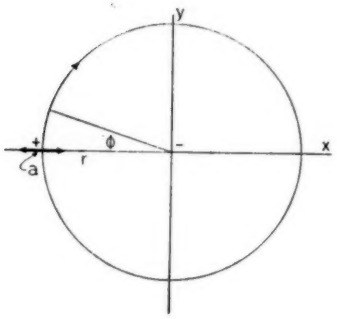

FIG. 6.

solution, in which it is suggested that the observed absorption in this instance is to be described as a principal absorption characterizing the intramolecular vibration together with a nearby subsidiary absorption representing the combination frequency of this high frequency intramolecular vibration with a low frequency intermolecular vibration occurring between the solute and solvent molecules.

If the OH group in phenol is constrained to lie in the plane of the ring, it presumably may librate with small amplitude about its equilibrium position. The restoring force is, of course, not yet known in this instance, but it is presumably sufficiently great to insure that the amplitude will not be large. This relatively low frequency of libration may in general be expected to combine with the principal vibration of the OH group along the valence bond, leading to subsidiary peaks on both sides of the principal frequency displaced by an amount depending on the magnitude of the force constraining the OH group to lie in the plane of the ring. The intensities of the sum and difference frequencies will, of course, differ, the intensity of the peak corresponding to the difference frequency being appreciable only if the restraining force is sufficiently small that the energy of the first quantum in the libration frequency is not too large compared to kT.

Since this factor of the restricted rotational motion of the absorbing group is of importance in discussing the shape of such OH absorptions as that in phenol, it seems worth while to describe here the difference between the absorption of a free dipole rotator and the absorption of such a restricted dipole rotator as we have been considering. In such cases classical theory gives a good approximation for the intensities. The result for a simple dipole rotator such as a free OH group is well known, but the expressions will be given in order that comparison can be made between these and the expressions for the restricted rotator. In Fig. 6 it can be seen that in the rotational motion of the dipole (drawn for simplicity in this case as if the dipole rotates around a very heavy or fixed center), the variation of the projection of the electric moment on the x axis will be identical to that on the y axis, except for a difference in phase of 90°. If the rotational frequency is designated as ω_r (i.e., $\phi=\omega_r t$) and the vibrational frequency as ω_v (i.e., $s=a\cos\omega_v t$), it is clear that the projection of the electric moment on the x axis may be written approximately as

$$M_x=(M_0+s(dM/dr)+\cdots)\cos\omega_r t$$
$$=r_0 e\cos\omega_r t+ae'\cos\omega_v t\cos\omega_r t, \quad (1a)$$

$$=r_0 e\cos\omega_r t+(ae'/2)[\cos(\omega_v+\omega_r)t+\cos(\omega_v-\omega_r)t]. \quad (1b)$$

Expression (1b) consists of three terms, each of which varies periodically. The first possesses the pure rotation frequency, the second possesses the sum of the vibration and rotation frequencies, while the third possesses the difference of the vibration and rotation frequencies. The electric moment associated with the first term $r_0 e$ is larger than that associated with the second and third terms $ae'/2$, but the first term has a lower frequency than the second and third and the intensities of the three may thus be at least comparable. Simple dipole molecules such as HCl illustrate such behavior.

Considering now the case of a restricted rotator, the angle ϕ instead of passing periodically through 2π is restricted to a libration of relatively low frequency ω_l and of small amplitude γ such that

$\phi=\gamma\sin\omega_l t$ where $\gamma\ll\pi/2$ and hence $\phi\leqq\gamma\ll\pi/2$.

In this case the projections on the x and y axes are different. Introducing the approximations $\sin\phi=\phi$, $\cos\phi=1$ and referring to (1a) above, the expression for M_x may be written

$$M_x=r_0 e+ae'\cos\omega_v t. \quad (2)$$

Thus M_x varies periodically with the pure vibration frequency and with an amplitude ae',

which is twice as great as the amplitude associated with the sum and difference frequencies in the case of the free rotator. Referring again to (1a) above, the expression for M_y becomes

$$M_y = r_0 e\gamma \sin \omega_l t + (ae'\gamma/2)[\sin (\omega_v+\omega_l)t + \sin (\omega_v-\omega_l)t]. \quad (3)$$

Expression (3) consists again of three terms, the first representing the pure libration frequency. The amplitude of this is, however, γ times smaller than the pure rotation frequency in the case of the free rotator, although the frequency is indeed slightly higher. The second and third terms are again the sum and difference respectively of the vibration and libration frequencies, but the amplitudes are γ times as small as the amplitude in the case of the free rotator. Since the intensities of emission or absorption are proportional to the square of these amplitudes, the sum and difference frequencies will evidently be very weak relative to the fundamental vibration frequency, if γ is small compared to $\pi/2$.

Thus if the OH group is constrained to lie in a preferred position in the molecule by forces which are sufficiently strong to insure that the amplitude of libration about this preferred position is small at ordinary temperature, the single peaks of absorption characteristically observed for these molecules in dilute solution would find a simple explanation. It seems evident without going through the derivation that, as the amplitude of motion about the preferred position increases, the intensity of the combination frequencies would increase relative to the intensity of the principal frequency. In this suggested explanation for the characteristic single peaks no remark has been made regarding the breadth of these peaks, and it seems necessary to look for some influence on the absorbing group either of an intramolecular or intermolecular nature which would lead to a roughly symmetrical distribution of the groups about a mean as mentioned earlier. This search is perhaps rendered a little more difficult than it would otherwise be by the need of having the distribution symmetrical. It is well therefore to emphasize that the observations indicate only a rough tendency toward symmetry and that an explanation of the breadth of the peaks, which would lead to asymmetrical broadening of such a nature as to develop pronounced asymmetry only at considerable distances from the maximum, would certainly be admissible.

Summary

Analyses have been made of a number of relatively complex infra-red absorption coefficient curves of certain OH-containing organic molecules in the region of the first overtone absorption of the OH group. The analyses have been based on the hypothesis that such complex curves are in reality the superposition of a number of single symmetrical peaks of varying intensities and positions, each one characteristic of a particular position and orientation of the OH group in the molecule. Relatively simple cases are given in which such resolution into component parts has seemed to be plausible from a consideration of the absorptions of simpler related molecules. In the more complicated cases such analyses appear to afford some information relative to the structure of the absorbing molecule. This has been illustrated in the two isomeric benzoin oxime acetates. In β-benzoin oxime acetate the OH group appears to have two orientations which it occupies to an appreciable extent. In the α-form of this substance four different orientations of the OH group appear, two of which are practically the same as the two orientations in the β-form. In the substance β-2,3,4,6-tetraacetyl-*d*-glucose there are also several orientations which the OH group may take up, presumably four in number, and these resemble those in α-benzoin oxime acetate. The variability in the properties of the β-2,3,4,6-tetraacetyl-*d*-glucose, depending on the method of preparation of the substance, is interpreted as arising from different mixtures of molecules with the OH group in the several orientations. The change with time which the properties of this substance undergo thermally is explained as a change in the relative numbers of molecules possessing the OH group in these several different orientations, and it is suggested that the spontaneous change appears to proceed in the direction in which unsaturated polarity, existing in the molecule and affecting the OH group, is saturated in the change. The observation that

the higher melting form could be obtained by recrystallization from a polar solvent, ether, would seem to be in accord with this. The origin of the single absorption peaks and their relative sharpness is discussed. An explanation for the former, that is, for the observation of what seems to be simply the pure vibration frequency of the group giving rise to the absorption is suggested, considering the absorbing group as constrained to lie in one or more particular orientations in the molecule by forces which prevent the group departing from such orientations by more than an amplitude small compared with that of rotation around the C−O bond.

NOVEMBER, 1938 JOURNAL OF CHEMICAL PHYSICS VOLUME 6

The Band Envelopes of Unsymmetrical Rotator Molecules. I. Calculation of the Theoretical Envelopes *

RICHARD M. BADGER AND LLOYD R. ZUMWALT
Gates and Crellin Laboratories of Chemistry, California Institute of Technology, Pasadena, California

(Received June 14, 1938)

Since the majority of molecules of chemical interest are too heavy to permit resolution of the rotational structure of the infra-red bands, it is of interest to find what information can be derived from a study of the band envelopes. Considerations of the type which Gerhard and Dennison have made for symmetrical molecules have been extended to the unsymmetrical rotator. By the use of an approximation method the envelopes of the three elementary types of band have been calculated for nine different sets of molecular parameters.

INTRODUCTION

THE number of molecules with moments of inertia small enough to permit the resolution and analysis of the rotational structure of the infra-red bands appears to be rather limited. In the majority of cases of interest to the chemist it is an idealization to speak of the bands as consisting of lines, since the spacing of the theoretical lines is less than their breadth must be under the conditions of experiment. Gerhard and Dennison[1] have considered the unresolved bands of symmetrical rotators and have shown that useful information can be obtained from the separations and relative intensities of the maxima. They have calculated a number of band envelopes which we have found very useful in qualitative comparisons. However, the majority of molecules are unsymmetrical and their calculations are inapplicable since with even moderate asymmetry the appearance of the bands is materially modified, especially near their centers.

We have recently observed the spectra of a number of moderately heavy unsymmetrical molecules and have found that the bands may vary considerably in appearance and frequently exhibit distinctive features. For example: In some cases there is only one broad maximum, in others there may be as many as five peaks of unequal intensity. The significance of these features has not always been immediately obvious but their variability suggests that useful information may be obtained from the shapes of the band envelopes alone. To make this possible the theoretical envelopes for various types of molecules must, of course, be known.

The discussions of the unsymmetrical rotator bands which have been given in the literature are quite inadequate for our purposes. Both Dennison[2] and Nielsen[3] have presented diagrams giving the positions and intensities of a few lines as functions of asymmetry, but these plots can give no idea of the intensity distribution in a band since only lines of very low J value are included. Aside from this fact they are restricted

* Contribution from the Gates and Crellin Laboratories of Chemistry, California Institute of Technology, No. 653.

[1] S. L. Gerhard and D. M. Dennison, Phys. Rev. **43**, 197 (1933).

[2] D. M. Dennison, Rev. Mod. Phys. **3**, 2 (1931).

[3] H. H. Nielsen, Phys. Rev. **38**, 1432 (1931).

to planar molecules. The elaboration of such diagrams to the point where they would be of general use is not practical owing to the amount of labor involved in calculating every line of appreciable intensity. Since we are not interested at all in individual lines it seems more sensible to follow a procedure similar to that used by Gerhard and Dennison for the symmetrical molecule. Even this is difficult in the unsymmetrical rotator case, but we have devised a method for calculating the intensity distribution in a band which can be carried out with a reasonable amount of labor. The method involves a number of approximations but the errors should not be excessive and the results are indeed justified by satisfactory agreement between calculated and observed band envelopes.

In the unsymmetrical rotator case one finds a number of complications which are not present in the symmetrical molecule. Two of these concern us at this point. In the first place it is comparatively seldom that the bands are of any simple type. If symmetry elements are entirely lacking the electric moment or change of moment may have components along all three principal axes of inertia. It is convenient, however, to consider any band as being built up of the three elementary types of structure which would be expected if the electric moment were parallel to the minor, intermediate or major axis in turn. We shall follow Nielsen in designating these structures by the letters A, B and C, respectively. There has been no consistent usage followed in the literature but it is convenient to adopt the convention that the three principal moments of inertia shall be designated by the same three symbols and always in the order $A<B<C$. The reciprocals, designated by small letters, will consequently be in the reverse order: $a>b>c$. An "A" band shall be one in which the electric moment or change of moment is parallel to the minor or A axis, etc.

In the second place the energy levels of the unsymmetrical rotator are arranged in a most inconvenient fashion and it is not possible accurately to represent the positions and intensities of the rotation lines by simple functions of the moments of inertia.

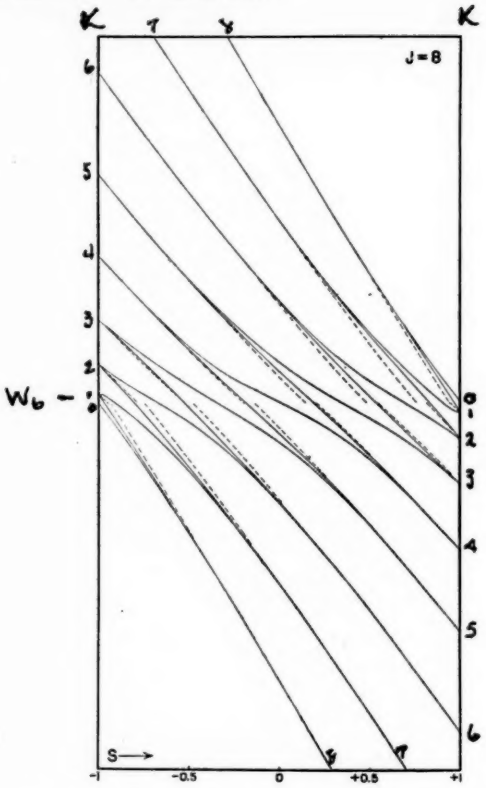

FIG. 1. The energy levels of an asymmetric rotator for $J=8$ plotted as a function of S, with $(a-c)$ and b kept constant. The continuous lines represent the levels given by the exact theory and the dashed lines indicate those given by approximate Eqs. (1) and (2). A horizontal line through the center of the figure would represent the energy $W_b=J(J+1)h^2b/8\pi^2$.

CALCULATION OF THE BAND ENVELOPES

Our first step in the calculation of the band envelopes was to find approximate expressions for the energy levels of the asymmetric rotator which are sufficiently accurate for our purposes and at the same time of a convenient form. These were obtained by an approximate solution of the secular determinant of Wang[4] using second-order perturbation methods.

In any particular case the secular determinant may be written in three different ways. To obtain reasonably accurate values for the energies with only second-order perturbation methods, it is necessary to use different forms depending on the energy ranges with which one is concerned. For levels with energy greater, or less, than $W_b=J(J+1)h^2b/8\pi^2$ the appropriate forms are those in which the diagonal terms are the same

[4] S. C. Wang, Phys. Rev. **34**, 243 (1929).

as they would be for symmetrical molecules with the reciprocals of the two like moments of inertia equal to the mean of b and c, or of a and b, respectively.

If one makes an approximation regarding the interaction terms by replacing $(J-\sigma)(J-\sigma+1)\times(J+\sigma)(J+\sigma+1)$ with $[J(J+1)-\sigma^2]^2$, one obtains general solutions for the two cases mentioned above, which may be written as follows:

$$W\approx(h^2b/8\pi^2)\left\{J(J+1)\left[1-\frac{\rho(5-3S)(1+S)}{8(3-S)}\right]+K'^2\frac{\rho(17-14S+S^2)}{8(3-S)}\right\}\quad\text{(Eq. (1)) for } W>W_b,$$

$$W\approx(h^2b/8\pi^2)\left\{J(J+1)\left[1+\frac{\rho(5+3S)(1-S)}{8(3+S)}\right]-K''^2\frac{\rho(17+14S+S^2)}{8(3+S)}\right\}\quad\text{(Eq. (2)) for } W<W_b,$$

where $\rho=(a-c)/b$ and $S=(2b-a-c)/(a-c)$, and K' and K'' are integers with maximum value J.

We prefer to take S as a measure of the symmetry of the molecule rather than Wang's b, since the latter quantity is not uniquely defined but may take three different values depending on how the determinant is written. It will be noted that S takes the values $+1$ for the symmetrical planar molecule, -1 for the symmetrical spindle, and 0 for those molecules which as regards arrangement of the energy levels we may regard as least symmetrical.

In restricting Eqs. (1) and (2) to their appropriate domains we may make use of an approximation suggested by an equation given in the second paper of Kramers and Ittmann.[5] For the lower limits of K' and K'' we may take $s'J$ and $s''J$, respectively, where

$$s'=(2/\pi)\tan^{-1}[(b-c)/(a-b)]^{\frac{1}{2}}$$

and $s''=1-s'$. The upper limit in each case is of course J.

As may be seen in Fig. 1, our approximation of the energy levels is entirely adequate except for a small "intermediate" region where the energy is not greatly different from W_b. On the scale to which the figure is drawn the levels calculated from Eqs. (1) and (2) cannot be seen to deviate from the actual ones up to the point at which the splitting becomes appreciable. From this point on they diverge along the dashed lines. Fortunately the failure of both equations in the transition region is not very serious. In the first place, only a small fraction of the energy levels are concerned. In the second place, the transitions involving levels in this region are the weakest in the cases where the predicted frequencies are most seriously in error, namely in the $\Delta J=\pm1$ branches of the B type bands and the $\Delta J=0$ branches of the A and C type bands. In the remaining cases where the transitions are strong the approximation is not so poor.

In a rough first approximation of the band envelopes we have assumed that the transition probabilities are the same as those of the symmetrical rotator, using of course the rules which will be appropriate for the levels given by the two equations, respectively. This will lead to considerable error only in the "intermediate" region, as has been discussed by Dennison.[6] Since our energy expressions are of the same form as those for the symmetrical rotator the procedure which Gerhard and Dennison[7] have worked out is directly applicable and it does not seem to be necessary to give further details of our calculation except to mention two modifications which must be introduced. In the first place, two sets of calculations have to be made in each case taking account of the two regions of energy levels separately. In the second place, some changes have to be made in the limits of integration to take account of the fact that the lower limits of K' and K'' are $s'J$ and $s''J$, respectively.

Although this first approximation just described gives a reasonably satisfactory representation of the intensity distribution in either the $\Delta J=0$ or the $\Delta J=\pm1$ branches of a band, the envelope obtained by combining the two may be considerably in error. It is easy to show that the sum of the transition probabilities between

[5] H. A. Kramers and G. P. Ittmann, Zeits. f. Physik **58**, 217 (1929).

[6] Randall, Dennison, Ginsberg and Weber, Phys. Rev. **52**, 160 (1937).

[7] The expressions given by Gerhard and Dennison contain several typographical errors and should not be used without careful examination.

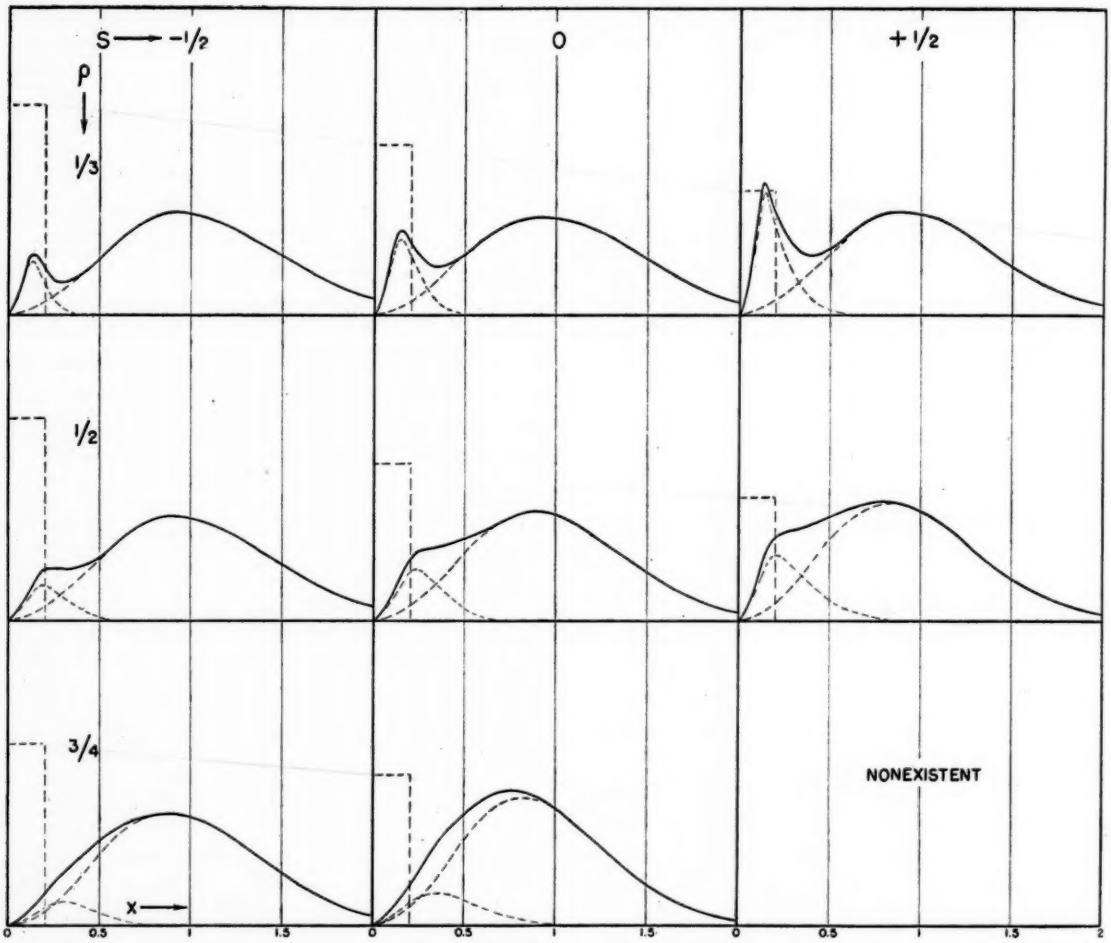

FIG. 2. The A bands (electric moment parallel to the minor axis of inertia) for eight different sets of parameters. The absorption coefficient is plotted as a function of x. One-half the band is shown, with the origin at the left. For further description see text.

levels of a given J value is independent of the symmetry of the molecule. Consequently this sum for any unsymmetrical molecule is the same as for the symmetrical rotator. A similar rule applies to transitions between levels which have J values differing by unity. In our approximation these rules are violated, though the ordinary sum rules are obeyed. This has the result that in the B type bands the branches with $\Delta J=0$ are robbed of a considerable fraction of their intensity while the $\Delta J=\pm 1$ branches are augmented by the same amount. In the A and C type bands the errors are in the opposite direction and are less serious.

Since the symmetrical rotator intensity expression must hold fairly well for transitions between the highest and lowest energy levels, respectively, it is evident that these errors must arise from a serious failure in the intermediate region. Besides the failure with respect to the normal transitions there are of course additional transitions which have no analog in the symmetrical rotator case. We have found it difficult to estimate the total contribution of these, though general considerations seem to show that it cannot be large. We shall assume that it may be ignored, which seems to be justified by the observations on the rotation spectrum of water vapor. Out of a total of well over two hundred lines of sufficient intensity to be observed only eight could be identified as due to anomalous transitions, and none of these was very strong.[6]

Considering this assumption to be justified it is possible to apply a simple correction to the

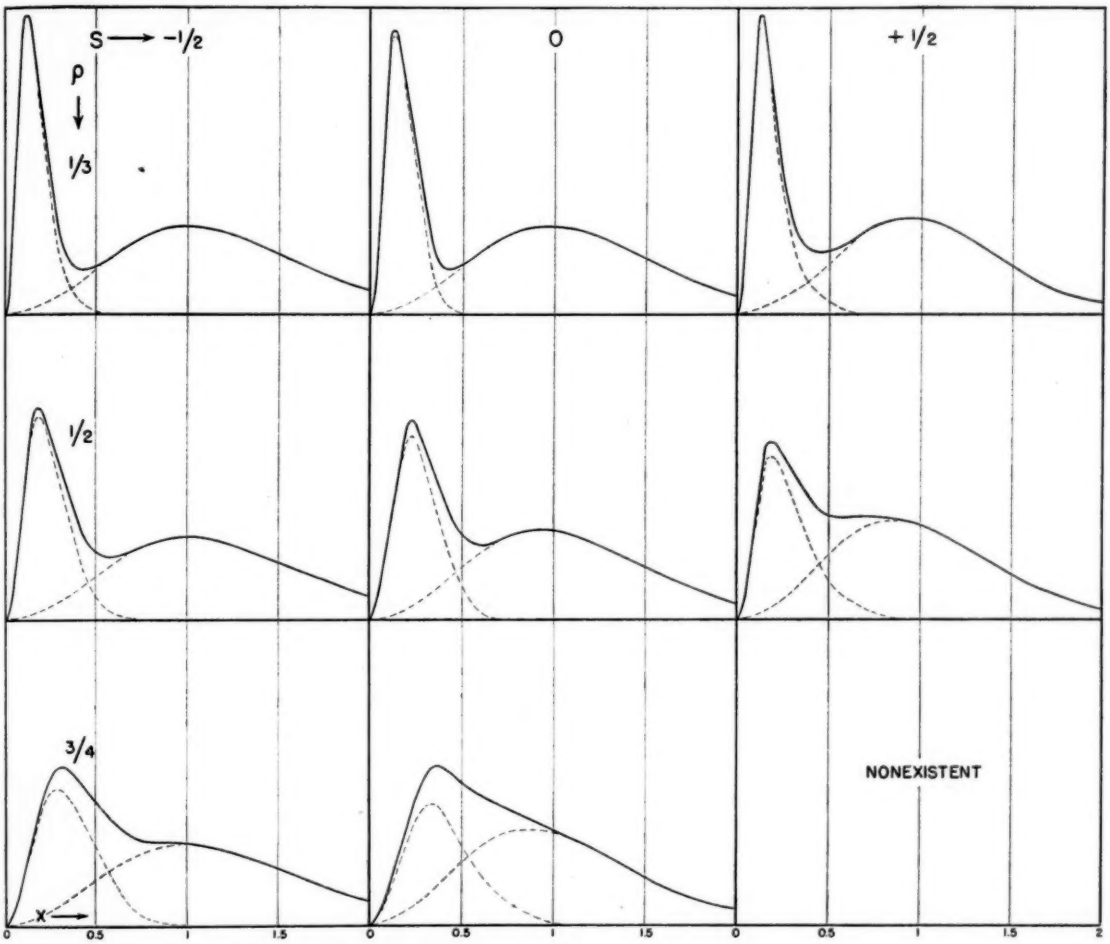

FIG. 3. The B bands (electric moment parallel to the intermediate axis of inertia).

band envelopes which takes into account the errors resulting from our approximation regarding the intensities. Actually of course we must expect that the symmetrical rotator expressions fit fairly well for the highest and lowest levels but fail more and more badly as one approaches the "intermediate" region. To compensate for this precisely would be difficult but it is simple to calculate two limiting envelopes between which the theoretically correct one should lie. In the one case one may assume that the intensity expressions are adequate except in the very center of the "intermediate" region where they abruptly fail, in the other case that they fail uniformly throughout.

In the former case the deficit or excess of the sum of probabilities for any set of transitions $(J \rightarrow J')$ may be accounted for by attributing it all to one transition in the very center of the "intermediate" region. Correction envelopes may then be calculated in a very simple manner, which have to be added to or subtracted from the envelopes obtained in our first approximation.

In the latter case the correction may be made by multiplying the probabilities of any given set of transitions by a constant factor. Since this factor is independent of J, one needs merely to multiply the ordinates of the $\Delta J=0$ and the $\Delta J=\pm 1$ branches by the appropriate constants before adding them to obtain the total envelope.

It turns out that the corrected envelopes obtained by these two different procedures do not differ materially. This is, of course, to be expected since in any given set of transitions the probability changes rather rapidly from one line to the next and a small part of the total set is

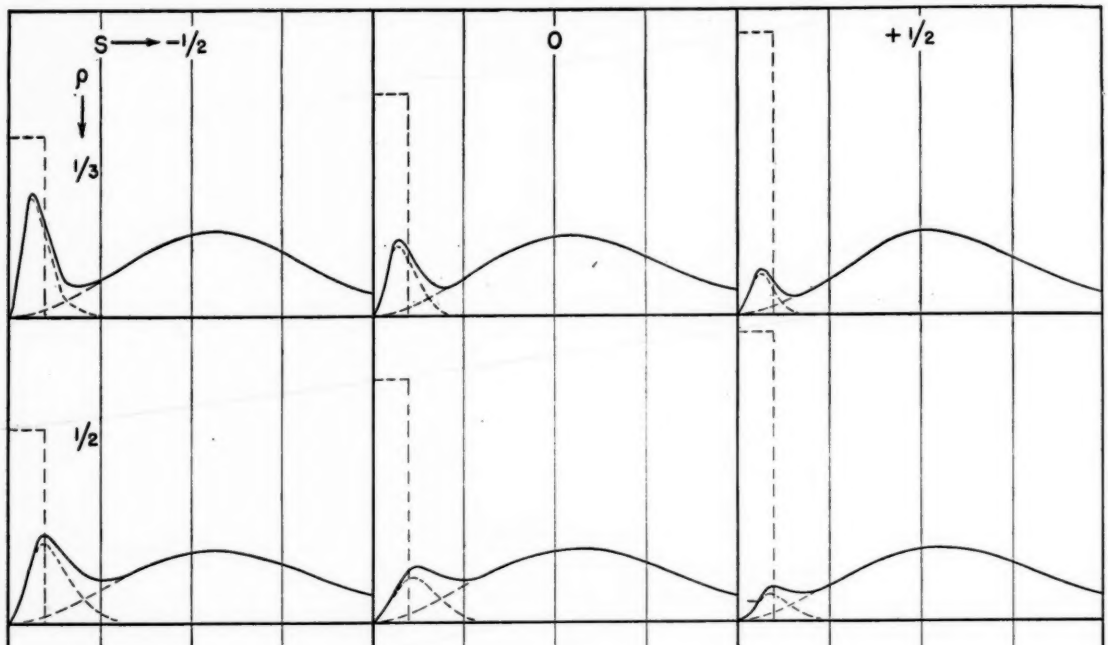

FIG. 4. The C bands (electric moment parallel to the major axis of inertia).

responsible for a large part of the intensity. Consequently we have been satisfied to calculate the envelopes by the second method and believe that they deviate less from the ideal theoretical ones than observed bands will normally do, owing to the nonrigidity of real molecules and other factors which we have not taken into account.

In Figs. 2, 3, 4 and 5 will be seen the three types of band envelopes for nine different sets of parameters. To save space only one-half the

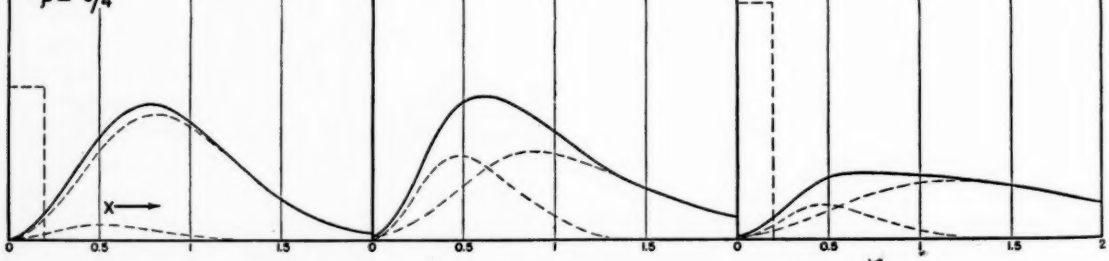

FIG. 5. The A, B and C bands for a molecule with $S=-\frac{1}{2}$ and $\rho=\frac{5}{4}$.

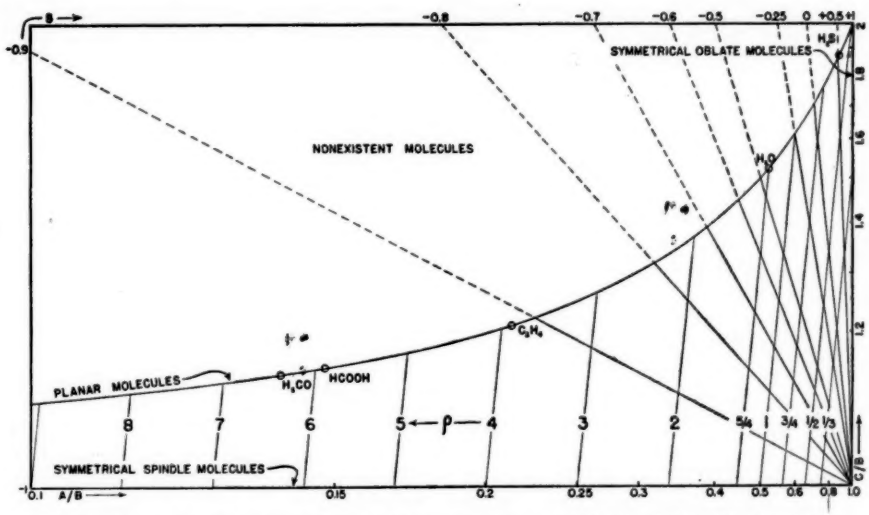

FIG. 6. Lines with constant S and with constant ρ plotted in a field with the dimensions a/b and c/b. The scales provided are in units of A/B and C/B rather than of the reciprocals.

band is shown in each case, with the origin at the left. The absorption coefficient has been plotted against x, where $x=(\nu-\nu_0)\pi(2B/kT)^{\frac{1}{2}}$, so that the figures are adaptable to molecules with any absolute moments of inertia and to any temperature. The frequencies are to be expressed in reciprocal seconds and B (the intermediate moment of inertia) and k in the usual units. The continuous lines represent the total envelopes while the dashed lines indicate the $\Delta J=0$ and the $\Delta J=\pm 1$ branches from which they are composed. In the A and C type bands the area of the dashed rectangle at the left represents one-half the amount of intensity in the collected "Q" branch. In the approximation to which we worked this branch should appear as a line of zero width. Actually this will not be the case, but in our experience the observed central branches have a width which is mainly due to the stretching of the molecule and to the difference in rotational constants in the normal and excited states and is much greater than would be expected for a rigid molecule with no interaction between rotation and vibration. In most cases this central branch can be well represented by a Gaussian function with width about $0.166x$ at half-height.

Our calculations have been confined to highly unsymmetrical and consequently little elongated molecules. These have been least investigated and seemed to us most interesting. The envelopes of spindle-shaped and slightly unsymmetrical molecules have become familiar through the investigation of several good examples.

Since one may wish to compare our curves with the envelopes of the "perpendicular" bands of the symmetrical rotator calculated by Gerhard and Dennison it may be worth while to call attention to the following facts. As S approaches $+1$ the A and B bands degenerate into perpendicular bands, which is likewise true of the B and C types when S approaches -1. In both limiting cases when $S=\pm 1$, $\rho S=-\beta$, where β is the parameter which Gerhard and Dennison have used to describe the symmetrical molecule.

Figure 6 may be of some assistance in the rapid estimation of the parameters S and ρ in any actual case. The lines of constant S and constant ρ are represented in a field with the dimensions a/b and c/b. For convenience the scales attached have been given in units of A/B and C/B, rather than of their reciprocals. Some molecules whose moments of inertia have been determined with some precision are located on the plot. It is of interest to note that in the extreme right portion of the figure the parameter S varies rapidly with the moments of inertia.

In a paper to follow we shall show how our calculated band envelopes have been of assistance in the interpretation of some observed bands.

Calculation of the Frequencies of the Symmetrical Modes of Vibration for Molecules with Various Types of Symmetry

H. J. BERNSTEIN
Chemistry Department, University of Toronto, Toronto, Canada

(Received August 1, 1938)

The secular equations for the frequencies of the symmetrical modes of vibration for molecules with various types of symmetry have been developed. The types of symmetry considered include a center of symmetry, and twofold, threefold, and fourfold axes of symmetry. Application to the problem of the configuration of oximes indicates that acetoxime has the following structural formula:

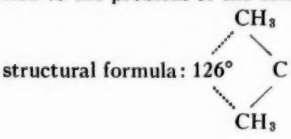

WHEN interpreting Raman spectra in terms of molecular models, it is customary to assume a certain configuration for the molecule, calculate the modes of vibration of such a molecule, and compare the calculated with the observed frequencies. For polyatomic molecules the calculation is very complicated and laborious, although the complete solutions have been given by others[1] for a number of molecular types. When there are a great many lines in the spectrum, it is, moreover, difficult to assign each observed line to a given mode of vibration of the model. The problem is greatly simplified if the data on the polarization of the Raman lines are available, since vibrations with a high degree of symmetry give rise to highly polarized lines (with depolarization factor approaching zero), while vibrations with lesser symmetry give rise to lines with depolarization factors approaching 6/7 as a limiting value.

It is indeed not necessary in most cases to calculate the frequencies of all the possible modes of vibration in order to decide whether an assumed molecular model is satisfactory. It is sufficient to calculate the frequencies of the symmetrical modes since these can be recognized in the spectrum if the depolarization measurements have been made. This calculation is much simpler than the complete calculation. The secular equations involving only the frequencies of the symmetrical vibrations have been developed for the following molecular types:

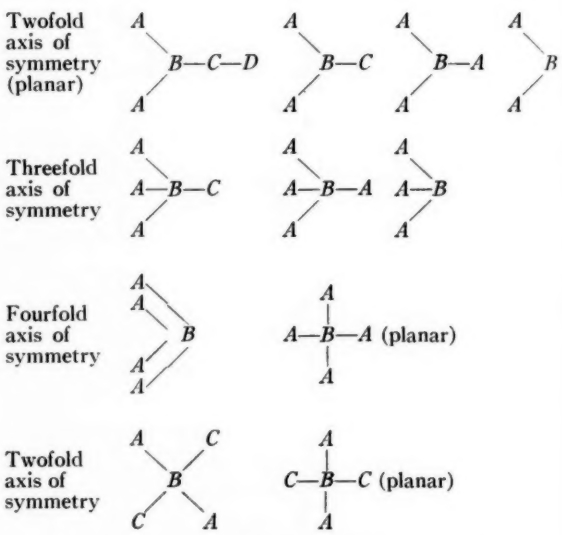

The equations will be developed for the first member of each of the above symmetry groups, and the equations for the special cases derived by simplification.

THE SECULAR EQUATION FOR THE SYMMETRICAL VIBRATIONS OF THE PLANAR CONFIGURATION

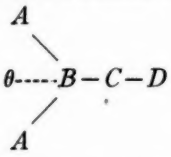

Since the discussion is limited to the symmetrical vibrations, it is sufficient to take one atom A as representative of the two.[2] The

[1] Dennison, Astrophys. J. **62**, 84 (1925).

[2] Glockler and Wall, J. Chem. Phys. **5**, 813 (1937).

atoms B, C, D are not to move out of the axis joining the three.

If m_a, m_b, m_c, m_d are the masses of the atoms A, B, C, D, respectively, and x_a, x_b, x_c, x_d their relative displacements in the x direction, then the kinetic and potential energies are given by

$$T=2/2m_a(\dot{x}_a^2+\dot{y}_a^2)+\tfrac{1}{2}m_b\dot{x}_b^2+\tfrac{1}{2}m_c\dot{x}_c^2+\tfrac{1}{2}m_d\dot{x}_d^2,$$

$$V=2/2K_1\xi_{ab}^2+\tfrac{1}{2}K_2\xi_{bc}^2+\tfrac{1}{2}K_3\xi_{cd}^2+2(2/2)d(r_{ab}\eta)^2,$$

where ξ_{ab}, ξ_{bc}, ξ_{cd} are the relative displacements of A with respect to B, B to C, C to D, respectively; $\eta=\theta-\theta_0$ (the displacement of the angle θ); K_1, K_2, K_3 are the force constants of the bonds $A-B$, $B-C$, $C-D$, respectively; and d is the deformation constant of the $\begin{matrix}A\\ \diagdown\\ B-\\ \diagup\\ A\end{matrix}$ group.

Since there are two atoms A, the first terms of the kinetic and potential energy expressions contain the factor 2. Since B, C, and D move in the x direction only, the expressions have no terms in y_b, y_c, y_d. The factor 2 is introduced into the last term of the potential energy expression since there are two angles (ABA and ABC) changing for each atom A—see treatment of Glockler and Wall.[2] If the configuration of the group $\begin{matrix}A\\ \diagdown\\ B-C-\\ \diagup\\ A\end{matrix}$ is approximately equilateral in the equilibrium position, the factor 2 can be used since for a small change in one of the angles there is an equal change in the other.

There exist linear relationships between the x's and y_a and the ξ's and η. From the geometry of the system it follows that

$$\xi_{ab}=(x_b-x_a)\cos\theta-y_a\sin\theta,$$

$$r_{ab}\eta=(x_b-x_a)\sin\theta+y_a\cos\theta,$$

$$\xi_{bc}=(x_c-x_b)\text{ etc.}$$

The secular equation is then

$$\begin{vmatrix} \alpha-2m_a\omega^2 & -\alpha & \beta & 0 & 0 \\ -\alpha & \alpha+K_2-m_b\omega^2 & -\beta & -K_2 & 0 \\ \beta & -\beta & \delta-2m_a\omega^2 & 0 & 0 \\ 0 & -K_2 & 0 & K_2+K_3-m_c\omega^2 & -K_3 \\ 0 & 0 & 0 & -K_3 & K_3-m_d\omega^2 \end{vmatrix}=0,$$

where

$$\alpha=2K_1\cos^2\theta+4d\sin^2\theta,$$

$$\beta=2(K_1-2d)\sin\theta\cos\theta,$$

$$\delta=2K_1\sin^2\theta+4d\cos^2\theta.$$

This becomes

$$\omega^8-L\omega^6+M\omega^4-N\omega^2+P=0, \qquad (1)$$

where

$$L=K_1\left(\frac{1}{m_a}+\frac{2\cos^2\theta}{m_b}\right)+K_2\left(\frac{1}{m_b}+\frac{1}{m_c}\right)+K_3\left(\frac{1}{m_c}+\frac{1}{m_d}\right)+2d\left(\frac{1}{m_a}+\frac{2\sin^2\theta}{m_b}\right),$$

$$M=K_1K_2\frac{2m_a\cos^2\theta+m_b+m_c}{m_am_bm_c}+K_1K_3\frac{m_bm_c+m_bm_d+(2m_am_c+2m_am_d)\cos^2\theta}{m_am_bm_cm_d}+K_2K_3\frac{m_b+m_c+m_d}{m_bm_cm_d}+2K_1d\frac{m_b+2m_a}{m_a^2m_b}+2K_2d\frac{2m_a\sin^2\theta+m_b+m_c}{m_am_bm_c}+2K_3d\frac{m_bm_c+m_bm_d+(2m_am_c+2m_am_d)\sin^2\theta}{m_am_bm_cm_d},$$

$$N=K_1K_2K_3\frac{2m_a\cos^2\theta+m_b+m_c+m_d}{m_am_bm_cm_d}$$
$$+2K_1K_2d\frac{2m_a+m_b+m_c}{m_a^2m_bm_c}$$
$$+2K_1K_3d\frac{m_bm_d+m_bm_c+2m_am_c+2m_am_d}{m_a^2m_bm_cm_d}$$
$$+2K_2K_3d\frac{2m_a\sin^2\theta+m_b+m_c+m_d}{m_am_bm_cm_d},$$
$$P=2K_1K_2K_3d\frac{2m_a+m_b+m_c+m_d}{m_a^2m_bm_cm_d}.$$

This equation gives the frequencies of the symmetrical modes of the model as in Fig. 1.

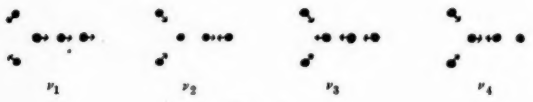

FIG. 1.

To obtain the secular equation for the symmetrical vibrations of the planar configuration

$$\begin{matrix} & & A \\ & \diagdown & \\ B & - & C \\ & \diagup & \\ & & A \end{matrix}$$

put $K_3=0$ in the equation for the pentatomic molecule (Eq. (1)). The equation thus obtained is identical with that obtained by the complete development for the simpler molecule.

The secular equation for the symmetrical vibrations of the triangular triatomic molecule

$$\begin{matrix} & & A \\ & \diagdown & \\ & & B \\ & \diagup & \\ & & A \end{matrix}$$

is obtained by putting $K_2=K_3=0$, and by substituting d for $2d$ since there are not two angles changing for each atom A. This gives the equation

$$\omega^4-\omega^2\left[K_1\left(\frac{1}{m_a}+\frac{2\cos^2\theta}{m_b}\right)+d\left(\frac{1}{m_a}+\frac{2\sin^2\theta}{m_b}\right)\right]$$
$$+K_1d\frac{2m_a+m_b}{m_a^2m_b}=0.$$

THE SECULAR EQUATION FOR THE SYMMETRICAL VIBRATIONS OF THE CONFIGURATION

$$\begin{matrix} & & A \\ & \diagdown & \\ A & - & B-C \\ & \diagup & \\ & & A \end{matrix}$$

Since the atoms A are symmetrical with respect to the threefold axis of symmetry, it is sufficient to take one of the atoms as representative of the three.

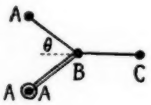

The kinetic and potential energies are given by

$$T=3\cdot\tfrac{1}{2}m_a(\dot{x}_a^2+\dot{y}_a^2)+\tfrac{1}{2}m_b\dot{x}_b^2+\tfrac{1}{2}m_c\dot{x}_c^2,$$
$$V=3\cdot\tfrac{1}{2}K_1\xi_{ab}^2+\tfrac{1}{2}K_2\xi_{bc}^2+2\cdot3\cdot\tfrac{1}{2}d(r_{ab}\eta)^2.$$

The secular equation is

$$\begin{vmatrix} \alpha-3m_a\omega^2 & -\alpha & \beta & 0 \\ -\alpha & \alpha+K_2-m_b\omega^2 & -\beta & -K_2 \\ \beta & -\beta & \delta-3m_a\omega^2 & 0 \\ 0 & -K_2 & 0 & K_2-m_c\omega^2 \end{vmatrix}=0,$$

where
$$\alpha=3K_1\cos^2\theta+6d\sin^2\theta,$$
$$\beta=3(K_1-2d)\sin\theta\cos\theta,$$
$$\delta=3K_1\sin^2\theta+6d\cos^2\theta.$$

This equation becomes

$$\omega^6-M\omega^4+N\omega^2-P=0, \qquad (2)$$

where

$$M=K_1\left(\frac{1}{m_a}+\frac{3\cos^2\theta}{m_b}\right)+K_2\left(\frac{1}{m_b}+\frac{1}{m_c}\right)$$
$$+2d\left(\frac{1}{m_a}+\frac{3\sin^2\theta}{m_b}\right),$$
$$N=K_1K_2\frac{3m_a\cos^2\theta+m_b+m_c}{m_am_bm_c}+2K_1d\frac{3m_a+m_b}{m_a^2m_b}$$
$$+2K_2d\frac{3m_a\sin^2\theta+m_b+m_c}{m_am_bm_c},$$
$$P=2K_1K_2d\frac{3m_a+m_b+m_c}{m_a^2m_bm_c}.$$

The secular equation for the symmetrical vibrations of a tetrahedral molecule $\begin{matrix} & A & \\ & \diagdown & \\ A-B-A & & \\ & \diagup & \\ & A & \end{matrix}$ is obtained by putting $K_2=K_1$ and $m_b=m_a$ in Eq. (2). The secular equation for the symmetrical vibrations of a pyramidal molecule $\begin{matrix} A & \\ \diagdown & \\ A-B & \\ \diagup & \\ A & \end{matrix}$ is obtained by putting $K_2=0$ in Eq. (2), and by substituting d for $2d$ since there is only one angle changing for each atom A.

The Secular Equation for the Symmetrical Vibrations of the Molecular Type

The kinetic and potential energies are given by

$$T=4\cdot\tfrac{1}{2}m_a(\dot{x}_a^2+\dot{y}_a^2)+\tfrac{1}{2}m_b\dot{x}_b^2,$$

$$V=4\cdot\tfrac{1}{2}K_1\xi_{ab}^2+4\cdot\tfrac{1}{2}d(r_{ab}\eta)^2.$$

The secular equation is

$$\begin{vmatrix} \alpha-4m_a\omega^2 & \beta & -\alpha \\ \beta & \delta-4m_a\omega^2 & -\beta \\ -\alpha & -\beta & \alpha-m_b\omega^2 \end{vmatrix}=0,$$

where

$$\alpha=4K_1\cos^2\theta+4d\sin^2\theta,$$

$$\beta=4(K_1-d)\sin\theta\cos\theta,$$

$$\delta=4K_1\sin^2\theta+4d\cos^2\theta.$$

The equation is therefore

$$\omega^4-\omega^2\left(\frac{K_1+d}{m_a}+\frac{\alpha}{m_b}\right)+K_1d\frac{m_b+4m_a}{m_a^2m_b}=0.$$

To obtain the secular equation for the planar configuration $\begin{matrix} & A & \\ & | & \\ A-B-A & & \\ & | & \\ & A & \end{matrix}$, we need only put $\theta=\pi/2$. In this case $\alpha=4d$, and the equation reduces to

$$\left(\omega^2-\frac{K_1}{m_a}\right)\left(\omega^2-d\frac{4m_a+m_b}{m_am_b}\right)=0.$$

The Secular Equation for the Symmetrical Vibrations of the Molecular Type

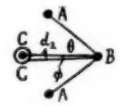

The kinetic and potential energies are given by

$$T=2\cdot\tfrac{1}{2}m_a(\dot{x}_a^2+\dot{y}_a^2)+\tfrac{1}{2}m_b\dot{x}_b^2+2\cdot\tfrac{1}{2}m_c(\dot{x}_c^2+\dot{z}_c^2),$$

$$V=2\cdot\tfrac{1}{2}K_1\xi_{ab}^2+2\cdot\tfrac{1}{2}d_1(r_{ab}\eta_1)^2+2\cdot\tfrac{1}{2}K_2\xi_{bc}^2+2\cdot\tfrac{1}{2}d_2(r_{bc}\eta_2)^2.$$

To obtain the equation for the planar type it is sufficient to put $\theta=\phi=\pi/2$. The secular equation then becomes $(\omega^2-K_1/m_a)(\omega^2-K_2/m_c)=0$ for the valence vibrations, and for the deformation vibrations

$$\begin{vmatrix} 2d_1-2m_a\omega^2 & -2d_1 & 0 \\ -2d_1 & 2d_1+2d_2-m_b\omega^2 & -2d_2 \\ 0 & -2d_2 & 2d_2-2m_c\omega^2 \end{vmatrix}=0.$$

The Structure of Acetoxime

In a previous investigation by the author[3] the Raman spectra of dimethyl-ketoxime (acetoxime), diethyl-ketoxime, and acetaldoxime were obtained. The spectra were interpreted satisfactorily on the basis of the following configuration for the symmetrical oximes

$$\begin{matrix} & R & \\ & \diagdown & \\ & C=N-OH. & \\ & \diagup & \\ & R & \end{matrix}$$

Treating the molecule from the dynamic point of view as of the type $\begin{matrix} & A & \\ & \diagdown & \\ B-C-D & & \\ & \diagup & \\ & A & \end{matrix}$ (in acetoxime A is the CH_3 group and D the OH group),

[3] Bernstein and Martin, Trans. Roy. Soc. Canada **31**, 105 (1937).

TABLE I.

RAMAN FREQUENCIES, cm^{-1}		MODE OF VIBRATION. SEE FIG. 1
CALC.	OBS.	
330	335	ν_1
795	812	ν_2
940	930	ν_3
1712	1682	ν_4

the frequencies of the symmetrical modes of vibration were calculated. The force constants were obtained from molecules in which the same groups appear. For example, the deformation force constant was obtained by calculations on the tetramethyl ethylene molecule, the N−O force constant from the hydroxylamine molecule, and the C=N force constant from the guanidine molecule.

It was necessary to make a decision between two possible lines in the Raman spectrum of acetoxime, which might arise from the deformation vibration. To make this decision we obtained the depolarization factors for these radiations and found that the line at 335 cm^{-1} was more polarized than the line at 474 cm^{-1}. The first line was therefore taken for the symmetrical deformation vibration.

To make the depolarization measurements two small pieces of polarizing film (Polaroid) were mounted in front of the slit of the spectrograph with their axes at right angles to each other, so that half the slit was covered by each piece. Thus two spectra are obtained, one immediately above the other, arising from the components of the scattered radiations polarized in directions parallel to and perpendicular to the path of the exciting beam. Density measurements were made with a Moll microphotometer, and the depolarizations obtained. An account of this method for obtaining depolarization data is being published in detail shortly.

The calculated and observed frequencies for the acetoxime molecule are given in Table I.

The closeness of the agreement is somewhat fortuitous, considering the assumptions used. The calculations however appear to assign definitely each of the four observed lines to one of the modes of vibration in Fig. 1. The observed frequencies were then used in Eq. (1) to obtain the force constants and the angle θ. The values are

$$2d = 0.66\times10^5 \text{ dynes per cm}$$
$$K_1 = 4.60\times10^5 \quad " \quad " \quad "$$
$$K_2 = 10.0\times10^5 \quad " \quad " \quad "$$
$$K_3 = 3.80\times10^5 \quad " \quad " \quad "$$
$$\theta = 63°.$$

The structure of acetoxime may therefore be represented by the planar configuration

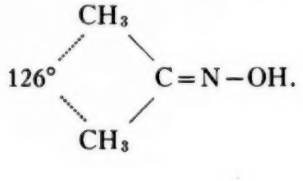

Modifications in the Near Infra-Red Absorption Spectra of Protein and of Light and Heavy Water Molecules When Water is Bound to Gelatin

JOSEPH W. ELLIS AND JEAN BATH
University of California, Los Angeles, California
(Received August 8, 1938)

Comparisons are made between the near infra-red absorption spectra of protein molecules in oven-dried gelatin and gelatin saturated with light and heavy water vapor respectively. The intensity of the first overtone valence N−H band at 1.50μ is greatly diminished by the addition of H_2O molecules, and this band is almost completely destroyed when D_2O molecules are taken on. The combination deformation-valence N−H bands at 2.05μ and 2.18μ are only partially destroyed in either instance. These facts suggest that the dipole moment oscillation of the N−H group constituting a part of the inter-molecular hydrogen bridge, C=O···H−N, is reduced when this bridge is broken and water molecules themselves become bridged to the N−H group; that the transverse dipole moment change is less affected than the parallel change; and that D_2O is much more effective than H_2O.

The 1.72μ and 2.28μ C−H bands do not change appreciably in intensity. However, at least the former shifts toward higher frequencies when water is taken on, indicating that the C−H groups are in a more vapor-like environment and corroborating the usual assumption that water molecules are attached only to the polar groups of the gelatin molecules.

The destruction of some of the usual absorption on the short and the long wave sides of the 1.44μ ($\nu_\sigma+\nu_\pi$) and 1.93μ ($\nu_\sigma+\nu_\delta$)H_2O bands indicates the nonexistence, or a reduction in number, of unperturbed vapor-like molecules as well as of the more highly perturbed molecules involving three and four hydrogen bridges. The presence of a sharpened and enhanced 1.79μ ($\nu_\sigma+\nu_\delta+\nu_R$) band indicates hindered rotation of H_2O molecules in a field more homogeneous than that in liquid water but having the same average value. A new weak band appears at 1.35μ and is believed to be ($\nu_\sigma+\nu_\pi+\nu_R$). Somewhat similar results occur with D_2O, requiring for complete interpretation, however, frequency contributions from hindered translation ν_T.

DURING the preparation of a monograph by Professor O. L. Sponsler on the subject of a molecular basis for a conception of protoplasm, embodying among other results those obtained at this institution by means of x-ray diffraction analysis, the question has arisen whether the methods of infra-red absorption spectroscopy can be used to corroborate some of the conclusions arrived at by other types of experimentation and reasoning. In particular, can use be made of the effects of hydrogen, or proton, bridging[1] upon certain well-identified absorption bands of molecules? We believe that the results thus far obtained indicate that these effects can be used.

The important types of protoplasmic materials are proteins, carbohydrates, fats and water. The scope of our investigations includes at least the first two and their interactions with water. Some preliminary results have been obtained with the protein of silk fibers and with the carbohydrates, sucrose crystals[2] and ramie cellulose fibers, using polarized infra-red waves in the region 1–2.5μ. Results which we believe to be more conclusive than these have been obtained with the protein gelatin, using unpolarized light. It is these results which are presented in the present paper. A preliminary report of this study already has been made.[3] Because of the variety in number and the complexities in form of the amino acid residues attached to the backbone of these long protein molecules in gelatin, as compared with the simple glycine and alanine residues of silk, and because of the presence of proline linkages in the backbone, the system being dealt with is complex. In spite of its complexity, gelatin is a protein upon which many different types of physical and chemical studies have been made. As a consequence, certain fairly definite conclusions have been deduced which lend themselves to spectroscopic verification.

In spite of the complexity of the gelatin molecule, its absorption spectrum in the 1–2.5μ region is relatively simple. In this region one has to deal

[1] For a comprehensive discussion of hydrogen bridges in organic compounds see Huggins, J. Org. Chem. **1**, 407 (1936). For recent summaries of and pertinent references to papers dealing with the spectroscopic consequences of hydrogen bridging see Gordy, J. Am. Chem. Soc. **60**, 605 (1938); also Errera and Sack, Trans. Faraday Soc. **34**, 728 (1938).

[2] Ellis and Bath, J. Chem. Phys. **6**, 221 (1938).
[3] Ellis and Bath, J. Chem. Phys. **6**, 108 (1938).

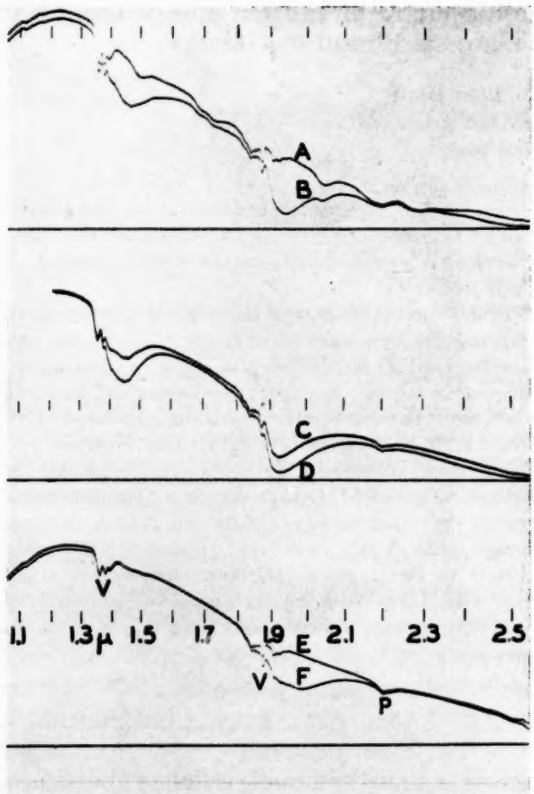

FIG. 1. A: 0.20 mm oven-dried gelatin. B: 0.28 mm gelatin+H_2O (weight of water 35.7 percent of total). C: 0.09 mm light water. D: 0.17 mm light water. E: Background distribution for F. F: 0.08 mm heavy water. G: 0.20 mm oven-dried gelatin. H: 0.30 mm gelatin+D_2O. I: 0.99 mm oven-dried gelatin. J: 1.49 mm gelatin+D_2O.

primarily, and perhaps entirely, with absorption bands associated with the overtone and combination vibrations of hydrogen atoms bonded to carbon, nitrogen and perhaps oxygen atoms. The only other type of oscillator which may have to be considered is the carbonyl group C=O. If the protein molecule is regarded as made up of approximately 300 amino acid molecules, then there exist on the backbone of the molecule this number each of C−H and C=O groups and about three-fourths of this number of N−H groups. The side chain residues contribute some thirty-one NH_2 groups, thirty-eight N−H, forty-nine O−H, eleven C=O groups and a large number of C−H pairs arising from CH, CH_2 and CH_3 groups.

In Fig. 1A is presented the absorption spectrum of a specimen composed of two sheets of gelatin, total thickness 0.20 mm, which had been oven-dried to constant weight at a temperature of 120°C. This spectrum was produced by the recording quartz spectrograph of the laboratory and is complicated by the presence of water vapor bands, *V*, of the atmosphere and by a quartz band, *P*, arising from the prisms. These vapor bands do not introduce appreciable difficulty when using such a spectrum with an appropriate background spectrum from which to obtain a percentage transmission curve, provided there is no change in the humidity of the room during the recording of the two spectra. Although there is no saving of time accomplished through the use of a recording instrument when it comes to reducing the records to a percentage transmission basis, nevertheless there is an obvious advantage in the use of such an instrument when the absorbing specimen is as optically imperfect as the typical sheet of gelatin. In the usual method of taking alternate galvanometer deflection readings with and without the specimen it becomes difficult to satisfactorily duplicate the alignment of the specimen in front of the slit.

Figure 1A shows five absorption bands of gelatin, none of them sharp, which we now interpret. The first overtone valence vibration band of NH and NH_2 occurs at 1.50μ. A band in this region is characteristic of primary and secondary amines[4] and its position in the spectrum is not particularly sensitive to the structure of the molecule. Similarly, the first overtone valence vibration band of CH, CH_2 and CH_3 groups oc-

[4] Ellis, J. Am. Chem. Soc. **49**, 347 (1927); **50**, 685 (1928).

curs at 1.72μ. At 2.05μ and 2.18μ are found bands arising from combinations of the fundamental valence and deformation vibrations of NH and NH_2; such bands also occur in the spectra of primary and secondary amines[3] and are structure-sensitive. In the spectrum of a molecule having an axis of symmetry coincident with the line of an N−H pair these two bands should coincide because of the degeneracy in the deformation vibration. A band resulting from a combination of the fundamental valence and deformation vibrations of C−H groups is found at 2.28μ. No bands characteristic of O−H groups appear, probably because there are few such groups. No apparent C=O band is found in this record; any C=O contribution falling within this region would arise from higher orders of overtones than are associated with the five bands just cited. Neither in this nor in the spectra of thicker oven-dried samples which we have studied do we find any evidence of residual water in the gelatin. This leads us to believe that the band at 3μ found by Buswell, Krebs and Rodebush[5] in the spectrum of a similarly prepared specimen and attributed by them to residual water in reality is produced by N−H valence vibrations.

When a gelatin sheet is allowed to stand in an atmosphere of ordinary water vapor it absorbs a maximum amount of water equal to about 35 percent of the total resulting weight. Such water is said to be bound to the gelatin. This process is accompanied by a 40 percent increase in thickness and a 6 percent increase in area. The amount of water taken on is the amount anticipated, provided every C=O, N−H, NH_2 and O−H group, unless restricted by space limitations, has attached to it the maximum number of water molecules possible through the mechanism of hydrogen bridging. It was anticipated, therefore, that if the spectrum of such a swollen sample were recorded and the absorption bands of the bound water plotted through a comparison of the records for dry and saturated gelatin specimens, differences should appear between these bands and those characteristic of an equivalent amount of ordinary water. Fig. 1B shows the record for such a specimen.

[5] Buswell, Krebs and Rodebush, J. Am. Chem. Soc. **59**, 2603 (1937).

In Fig. 2A there is plotted against wave-lengths the percentage transmission of a 0.08 mm layer of ordinary distilled water at 22°C. This was obtained by dividing the ordinates in a 0.17 mm record, Fig. 1D, by those in a 0.09 mm record, Fig. 1C, and multiplying throughout by a factor obtained from the ratio of ordinates at some wave-length where there is no absorption. This procedure corrects for an inability to adjust the galvanometer deflections between two records and also corrects for reflection losses. In this spectrum are seen the well-known broad bands at 1.44μ ($\nu_\sigma+\nu_\pi$) and 1.93μ ($\nu_\sigma+\nu_\delta$) as well as the weaker band at 1.79μ ($\nu_\sigma+\nu_\delta+\nu_R$). Here ν_π and ν_σ are the frequencies of symmetrical and unsymmetrical valence vibrations, respectively, ν_δ and ν_R those of deformation vibration and hindered rotation respectively. The width of the slits is indicated by the width of the vertical line marked *S* on the graph.

In Fig. 2B is the percentage transmission curve for an amount of water equivalent to that in Fig. 2A, but bound to gelatin. It was obtained by a reduction of the data of Figs. 1A and 1B. Several significant differences between the spectra of Fig. 2A and 2B appear. Although the gelatin-bound water band at 1.44μ is slightly deepened, portions of both its short and long wave-length sides are missing. The sharpening on the short wave side was anticipated and is associated with the absence of free vapor-like molecules. It is

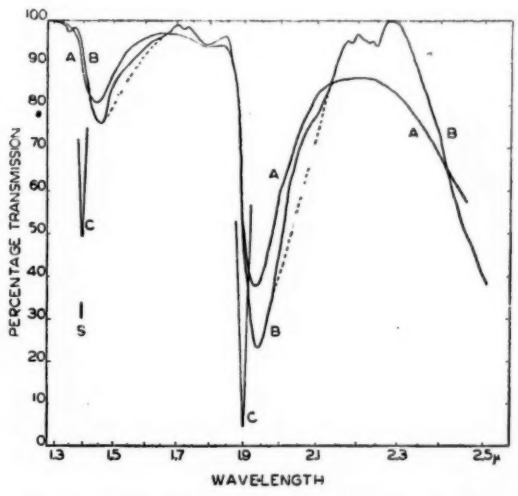

FIG. 2. A: 0.08 mm light water. B: 0.08 mm gelatin-bound light water. C: H_2O in CCl_4.

believed[6] that there are some free unassociated molecules in liquid water. That the extreme short wave side of the band is the location for the contribution of free molecules is indicated by the sharp band plotted in Fig. 2C which represents the greatly enhanced central Q-branch[7] as it appears in the partially resolved vapor-like rotation-vibration band of water molecules in dilute CCl_4 solution.

In our interpretation of the alteration of the long wave portion of the 1.44μ band, we are guided by an analysis of the Raman bands of water by Cross, Burnham and Leighton.[8] They regard the water-vapor molecule so far as its valence vibrations are concerned, as made up of two coupled O−H oscillators, and the molecule of liquid water as such a molecule perturbed through hydrogen bridges by one, two, three or four other molecules. Their picture of the liquid water state is that of Bernal and Fowler.[9] Cross, Burnham and Leighton assume that the shift of frequency from the vapor position resulting from perturbation is greater when the oscillating molecule is the donor of the hydrogen in the bridge than when it is the acceptor. They also assume that the effects of perturbation are additive, the molecules which undergo the maximum fourfold perturbation contributing to the portion of the band furthest away from the vapor-like position. The absorption throughout the region 1.6–1.7μ in Fig. 2A is real and must be interpreted as the contribution to the 1.44μ band by molecules which are most highly perturbed, that is, perturbed by three and four hydrogen bridges. The fluctuating conditions of the liquid state can account for the continuity of absorption in such a band. The total width in frequency units of the 1.44μ ($\nu_\sigma+\nu_\pi$) band is considerably greater than the width of the Raman band (ν_π) or of the infrared band (ν_σ) in the 3μ region.[7] This is to be expected from the theory of perturbation. In fact, a comparison of the separation $\Delta\nu$ of perturbed and unperturbed O−H bands of alcohols in the fundamental[10] and first overtone[11] regions shows that the latter is about 13/5 as great as the former. This is the amount predicted by the quantum mechanics first order perturbation expression, $\Delta\nu \propto (2v^2+2v+1)$, in which v is the vibration quantum number.

The disappearance in Fig. 2B of some of the absorption in the 1.6–1.7μ region indicates that the gelatin-bound water molecules are in general not subjected to three and fourfold perturbations. This is consistent with the assumed model, which permits the absorbing water molecule to have no more than a twofold perturbation by N−H and C=O groups. The 1.44μ band in Fig. 2B seems to have two distinct parts, indicating two distinct types of perturbation. We shall show later that this interpretation is incorrect.

In the 1.93μ ($\nu_\sigma+\nu_\delta$) band of Fig. 2A–C occur effects similar to those in the 1.44μ band, and we offer similar explanations. The alteration of the long wave portion is even more noticeable than in the previous instance. The lesser alteration of the short wave portion, resulting in a smaller displacement of the whole band than in the 1.44μ band, is to be expected; for, the 1.93μ band should show some of the characteristics of both fundamentals, ν_σ and ν_δ, of which it is the combination. As pointed out by Cross, Burnham and Leighton,[8] and perhaps as shown even better by the hydration experiments of Ganz,[12] ν_δ behaves oppositely to ν_σ in regard to shifting when perturbed through hydrogen bridging, That is, ν_δ shifts to a higher frequency.

The behavior of the 1.79μ ($\nu_\sigma+\nu_\delta+\nu_R$), as displayed by Fig. 2A–B, is interesting. The existence of this band was first discovered by one of us,[13] was later challenged by Miss Kellner,[14] and finally was made a subject of special study by Collins.[15] It arises from simultaneous excitations of oscillation frequencies ν_σ and ν_δ and the hindered rotation frequency ν_R (510 cm^{-1}). It is interesting to notice that this band has the same location in liquid and gelatin-bound water, but is sharpened and intensified in the latter instance. These facts indicate that the potential field in which the absorbing molecule swings in hindered rotation in the gelatin medium is of the same magnitude but more homogeneous than in water.

[6] Kinsey and Ellis, Phys. Rev. **51**, 1074 (1937).
[7] Ellis and Kinsey, Phys. Rev. **54**, 599 (1938); also reference 6.
[8] Cross, Burnham and Leighton, J. Am. Chem. Soc. **59**, 1134 (1937).
[9] Bernal and Fowler, J. Chem. Phys. **1**, 515 (1933).
[10] Errera and Mollet, Nature **138**, 882 (1936).
[11] Kinsey and Ellis, J. Chem. Phys. **5**, 399 (1937).
[12] Ganz, Ann. d. Physik **28**, 445 (1937).
[13] Ellis, Phys. Rev. **38**, 693 (1931).
[14] Kellner, Proc. Roy. Soc. **159**, 410 (1937).
[15] Collins, Phys. Rev. **52**, 88 (1937).

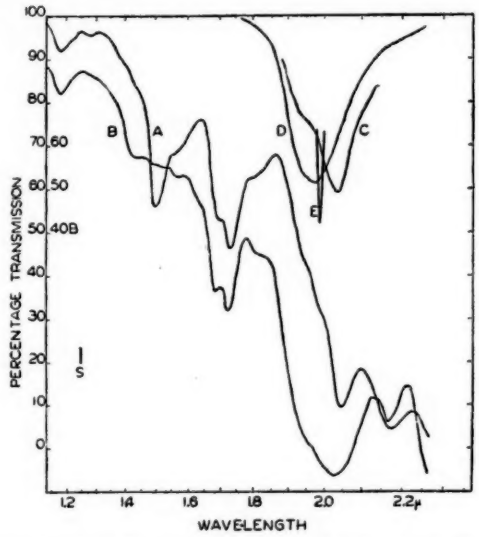

FIG. 3. A: 0.99 mm oven-dried gelatin. B: 1.49 mm gelatin + D_2O. (Percentages in B have been displaced downward 10 percent.) C: 0.30 mm gelatin + D_2O. D: 0.08 mm D_2O. E: D_2O in CCl_4.

This effect of intensification is probably responsible for the appearance for the first time of a weak band at 1.35μ, also shown in Fig. 2B. This we interpret as $(\nu_\sigma+\nu_\pi+\nu_R)$.

A similar effect is doubtless responsible for the unequal rates of descent toward the 2.6μ region in which $(\nu_\sigma+\nu_R)$ is located.

The irregularity in Fig. 2B at 1.7μ is caused by the nonsuperposition of C−H bands in this region. The slight shift in the C−H bands producing this irregularity is clearly shown in Fig. 1I–J, representing the effects of bound heavy water, and will be discussed more fully later. Peculiarities of absorption in the 2.2–2.3μ region will also be discussed later.

It was our opinion, after inspecting Fig. 2B, that we were wrong in our original assumption that the gelatin bands would not be greatly altered upon saturating the specimen with water. We conclude that the 1.50μ and 2.05μ N−H bands diminished appreciably in intensity, thus falsifying in Fig. 2B the shapes of the two water bands which overlap these N−H regions. Guided by Fig. 2A, we have drawn with broken lines the probable contours that would appear if there were no falsification. We thus estimate that the 1.50μ and 2.05μ NH bands have diminished to at least one-half and three-fourths of their original intensities, respectively.

To test the preceding assumption we repeated the experiments outlined above, using 99.9 percent heavy water whose absorption bands do not overlap the 1.44μ region. During the first attempt it was found that condensation of heavy water was occurring on the glass plates between which the gelatin specimens were sealed. This was caused by an air jet which, as in the previous experiments, was used to keep the temperature from rising. Consequently, the air jet had to be dispensed with and the plates dried and resealed. The spectrum showed the presence of light water. Replacement of H atoms of the protein by D atoms from the heavy water was suspected. But the probability of this having happened was removed when, upon drying the specimen, it was found to yield the same N−H and C−H bands and no new ones. The experiment was again repeated with every precaution taken to prevent contamination with light water vapor. The record, showing no light water absorption at 1.44μ and perhaps none at 1.93μ, is shown in Fig. 1H. A dry specimen record is given in Fig. 1G for comparison.

The suspicion of falsification of the absorption bands of Fig. 2B is now corroborated. For, with heavy water the 1.50μ N−H band is completely removed and the 2.05μ and 2.18μ N−H bands are greatly reduced in intensity. It is also apparent from Fig. 1G–H that there is a continuous absorption, extending from the 2.05μ band to 2.42μ ,which characterizes the oven-dried gelatin spectrum. This continuous absorption is greatly diminished in the spectrum of the water-bound specimen.

To demonstrate further the effects referred to in the preceding paragraph, the experiment was repeated with specimens which were five times as thick as before. These were made by immersing ten sheets of gelatin in a mixture of CCl_4 and CS_2. Thus by matching the index of refraction of the mixture with that of the gelatin, it was possible to make a fairly transparent specimen. CCl_4 and CS_2 are the two common liquids which do not have absorption bands of their own in the region studied. They mix readily and fortunately have indices below and above that of gelatin, respectively. The records for 0.99 mm oven-dried and 1.49 mm D_2O saturated specimens are shown in Fig. 1I–J.

The records of Fig. 1I–J have been reduced to percentage transmission curves, using an appropriate background record. These curves are plotted in Fig. 3A–B. The deep 1.50μ N−H valence band of Fig. 3A is nearly, or possibly entirely, gone in Fig. 3B. Because of the appearance of a complicated structure in the N−H valence bands of primary and secondary amines, it is impossible to say if the long wave shoulder of this band is to be attributed to N−H valence oscillators which are more highly perturbed than those contributing to the deeper short wave portion of the band. That there is such an effect in aniline, a primary amine, has been shown by Kinsey and Ellis [11] through the disappearance of the long wave portion of the 1.5μ band when aniline is dissolved in CCl_4. A search for a similar effect in a secondary amine, di-*n*-butylamine, during the present investigation led to negative results. All, or most, of the gelatin N−H oscillators contributing to the 1.50μ gelatin band must be perturbed by hydrogen bridging according to the model of Astbury and Lomax.[16] The bridges should occur between the N−H groups of one molecule and the C=O groups of another.

The surprising thing in connection with the 1.50μ band is its partial disappearance when H_2O molecules are attached to the N−H groups and its almost complete disappearance when D_2O molecules are attached. It is not likely, in view of the relative strengths of ordinary chemical bonds and hydrogen bridges, and also in view of the nature of the spectrum resulting when a D_2O swollen specimen had been carefully re-dried, that the N−H groups are actually destroyed by the addition of water. It is more likely that the dipole moments in the N−H groups have been greatly reduced when the water molecules are bridged to them, and that D_2O is much more effective than H_2O. Also it is possible that the C=O···H−N bridging enhances the intensity of the band of the dried gelatin. This possibility is suggested by the results of Gordy[17] which show that the intensities of the N−H fundamental valence bands of aniline and the C=O fundamental valence band of acetone are both enhanced when these two liquids are mixed. This effect, as Gordy suggests, probably results from C=O···H−N bridging. A more startling, but less analogous, example of such an intensity alteration is found in the 100-fold increase of absorption by H_2O molecules in solutions of dioxane or pyridine[18] over the absorption that they possess in the inactive solvents CCl_4 and CS_2. It should be pointed out in this connection that Fig. 2A–B shows that the total absorption by water molecules is not increased when these are bound to gelatin. If the preceding analysis is correct, a cause for the opposite effects produced by C=O and D_2O (and H_2O) may be that in the former instance the N−H group is the donor of the H for the bridge, whereas in the latter instance it may be the acceptor as well as the donor.

The 2.05μ and 2.18μ N−H bands behave similarly to the 1.50μ band, but to a lesser degree. Fig. 1G–H clearly shows that these bands have intensities diminished when D_2O is added. That there is a similar but smaller effect with H_2O is seen from the appearance of Fig. 2B in the regions 2.05μ and 2.18μ, Only a small portion of this diminution could be caused by the 6 percent increase in area of the gelatin specimen when the water is taken on. The difference in the behavior of the 1.50μ and the 2.05μ, 2.18μ bands may be caused by a smaller alteration of the dipole moment change perpendicular to the N−H groups than parallel to the groups. The oscillations producing the 2.05μ and 2.18μ bands have transverse components.

The best explanation for the presence of continuous absorption in the 2.18–2.42μ region of the spectrum of the dried gelatin is that in this region there are long wave contributions to the 2.05μ and 2.18μ bands similar to the shoulder of the 1.50μ band. These long wave contributions may arise from the more highly perturbed N−H or NH_2 groups. Variations in the strength of the hydrogen bridge may be caused by the frequent occurrence of proline linkages in the backbone. These proline linkages probably cause a warping in the backbone, resulting in closer approaches of some C=O and N−H groups than of others. It is possible that the investigation of silk, in which there are fewer proline linkages, will give additional information in this respect.

[16] Astbury, Trans. Faraday Soc. **29**, 193 (1933); Astbury and Lomax, J. Chem. Soc. London, p. 846, June, 1935.
[17] Gordy, J. Am. Chem. Soc. **59**, 464 (1937).
[18] Errera, Physica **4**, 1097 (1937).

Figure 3A shows a weak band at 1.28μ and a very weak one at 1.22μ which disappear in Fig. 3B. These bands doubtless bear the same relation to the 1.50μ overtone as the 2.18μ and 2.05μ bands bear to the valence vibration fundamental near 3.0μ.

The 1.18μ, 1.72μ and 2.28μ bands arise from C−H vibrations. The most conspicuous of these, namely the one at 1.72μ, shifts toward shorter wave-lengths upon the addition of water, as is clearly shown by Figs. 1I–J and 3A–B. This is to be expected since the C−H groups contributing to it have fewer near neighboring atoms when the gelatin molecules are pushed apart by water molecules. No bridging of water molecules to C−H groups is probable. This shift toward shorter wave-lengths when conditions are more vapor-like for the C−H groups is consistent with general observations of differences in band positions in vapor, liquid and solution spectra.[19] Some of the change of form in the 1.72μ band is doubtless significant. However, it is also partly caused by a partially overlapping D_2O band.

Weak absorption bands at 1.94μ and 1.99μ in Figs. 1I and 3A may well be attributed to carbonyl groups C=O.[20]

The main band of D_2O occurs at 1.98μ. This is $(\nu_\sigma+\nu_\pi)$. Its position in Fig. 3B is certainly too far to the right, owing to the overlapping of a residual of the 2.18μ N−H band. This band is also shown in Fig. 3C, which is a similar reduction of the record of Fig. 1H. Fig. 3B–C shows a short wave-length shoulder in this band. This absorption and that at 1.44μ in Fig. 3B indicate that there has been slight contamination by light water. That the short wave portion of the 1.98μ band is not entirely caused by light water impurity is shown by Fig. 3D. This represents a reduction of the record for the 0.08 mm sample of 99.9 percent D_2O shown in Fig. 1F. This record shows no impurity band at 1.44μ. The additional 1.9μ contribution can arise from $(\nu_\sigma+\nu_\pi+[\nu_T, \nu_R])$ and is analogous to $(\nu_\delta+[\nu_T, \nu_R])$ found by Ellis and Sorge[21] at 6.85μ. Here ν_T and ν_R are the frequencies of hindered translation and hindered rotation. That we are dealing with the weighted unresolved mean $[\nu_T, \nu_R]$ of these two frequencies follows from Cartwright's[22] measurements of the magnitudes of these frequencies, 160 cm^{-1} and 360 cm^{-1}, respectively. The center of the broad 6.85μ is separated by 240 cm^{-1} from the 8.20μ(ν_δ) band. It was pointed out by Ellis and Sorge that the extramolecular absorption contributing to the 6.85μ band and to the 1.56μ band $(\nu_\sigma+\nu_\pi+\nu_\delta+[\nu_T, \nu_R])$ is more intense than that contributing to corresponding bands in light water. The 1.56μ band is clearly shown in Figs. 1H and 3B. Also the 1.65μ band $(\nu_\sigma+\nu_\pi+\nu_\delta)$ associated with the 1.56μ is seen best in Fig. 1H.

In Fig. 3E is drawn a portion of the partially resolved $(\nu_\sigma+\nu_\pi)$ band of D_2O in CCl_4 solution.[7] Because of the similarity between this and the corresponding bands of Fig. 2C we identify this as the unresolved *Q*-branch of D_2O vapor-like molecules. That a considerable portion of the liquid band lies to the left of this sharp 1.98μ band, in contrast to the H_2O band behavior at 1.44μ, indicates again that there is an additional contribution in this instance.

[19] Ellis and Kinsey, J. Chem. Phys., **6**, 497 (1938).
[20] Ellis, J. Am. Chem. Soc. **51**, 1384 (1929).
[21] Ellis and Sorge, J. Chem. Phys. **2**, 559 (1934).
[22] Cartwright, Phys. Rev. **49**, 470 (1936).

Wave Functions and Potential Curves for Excited H_2

ALBERT SPRAGUE COOLIDGE AND HUBERT M. JAMES
Harvard University, Cambridge, Massachusetts, and Purdue University, Lafayette, Indiana

(Received August 29, 1938)

Results on wave functions and energy values for the $1s\sigma 2p\sigma\,^3\Sigma_u$ and $1s\sigma 2s\sigma\,^3\Sigma_g$ states of H_2, obtained by a variational method, are given. The nuclear separations considered range from $1.3a_H$ to $2.9a_H$. The errors in the computed energies for the $^3\Sigma_u$ state are of the order of 0.001 atomic unit, while the computed energies for the $^3\Sigma_g$ state are in general more accurate. Root-mean-square errors in the wave functions are of the order of 2 percent.

IN order to carry out a calculation of the energy distribution in that continuous spectrum of H_2 which is produced by transitions from the stable $1s\sigma 2s\sigma\,^3\Sigma_g$ state to the repulsive state $1s\sigma 2p\sigma\,^3\Sigma_\mu$, we have required reasonably accurate approximations to the electronic wave functions of these states, and knowledge of the respective potential curves, over a considerable range of nuclear separation. To determine the electronic functions and the repulsive potential curve the only available method of adequate accuracy is that applied by us to the treatment of the ground state[1] and extended by Present and ourselves[2, 3] to various two-quantum excited states of this molecule. In these latter papers will be found computed wave functions and energies for one nuclear separation in the case of the $^3\Sigma_g$ state,[2] and three in the case of the $^3\Sigma_u$ state.[3] We here report on extensive calculations on both states by this method, of high accuracy and covering the range from $R=1.3a_H$ to $R=2.9a_H$. A complete description of the method will be found in the references given, the notation of which will be used in the present report.

Before presenting our numerical results, a discussion of their theoretical significance may be in order. It is well understood that the familiar two-stage method of treating molecular problems in quantum mechanics is based upon a forced separation of variables, whereby certain small terms are ignored. The resulting errors in the wave functions are undoubtedly negligible in comparison with those which are introduced by the further approximations (such as the use of a finite number of terms in a series) upon which it is necessary to fall back in order to treat the electronic motion in the separated problem. On the other hand, the energy values are more accurate than the wave functions with which they are obtained, and in comparing them with experiment the separation errors should be considered.

Van Vleck[4] has discussed the corrections to be applied to computations of energy levels based on the separation of nuclear and electronic coordinates, assembling formulas for the first- and second-order perturbations arising from all terms neglected in such treatments. He omits from consideration spin terms in the energy, negligible in H_2. According to Van Vleck, all diagonal perturbation terms (i.e., terms arising between states having the same electronic quantum numbers) may be accounted for by using a potential curve corrected at each value of R (the nuclear separation) by adding to the energy of the corresponding fixed-nuclei problem three small terms $P_{nn}(R)+Q_{nn}(R)+S_{nn}(R)$. (For infinite separation, this correction becomes just that required to convert the fixed- into the free-nuclei problem, and we may call it the correction for nuclear motion.) Insofar as nondiagonal perturbations can be neglected, this corrected potential curve should agree with the empirical potential curve which reproduces observed energy levels (to the degree to which such an empirical curve is defined). It is such a comparison that we make in this paper. Nondiagonal perturbations cannot be expressed as corrections to a computed potential curve, and prevent the exact representation of observed energy levels by any empirical potential curve. Our comparison of theory with experi-

[1] H. M. James and A. S. Coolidge, J. Chem. Phys. **1**, 825 (1933).
[2] R. D. Present, J. Chem. Phys. **3**, 122 (1935).
[3] H. M. James, A. S. Coolidge and R. D. Present, J. Chem. Phys. **4**, 187 (1936).
[4] J. H. Van Vleck, J. Chem. Phys. **4**, 327 (1936).

ment thus depends for its validity on the absence of such perturbations, which fortunately seem to be safely negligible in the present cases.

The Repulsive State $1s\sigma 2p\sigma\,{}^3\Sigma_u$

Wave functions for this state have already been given for $R=1.5$, 1.6, and 1.87.[3] (R is the internuclear distance in Bohr radii.) Of these, the first, which was based upon a careful selection of terms, was retained for the present work. The second was not used, as the difference in R was too small, while the third was discarded because it seemed likely (and proved true) that a better function could be constructed by including some terms which had proved to be useless at the smaller R. New functions were computed for $R=1.3$, 1.7, 1.87, and 2, using 12 terms of a series with the same form:

$$\psi=\sum_{mnjkp} C_{mnjkp}[mnjkp],$$

where

$$[mnjkp]=\frac{1}{2\pi}\{e^{-\delta_1\lambda_1-\delta_2\lambda_2}\lambda_1{}^m\lambda_2{}^n\mu_1{}^j\mu_2{}^k - e^{-\delta_2\lambda_1-\delta_1\lambda_2}\lambda_1{}^n\lambda_2{}^m\mu_1{}^k\mu_2{}^j\}\rho^p,$$

with $j+k$ odd, $\delta_1=0.5$, and $\delta_2=1$. (We wish to acknowledge our indebtedness to Dr. Present for the use of his tables of matrix elements in this part of our work.)

For larger separations it was clearly necessary to work with larger values of the exponential parameters, and, indeed, it seemed probable that a series of a different form might be found to converge more rapidly. The series previously used may be regarded as developed from a leading term which describes a $1s\sigma$ and a $2p\sigma$ molecular orbital, and is thus adapted to the "united atom" or Hund-Mulliken point of view. At a large enough distance, we know that the "separated atom" or Heitler-London point of view must be correct; it therefore seemed promising to explore the possitilities of a series with the Heitler-London (or the Wang) function as its leading term. Such a series (which we may call the H-L series) is that having the typical term

$$[mnjkp]=\frac{1}{2\pi}e^{-\delta(\lambda_1+\lambda_2)}\rho^p \times[\lambda_1{}^m\lambda_2{}^n\mu_1{}^j\mu_2{}^k(e^{\delta(\mu_1-\mu_2)}-(-1)^{j+k}e^{-\delta(\mu_1-\mu_2)}) - \lambda_1{}^n\lambda_2{}^m\mu_1{}^k\mu_2{}^j(e^{\delta(\mu_2-\mu_1)}-(-1)^{j+k}e^{-\delta(\mu_2-\mu_1)})].$$

Table I.

Series	Number of Terms (none involving r_{12})	Energy (atomic units)	Number of Terms (some involving r_{12})	Energy
H-L	8	−0.9430		
One-parameter	13	−0.9440	14	−0.9450
Two-parameter	14	−0.9430	16	−0.9446

A third possibility is the "one-parameter" series in which δ_1 and δ_2 of the two-parameter series are taken equal to each other, thus dropping the distinction between the normal and the excited electron, but retaining the molecular, rather than the atomic character of the orbitals.

For an orienting calculation, the distance $R=2.5$ was selected, using $\delta=1.25$ in the H-L and one-parameter series, and $\delta_1=\frac{5}{6}$, $\delta_2=\frac{5}{3}$ in the two-parameter series, so that (for the second and third series) the values of the δ's might bear to each other and to R the same ratio as in Present's corresponding exploration at $R=1.5$. The results of this calculation are given in Table I. Except with the one-parameter series, no careful search was made for the best possible selection of terms. It appears that, in agreement with expectation, the H-L series is the most rapidly converging, and, contrary to the case when $R=1.5$, the one-parameter series is somewhat superior to the two-parameter one. The latter fact may be referred to the slightness of the promotion effect upon the $2p\sigma$ electron at this distance.

In spite of its slight inferiority to the others, the two-parameter series was selected for the final computations, since, on the one hand, it seemed good enough for our purposes if sufficient terms were taken, and, on the other, it was found to be suitable for the ${}^3\Sigma_g$ state, and a great saving of labor could be secured by using the same series for both states. Doubtless the H-L series could also have been made to serve for both states, but the computations with this series were much complicated by the exponentials in the μ's, and it was therefore rejected. Functions using 16 terms of the two-parameter series were calculated for $R=2.1$, 2.3, 2.5, 2.7, and 2.9.

In Table II are shown the coefficients of all functions for the repulsive state, the energies actually computed, and the estimated convergence limits. In stating the extrapolated energy

TABLE II. *The $1s\sigma 2p\sigma\,^3\Sigma_u$ state.*

	$\delta_1=1/2,\ \delta_2=1$					$\delta_1=5/6,\ \delta_2=5/3$				
R IN aH	1.3	1.5	1.7	1.87	2.0	2.1	2.3	2.5	2.7	2.9
				Energy values						
Calc. (at. units)	−0.75406	−0.80906	−0.85021	−0.87781	−0.89492	−0.90849	−0.92870	−0.94460	−0.95687	−0.96587
Extrap. (at. units)	−0.756	−0.810	−0.851	−0.879	−0.896	−0.910	−0.930	−0.946	−0.958	−0.967
Repulsion (ev)	6.61	5.14	4.03	3.28	2.82	2.44	1.90	1.46	1.14	0.89
				Coefficients of terms in wave functions						
[00100]	0.979050	1.548772	2.239678	2.599628	2.659882	1.936894	2.234818	2.941302	3.575884	4.041758
[01100]	0.170157	−0.027247	−0.321723	−0.515224	−0.590717	0.633018	0.832691	0.426836	−0.143139	−0.714533
[02100]	0.006601	——	0.011082	0.023675	0.029833	0.423497	0.164173	0.067069	0.048085	0.072247
[10100]	0.472356	0.204526	−0.188502	−0.459722	−0.571635	0.827257	0.011657	−0.869994	−1.555611	−2.019773
[11100]	−0.013866	−0.048833	−0.010614	0.026871	0.046351	−0.247715	−0.247237	−0.081591	0.113698	0.287866
[20100]	−0.000468	——	0.014215	0.032764	0.040667	−0.139321	−0.030849	0.083321	0.168937	0.223823
[00120]	0.130312	0.683718	0.942823	1.089500	1.138531	0.972096	2.067164	2.828300	3.311904	3.555939
[01120]	0.138519	0.039157	−0.048175	−0.089747	−0.109526	1.786428	1.279151	0.847516	0.499280	0.232730
[10120]	0.145136	——	−0.062575	−0.108259	−0.128555	−0.072024	−0.420895	−0.657306	−0.805350	−0.882633
[00300]	0.183226	0.205257	0.213798	0.212291	0.206694	1.096518	1.256921	1.368414	1.426851	1.425551
[10300]						−0.047583	−0.160486	−0.253337	−0.320530	−0.358368
[00320]						0.661987	0.762547	0.834345	0.880178	0.909575
[00010]						−0.170930	−0.195044	−0.214049	−0.230343	−0.235046
[00101]	0.192528	0.248869	0.224885	0.197417	0.170286	0.318177	0.625430	0.809566	0.895080	0.924795
[10101]	0.020854	−0.017416	−0.023218	−0.025499	−0.024072	0.051059	−0.036792	−0.086760	−0.110019	−0.118585
[01101]						0.199616	0.032409	−0.085467	−0.161526	−0.209103

no correction for nuclear motion has been made, since there is in this case no possibility of a correspondingly accurate comparison with experimental evidence. The extrapolated energies may be expected to be correct to within 0.001 atomic unit; comparison with the corresponding computations on the $1s\sigma 2s\sigma\,^3\Sigma_g$ state indicates that for the intermediate values of R corresponding to either choice of δ_1 and δ_2 the allowance for convergence may well be too great. Upon converting to electron volts and referring to the energy of the separate normal atoms as zero, we obtain a potential curve which lies within the limits suggested in a previous paper,[5] somewhat nearer the lower than the upper limit.

The coefficients are given to sufficient places to ensure that the function is accurately normalized, but it is not to be imagined that the minimum problem has been solved with corresponding accuracy. We have found that, in general, properly related variations of several percent in the coefficients can be made without appreciably affecting the energy. Thus, a recalculation at $R=1.5$ in order to supply the coefficients of the three missing terms would not be worth while, since we already knew that those terms were useless at this distance. A rough interpolation from the table shows that they must all be small. On the other hand, at $R=1.87$ these coefficients have all increased (in absolute magnitude), and by including them we improve the energy from -0.87472 to -0.87781. The root-mean-square errors of the wave functions can be estimated by a method applied in reference 1, and further discussed in a separate paper.[6] The computations on He to be found in this latter paper indicates to us that in reference 1 the values estimated for ϵ_x (there called ΔE) are somewhat too low, the estimated root-mean-square errors in the functions somewhat too high. For the best functions in reference 1 we now believe a better estimate of the root-mean-square error would be 1–2 percent, an estimate which applies also to the functions of Table II.

THE STABLE STATE $1s\sigma 2s\sigma\,^3\Sigma_g$

For this state, Present's wave function was available for the equilibrium distance $R=1.87$.[2]

[5] A. S. Coolidge, H. M. James and R. D. Present, J. Chem. Phys. **4**, 193 (1936), (Fig. 2).

[6] H. M. James and A. S. Coolidge, Phys. Rev. **51**, 860 (1937).

TABLE III. *The* $1s\sigma 2s\sigma\,{}^3\Sigma_g$ *state.*

	$\delta_1=1/2,\ \delta_2=1$					$\delta_1=5/6,\ \delta_2=5/3$				
R IN aH	1.3	1.5	1.7	1.87	2.0	2.1	2.3	2.5	2.7	2.9
				Energy values (Binding energy includes correction for nuclear motion)						
Calc. (at. units)	−0.69730	−0.72350	−0.73427	−0.73609	−0.73449	−0.73115	−0.72702	−0.72001	−0.71164	−0.70275
Binding (ev)	1.957	2.667	2.958	3.007	2.964	2.874	2.762	2.572	2.345	2.105
Experiment	1.988	2.683	2.975	3.035	3.006	2.954	2.794	2.589	2.362	2.126
				Coefficients of terms in wave functions						
[00000]	7.334504	2.676890	0.000000	−1.161959	−0.834000	15.648688	9.068104	5.624794	3.077609	1.674374
[01000]	1.585267	0.905995	0.334730	——	−0.027924	3.367721	2.038518	1.798262	1.293116	0.981765
[10000]	−2.258956	−0.700890	0.143395	0.499368	0.376281	−8.589064	−5.007215	−3.035991	−1.642966	−0.871511
[11000]	−0.260871	−0.172787	−0.112603	−0.077834	−0.079971	−0.999031	−0.533742	−0.442045	−0.316694	−0.259331
[20000]	0.304102	0.129032	0.039516	——	0.007870	1.681193	1.015974	0.648982	0.399628	0.258872
[00200]						0.794005	0.312874	−0.029954	−0.258188	−0.424428
[10200]	0.053391	0.049071	0.042381	0.034815	0.028552	0.024387	0.124910	0.186825	0.219285	0.233503
[00020]						1.926092	0.922516	0.128024	−0.475760	−0.957345
[10020]	−0.033654	0.013360	0.049868	0.071975	0.082826	−1.984110	−1.185013	−0.518044	0.012731	0.455800
[20020]						0.500301	0.371342	0.258578	0.169435	0.091070
[11020]	−0.000037	−0.008961	−0.015106	−0.018709	−0.020754	0.233960	0.139793	0.059715	−0.005355	−0.060504
[10110]	−0.009887	−0.008209	−0.011727	−0.014422	−0.016033					
[11110]						−0.168156	−0.157347	−0.148075	−0.142058	−0.133054
[00001]	0.169002	0.090723	0.092908	0.091777	0.153050	0.898820	0.406936	0.223444	0.162129	0.196296
[10001]	−0.032174	−0.001510	−0.001499	−0.004742	−0.019470	−0.443052	−0.159783	−0.045550	0.008296	0.011954
[11001]	0.013321	0.001016	−0.001149	−0.000503	0.001138	0.247307	0.111747	0.047792	0.009993	−0.006960
[10021]	0.028654	0.020566	0.013686	0.009030	0.006414	0.020252	0.026095	0.031614	0.035153	0.038348

We have made new computations for all nuclear separations for which the repulsive state was treated, employing series of the same form, with the same values for the parameters δ_1 and δ_2, but differing in that the terms employed had $j+k$ even, in keeping with the *gerade* symmetry of this state. Since this state, in contrast to the repulsive one, gives an excited atom upon dissociation, it is to be expected that the best values of δ_1 and δ_2 will remain different as R increases; as we have mentioned, the values employed were chosen as appropriate for this state rather than the repulsive one, though no extensive investigation was made in selecting these values. Our experience has always been that moderate deviations from the best choice of parameters can be compensated by increasing the number of terms in the series, which, for the larger values of R, is 16 in the present investigation.

Since our main purpose was connected with the wave functions rather than with the computed energy we have not attempted to attain the maximum accuracy for all values of R, nor have we attempted any careful estimate of the convergence limits at the different distances. It was clear that the computations at $R=1.5$ and $R=2.5$ were of high accuracy, apparently being about 0.01 ev from the convergence limit, while for the extreme values of R associated with either choice of δ_1 and δ_2 the error was rather greater. In particular, extrapolations of the two sets of computations to intermediate values of R do not join smoothly, because of the increasing error in either curve in this region.

In Table III will be found, together with the wave functions for the various nuclear separations, values of the energy as computed, values for this energy corrected for nuclear motion, but not for imperfect convergence, and, finally, empirical values for the correct energy.

The estimate for the correction due to nuclear motion was made as follows. For the ground state, Van Vleck estimates that at the equilibrium distance the correction is 114 cm^{-1} or 0.014 ev, and this is also its value for infinite separation. For our state, the value at infinite separation is $\frac{5}{8}$ of this amount, 0.009 ev. Van Vleck estimates that in the two-quantum states $^1\Sigma$ and $^1\Pi$ at the equilibrium distances the inner electron is responsible for a correction of 0.007 ev. If we raise

this by 0.002 ev to allow for the effect of the outer electron we obtain, as in the ground state, the same correction as at complete separation. We have, therefore, taken this correction as 0.009 ev at all values of R.

The empirical results are taken from a paper[7] in which we have discussed methods of obtaining empirical potential curves of high accuracy, using as illustrative material computations on this state. The relation of our theoretical results to our best empirical determination is precisely what our experience with the theoretical computations has led us to expect. It will be noted, however, that these theoretical results are definitely incompatible with some of the empirical curves set up by less accurate and more usual methods, lying below rather than above the presumptive "observed" curve.

From the varying energy errors of the several functions it will be clear that there is also a considerable variation in the root-mean-square error of these functions. An estimate of 1 percent for this quantity for the best functions, 3 percent for the worst, should not be far from the mark.

[7] A. S. Coolidge, H. M. James, and E. L. Vernon, Phys. Rev. **54**, 726 (1938).

NOVEMBER, 1938 JOURNAL OF CHEMICAL PHYSICS VOLUME 6

The Negative Bands of $N^{14}-N^{15}$

R. W. Wood and G. H. Dieke
Johns Hopkins University, Baltimore, Maryland

(Received August 8, 1938)

The negative bands of nitrogen were photographed with a mixture which contained about 15 percent of N^{15}. The 0→0, 1→0 and 0→1 bands of the $N^{14}-N^{15}$ molecule were analyzed. Their position is within the limits of experimental errors where the elementary theory of the isotopic shifts predicts them. The bands do not show any intensity alternations and there are no perturbations at the places where the corresponding bands of ordinary nitrogen have them.

Introduction

THE availability of mixtures with a considerable percentage of the heavy nitrogen isotope N^{15} now makes possible a study of the molecules which contain one or more atoms of N^{15}. The most interesting of these molecules would be $N^{15}-N^{15}$ because with its help the spin of the N^{15} atom can be determined. With the determination of the spin as chief aim we have begun the investigation of some bands of the nitrogen molecule. This research was made possible through the courtesy of Professor H. C. Urey, who supplied us with a small amount of ammonium nitrate prepared in his laboratory which yielded nitrogen with a concentration of about 15 percent of the heavy isotope.

The present communication gives some of the preliminary results. Although we have photographed several $N^{15}-N^{15}$ bands, they are, with the available sample, relatively weak compared to the $N^{14}-N^{15}$ and the $N^{14}-N^{14}$ bands, so that reliable intensity measurements necessary for the determination of the spin would be difficult. The $N^{14}-N^{14}$ bands are naturally by far the strongest bands. Therefore we hope to repeat the experiments with more concentrated samples in order to obtain the spin. In this paper we report on some bands of $N^{14}-N^{15}$.

The nitrogen molecule has many band systems in the ultraviolet and visible. Most of these, e.g., the first and second positive groups, are of a rather complicated structure, and can be completely resolved only with difficulties. It is obvious that weak bands of $N^{14}-N^{15}$ or $N^{15}-N^{15}$ partly overlapped by the much stronger $N^{14}-N^{14}$ bands would represent rather unfavorable objects for analysis. However, the so-called negative bands due to the N_2^+ ion have a relatively simple structure and therefore we have chosen them for a first study. The present paper contains the three bands 0→0, 1→0 and 0→1 of the positive $N^{14}-N^{15}$ ion.

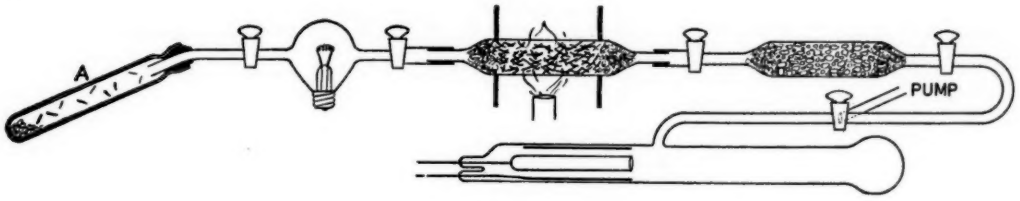

FIG. 1.

EXPERIMENTAL PROCEDURE

Owing to the limited amount of material available, it seemed best to construct a generator for the preparation and purification of the gas, with as small a capacity as possible.

The salt was decomposed by heating in contact with sodium hydroxide, the liberated ammonia broken down by the incandescent filament of a 6-volt automobile lamp, the hydrogen removed by hot copper oxide, and the water vapor and any residual ammonia absorbed by granulated barium perchlorate. The purified nitrogen was then admitted to the discharge tube, which was furnished with a hollow cathode and a coaxial anode of sheet nickel. It is well known that this type of tube emits the negative bands with great intensity and suppresses the otherwise very strong second positive bands. Fig. 1 shows the gas generator and discharge tube on a scale of about one-third natural size.

In charging the generator tube *A*, a short stick of caustic soda was first fused and boiled in the tube until the liberation of steam had almost subsided. It was then corked and rotated in a nearly horizontal position until cool, thus coating the inner wall with a thin layer of the anhydrous salt, which served as a drying agent for any water vapor liberated from the mixture of ammonium nitrate and sodium hydroxide, subsequently introduced. The cracks which form in the vitreous layer of sodium hydroxide should not be mistaken for cracks in the glass. The tube *A* was then cemented to the rest of the system with sealing wax, and the whole exhausted with an oil pump, after which the stopcocks were closed and the mixed salts heated with a small flame, the effervescence being watched carefully to avoid too high a pressure; the proper amount of heating was soon learned from experience. After the tube had cooled, the lamp filament was brought to a dull red heat and the first stopcock opened, the diminution of the light furnishing a rough measure of the pressure of the gas. The stopcock was then closed and the filament raised to incandescence for about five minutes.

The copper oxide, in a tube of fused quartz (the wax seals screened from radiation by asbestos disks) was then heated to a dull red by a Bunsen flame and the second stopcock opened and closed. After about ten minutes, the third cock was opened and closed, admitting some of the gas into the barium perchlorate desiccating tube. After half an hour the three-way stopcock was turned into such a position that the highly exhausted discharge tube was cut off from the pump and put in communication with the desiccating tube. The fourth stopcock was now turned very slowly until the pressure, indicated by the appearance of the discharge, amounted to a few millimeters. If no luminosity appeared in the interior of the hollow cathode, the pump was operated until the blue glow filled its interior at maximum brilliancy.

Ordinary nitrogen was prepared by substituting a tube containing a small amount of sodium azide for the tube *A*.

The discharge tube was excited by a small 5000-volt transformer in connection with a mercury rectifier, and the spectra photographed in the second order of a six-inch, 21-foot radius, concave grating ruled with 30,000 lines to the inch on aluminized Pyrex glass. The dispersion is about 0.6A per mm. Exposure times varied from one to four hours, according to the intensity of the bands, an absorbing filter for suppressing ultraviolet of higher order being used when necessary. After long operation with heavy nitrogen, it was found that the electrodes had absorbed a great deal of the gas. Repeated fillings with pure N_2 obtained from ordinary sodium azide and long operation of the tube with this

TABLE

K	P BRANCH ν	I	K	R BRANCH ν	I	K	P BRANCH ν	I	K	R BRANCH ν	I
	1→0 band						0→0 band				
0	—	—		27,900.87	0	0				25,568.34	1
1	27,893.20	1		05.10	1	1	25,560.61	1		72.67	2
2	89.71	1		09.81	2†	2	57.15	2		77.23	2
3	86.57	1		14.35	1c	3	54.04	2		82.14	3
4	83.54	2		19.29	0c	4				87.32	3
5	80.84	2b		24.32	1c	5	P_4 to P_{22}			92.79	3
5				24.57	2†	6	Confused with the			98.58	3
6	78.30	1c		29.93	6b	7	head of the $N^{14}-N^{14}$			25,604.64	3
6	78.47	1c				8	band			11.01	3
				35.53	3†	9				17.69	3
7	76.11	1		35.85	3	10				24.64	3b
7	76.29	1				11				31.86	3b
				41.46	4†	12				39.42	3b
8	74.11	1		41.86	3	13				47.18	2
8	74.32	1		P BRANCH		13				47.32	2
9	72.39	1	21	71.39	0	14				55.27	2
9	62.65	1	21	72.05	0	14				55.44	2
10	70.87	1c	22	73.03	0	15				63.64	2
10	71.30	1c	22	73.58	0	15				63.84	2
11	69.66	2*	23	74.87	0	16				72.38	2
11	70.11	2*	23	75.42	0	16				72.57	2
12	68.79	2*	24	76.87	0	17				81.34	2
12	69.14	2*	24	77.46	0	17				81.66	2
13	67.96	4d*	25	79.25	0	18				90.50	2
13	68.35	1*	25	79.75	0	18				90.83	2
14	67.96	4d*	26	81.77	0	19				25,700.17	2
14			26	82.33	0	19				00.50	2
15	67.45	2*	27	84.59	0	20				10.04	2
15	67.96	4d*	27	85.14	0	20				10.26	2
16	67.45	2*	28	87.66	0	21				20.15	2
16	67.96	4d*	28	88.30	0	21				20.42	2
17	67.96	4d*	29	91.01	0	22				30.60	2
17	68.35	1*	29	91.56	0	22				30.83	2
18	68.35	1*	30	94.52	0						
18	68.79	2*	30	95.17	0c						
19	69.14	2*	31	98.32	0						
19	69.66	2*	31	98.86	0						
20	70.11	2*	32	02.39	00						
20	70.69	0	32	03.04	[5]Ni						

gas did not remove from the spectrum traces of the bands of the heavy isotope.

ANALYSIS

On the second-order plates which we obtained, the principal $N^{14}-N^{15}$ bands are well developed and we have measured and analyzed the 0→0, 1→0 and 0→1 bands. Other bands are also present, but we want to postpone their analysis until we can obtain more favorable plates. The head of the 1→0 band of $N^{15}-N^{15}$ was also present, but the band was too weak for obtaining

TABLE I—*Continued*

K	P BRANCH ν	I	K	R BRANCH ν	I	K	P BRANCH ν	I	K	R BRANCH ν	I
	0→0 band						0→0 band				
23	53.33	1*d*		41.27	2	27	67.37	1		86.93	0
23	53.57	1		41.55	1	27	67.62	1		87.17	0
24	56.45	1		52.27	2	28	71.67	1		98.82	0
24	56.66	1		52.53	2	28	71.86	1		99.25	0
25	59.75	1		63.60	1	29	76.07	0		10.50	1?
25	60.02	1		63.82	1	29	76.33	0		11.56	0
26	63.41	1		75.13	1	30	80.68	0			
26	63.65	1		75.39	1	30	81.07	0			
	0→1 band						0→1 band				
0	—	—									
1				23,434.01	[6*b*]†	14	04.04	1*c**†		20.22	1
2	23,418.57	1*b*		38.58	1	14	04.24	1*c**		20.39	1
3	15.39	[5*b*]†		43.54	1*r*	15	unresolved part between 04.75 and 05.35			29.12	1
4	12.77	1		48.88	2					29.34	1
5	10.42	2		54.54	2	16	06.27	1		38.45	1
6	08.41	2		60.53	2	16	06.49	1		38.71	1
7	06.71	2		66.84	2	17	07.87	1		48.02	1
8	05.35	1*c*		73.49	2	17	08.10	1		48.23	1
9	04.24	1*c*		80.40	[5]†	18	09.90	[4*b*]†		57.95	1
10	03.64	1*c**†		87.81	2*b*	18				58.16	1
11	03.17	1*c**		95.37	1*c*	19	12.12	1		68.19	1
11	03.35	1*c**		95.50	1*c*	19	12.31	1		68.40	1
12	03.17	1*c**		23,503.33	1*c*	20	14.65	2*b*†		78.76	1
12	03.35	1*c**		03.46	1*c*	20	14.94	0		78.98	1
13	03.35	1*c**		11.62	1*c*	21	17.65	0		89.64	0
13	03.64	1*c**†		11.76	1*c*	21	17.88	0		89.86	0
						22		†			
						22		†			
						23	24.54	0			
						23	24.73	0			

* means that the line is a blend with another $N^{14}-N^{15}$ line; † means that the line is a blend with a $N^{14}-N^{14}$ line.

a satisfactory analysis. In addition, the strongest bands of the second positive nitrogen group are found on the plates with the corresponding $N^{14}-N^{15}$ and $N^{15}-N^{15}$ bands. On some plates a few nickel lines appear.

As could be expected, the position of the $N^{14}-N^{15}$ bands with respect to the corresponding bands of ordinary nitrogen is different for the three bands under investigation. The origins of the 0→0 bands lie less than 2 wave numbers apart, and the head of the $N^{14}-N^{15}$ band is just 0.14A inside the head of the $N^{14}-N^{14}$ band. As the lines of the *P* branch which form the head are so crowded together that their resolution is incomplete in the vicinity of the head, the lines P_4 to P_{22} of $N^{14}-N^{15}$ are lost among the much stronger $N^{14}-N^{14}$ lines. The other lines of this band appear near the corresponding lines of the ordinary band but well separated from them and there are practically no superpositions.

The head of the 1→0 band lies near 3587.4A. The part of the band between its head and 3582.3A, the head of the corresponding ordinary

band,* is quite free from superposition with any lines of ordinary nitrogen.

The lines R_2 to R_8, however, lie on the short wave-length side of this last head and are very much interfered with by the strong lines of the ordinary band. The lines beyond R_8 are covered by the dense band 3577 of the second positive group and no attempt was made to locate them.

The 0→1 band lies entirely within the ordinary 0→1 band. The position of the heads is at 4271.7A and 4278.1A, respectively. Owing to the high dispersion of the plates there is, however, relatively little disturbance of the $N^{14}-N^{15}$ band by the much stronger $N^{14}-N^{14}$ band.

Table I gives the frequencies and intensities of the three bands. The plates were measured in the usual way under the comparator against iron standards. As we were chiefly interested in a comparison with the corresponding bands for ordinary nitrogen, we applied a small correction to our wave-lengths so as to make those of ordinary nitrogen agree with the measurements of Coster and Brons. We are unable to say whether this means that there was a slight shift between the nitrogen lines and the iron comparison on our plates, or whether that shift was on the plates of Coster and Brons, who also admit the possibility of such a shift on their plates.

The negative bands of ordinary nitrogen have been the subject of considerable study. The most accurate data of the bands in question are probably those by Coster and Brons.[1] There are older measurements as well as the first analysis of the principal bands by Fassbender[2] and the measurements by Childs[3] of the bands 0→0 and 0→1 obtained from an arc discharge in nitrogen, which go up to very high values of the rotational quantum number.

The best procedure would be to obtain the rotational and vibrational constants from the $N^{14}-N^{15}$ bands and compare them with those for the $N^{14}-N^{14}$ molecule. However, the new bands are not known yet with the same completeness as those of ordinary nitrogen, and therefore the constants cannot be obtained with as high degree of reliability. Therefore we have taken the constants for $N^{14}-N^{14}$ and calculated from them those for $N^{14}-N^{15}$ and then tested whether they account with sufficient accuracy for the observed new bands. The outcome is that they do.

Table II.

		$N^{14}-N^{14}$		$N^{14}-N^{15}$	
		Initial	Final	Initial	Final
Y_{10}	ω_e	2419.84	2207.19	2379.28	2170.20
Y_{20}	$-x$	−23.189	−16.136	−22.418	−15.600
Y_{30}	y	− 0.5375	− 0.0400	− 0.5109	− 0.0380
Y_{40}	z	− 0.04949	—	− 0.04626	—
Y_{01}	B_e	2.085	1.930	2.016	1.866
Y_{02}	D_e	$4.3\cdot10^{-6}$	$2.9\cdot10^{-6}$	$4.02\cdot10^{-6}$	$2.71\cdot10^{-6}$
Y_{11}	α	0.0242	0.020	0.0230	0.019

In order to calculate the constants of $N^{14}-N^{15}$ from those of $N^{14}-N^{14}$ it is necessary to multiply each of the constants of the latter molecule by a certain power of the isotopic factor $\rho=\sqrt{(\mu_1/\mu_2)}$ in which μ_1 and μ_2 are the reduced masses of the two molecules. From the masses[4]

$$N^{14}=14.0076, \quad N^{15}=15.0050$$

for the two nitrogen atoms we find

$$\rho=0.983242.$$

In Table II the rotational and vibrational constants of the ordinary N_2^+ molecule are given, obtained from the data of Coster and Brons together with those of $N^{14}-N^{15}$ calculated from them. The constants are defined by the formula

$$E=\sum_{n,\,m} Y_{nm}(V+\tfrac{1}{2})^n K^m(K+1)^m$$

for the rotational and vibrational energy. The second column gives the more conventional symbols for these constants.

With the constants in Table II the rotational energies for final and initial state can be calculated and it is found that the frequencies of the individual lines of the bands can be represented with good accuracy by means of these calculated values. For low values of K the agreement is

* This 1→0 band of ordinary N_2 apparently has never been analyzed, undoubtedly due to the fact that a considerable part of it is hidden under the head (at 3577A) of the very strong 0→1 band of the second positive group. We measured and analyzed it and shall include the results in a future paper.

[1] D. Coster and H. H. Brons, Zeits. f. Physik **73**, 747 (1932).

[2] M. Fassbender, Zeits. f. Physik **30**, 73 (1924).

[3] W. H. J. Childs, Proc. Roy. Soc. **A137**, 641 (1932).

[4] K. T. Bainbridge and E. B. Jordan, Phys. Rev. **51**, 384 (1937).

within the limits of the errors of measurement. But for the higher K values there are small systematic deviations. They are of the same kind as those found in the $N^{14}-N^{14}$ bands and result from the imperfection of the formula used.

The origins of the three bands are found to be

1→0	27,896.90
0→0	25,564.33
0→1	23,425.46

The difference between the first two of these numbers is the first vibrational difference of the initial state and the difference of the last two numbers yields the same quantity for the final state.

The values are:

	Initial	Final
Obs.	2332.57	2138.87
Calc.	2332.56	2138.86

The values of the second row are those calculated with the constants of Table II. The agreement between calculated and observed values is perfect.

Finally we find as the origin of the whole band system

25,461.56 for $N^{14}-N^{15}$
25,461.48 for $N^{14}-N^{15}$

These two values agree also within the limits of experimental errors.

We have found so far that the relation between the negative bands of $N^{14}-N^{14}$ and of $N^{14}-N^{15}$ is exactly that postulated by the elementary theory of band spectra. The good agreement shows that there are no exceptional interactions which would behave in an anomalous way. Such anomalous behavior is often found e.g., in the H_2 bands.

There are, however, some points in which the bands of the light and the heavy molecule differ. In the first place, the characteristic intensity alternations found in the $N^{14}-N^{14}$ bands have disappeared, as they should, as $N^{14}-N^{15}$ is not a symmetric molecule. Furthermore, for both molecules the lines are all narrow doublets except those with the lowest K values which are not resolved. This doublet separation is due to the interaction of rotation and electron spin, but is influenced greatly by the interaction of the initial state with a neighboring Π state. If this interaction becomes considerable, perturbations are observed. As the character of the perturbation is chiefly determined by the close approach of rotational levels with the same J value, and as this occurs more or less accidentally, the state of affairs will be different for the two isotopic molecules, and perturbations will occur at different places.

This is borne out by the facts. There is a very pronounced perturbation for $V'=1$ in $N^{14}-N^{14}$ of which there is no trace in $N^{14}-N^{15}$. It is true that the lines which should show the maximum perturbation are those in the unresolved part of the head. But in such a perturbation a large number of lines are affected and it could not have escaped notice if it existed. We hope to come back to the interesting problem of doublet separation and perturbations, when we have accumulated more material.

We wish to express our great indebtedness to Professor H. C. Urey for the heavy ammonium nitrate without which this investigation could not have been accomplished. We wish to thank also Dr. N. Ginsburg for his help with taking the plates.

Nuclear Spin and Symmetry Effects in the Heat Capacity of Ethane Gas

E. BRIGHT WILSON, JR.
Mallinckrodt Chemical Laboratory, Harvard University, Cambridge, Massachusetts

(Received August 22, 1938)

The heat capacity of ethane gas has been calculated for a number of values of the internal potential barrier from zero to high barriers. Detailed account of the presence of noncombining species and of the exact nuclear spin statistical weights was taken. It was found that down to temperatures at least as low as 90°K these phenomena are entirely unimportant and that the partition function calculated in the usual way is correct. It is concluded that the observed experimental data are best explained by the assumption of a high restricting potential. Tables of statistical weights for the rotational levels of C_2H_6 and C_2D_6 are given.

THE heat capacity of ethane gas at low temperatures[1] (100°K) provides a particularly important piece of evidence pointing to a high barrier of about 3000 calories restricting internal rotation in this molecule. This interpretation has, however, been challenged by Hunsmann,[1c] who suggests that the observed result might be due to nuclear spin quantum effects such as occur in ortho- and parahydrogen. As previously pointed out in a preliminary report,[2] this suggestion is not acceptable since detailed calculations show that such spin effects are entirely negligible at the lowest temperatures at which measurements have been made. Although in a sense this conclusion is a negative one, it is an important link in the determination of the potential barrier, so that it seemed worth while to present the arguments which support it.

The method used is an extension of the group theory technique described earlier[3] for determining the statistical weights of the rotational levels of rigid molecules. The exact spin weight of each of the rotational states for each spin species is obtained and used to calculate the partition functions of the different noncombining species.

THE WAVE EQUATION

The assumption is usually made that the internal potential energy is of the form

$$V=\tfrac{1}{2}V_0(1-\cos 3\chi'),$$

χ' being the internal angle and V_0 the height of the potential barrier. The wave equation for ethane, treated as two connected rigid bodies, has been found[4] to be separable into two equations, one a function of the external Eulerian angles, the other a function of the angle between the methyl groups. The first equation is simply the wave equation for the ordinary rigid symmetrical rotator, whose solutions $\psi_e=\psi_{JKM}(\theta, \chi, \varphi)$ have been amply studied. The other equation can be written in the form

$$(d^2\psi_i)/(d\gamma^2)+(\beta+2\lambda\cos 6\gamma)\psi_i=0, \qquad (1)$$

where $\gamma=\frac{1}{2}\chi'$, $W_i=\frac{1}{2}V_0+(h^2/8\pi^2C)\beta$, and

$$\lambda=(8\pi^2C/h^2)V_0/4.$$

Here W_i is the internal energy, V_0 is the height of the potential barrier, h is Planck's constant, and C is the moment of inertia of ethane about the principal symmetry axis.

When either methyl group is turned through an angle of 2π radians, the wave function must return to the original value. This rotation adds π to the external Eulerian angle χ which is defined as one-half the sum of the Eulerian angles of the two methyl groups. It, therefore, multiplies the wave function by $e^{iK\pi}=(-1)^K$. The same rotation changes χ' by 2π and therefore γ by π. Consequently if K is even, $\psi_i(\gamma+\pi)$ must equal $\psi_i(\gamma)$, while with K odd $\psi_i(\gamma+\pi)$ must equal $-\psi_i(\gamma)$. Both of these are periodic in 2π, so the problem is to find all solutions ψ_i

[1] (a) Eucken and Weigert, Zeits. f. physik. Chemie **B24**, 277 (1934). (b) G. B. Kistiakowsky and F. Nazmi, J. Chem. Phys. **6**, 18 (1938). (c) W. Hunsmann, Zeits. f. physik. Chemie **B39**, 1 (1938). (d) G. B. Kistiakowsky, J. R. Lacher, and Fred Stitt, J. Chem. Phys. **6**, 407 (1938). See also E. Teller and K. Weigert, *Gött. Nach.* (1933), p. 218, for a calculation of the heat capacity.

[2] E. B. Wilson, Jr., J. Phys. Chem. **6**, 408 (1938).

[3] E. B. Wilson, Jr., J. Chem. Phys. **3**, 276 (1935).

[4] H. H. Nielsen, Phys. Rev. **40**, 445 (1932). See also J. B. Howard, J. Chem. Phys. **5**, 442, 451 (1937).

periodic in 2π. Half of these are to be used when K is even, the other half when K is odd.

Equation (1) is invariant under the 12 operations $\gamma\rightarrow\gamma$; $\gamma\rightarrow\gamma+\pi$; $\gamma\rightarrow\gamma\pm 2\pi/3$; $\gamma\rightarrow\gamma\pm\pi/3$; $\gamma\rightarrow-\gamma$, $-\gamma\pm 2\pi/3$; $\gamma\rightarrow-\gamma+\pi$, $-\gamma\pm\pi/3$; which fall into the six classes indicated by the above arrangement. These operations form a group which is isomorphous with the standard symmetry point group $\mathbf{D}_6$. The solutions of the differential equation (1) can therefore be classified according to their symmetry in terms of this group, as will be done below.

When $\lambda=0$, there is complete free rotation and the solutions are

$$\psi_i=\sin m\gamma \text{ and } \cos m\gamma, \tag{2}$$

with $\beta=m^2$, $m=0, 1, 2, 3, \cdots$. The normalizing constant has been omitted. These solutions may be classified according to their symmetries, since the solutions for any one energy must form a representation of the point group. It is quickly found that these symmetries are

$$\begin{array}{ll} m=0 & A_1 \\ m=6p & A_1+A_2 \\ m=6p\pm 1 & E_1 \\ m=6p\pm 2 & E_2 \\ m=6p+3 & B_1+B_2. \end{array} \tag{3}$$

Here p is a positive integer, while the symbols A_1, A_2, etc., represent the irreducible representations of the point group $\mathbf{D}_6$, whose characters[5] are given in Table I. The result shows that when λ increases from zero, the levels with m a multiple of 3 will split into two levels (except the lowest level), while the others will retain their twofold degeneracies. For very high values of λ, the lower levels approach those of a harmonic oscillator. By expanding $\cos 6\gamma$ in the expression for V and dropping higher terms it is found that as

$$\lambda\rightarrow\infty, \quad \beta\rightarrow(2k+1)6\sqrt{\lambda}-2\lambda, \tag{4}$$

with $k=0, 1, 2, \cdots$. Each of these levels is sixfold degenerate in the limit but the boundary conditions previously mentioned require that for each K value only three of the solutions can be used, one set of three being used when K is even, the other set when K is odd.

For intermediate values of λ, no simple form for β exists. The differential equation is a form of Mathieu's equation. Tables of values for β have been published[6] for the solutions with symmetries A_1, A_2, B_1, and B_2 but the degenerate levels have not been tabulated, although estimates of their positions have been made.[4, 7] Some of these levels have been calculated by an extension of the method described by Goldstein.[6] The principle is as follows. The unknown function ψ_i is expanded in a Fourier series with

TABLE I. *Character table for* $\mathbf{D}_6$.

	E	C_2	$2C_3$	$2C_6$	$3C_2'$	$3C_2''$
A_1	1	1	1	1	1	1
A_2	1	1	1	1	−1	−1
B_1	1	−1	1	−1	1	−1
B_2	1	−1	1	−1	−1	1
E_1	2	−2	−1	1	0	0
E_2	2	2	−1	−1	0	0

undetermined coefficients:

$$\psi_i=A_1\cos\gamma+A_5\cos 5\gamma+A_7\cos 7\gamma+A_{11}\cos 11\gamma+\text{etc.} \tag{5}$$

It is necessary to use only those cosines which have the desired symmetry, in this case E_1. This series is substituted into the differential equation and the coefficient of $\cos k\gamma$ in the reduced result equated to zero. This yields the following recursion formulas

$$\begin{aligned} (\beta-1)A_1+\lambda A_5+\lambda A_7&=0, \\ (\beta-25)A_5+\lambda A_1+\lambda A_{11}&=0, \\ (\beta-49)A_7+\lambda A_1+\lambda A_{13}&=0, \\ (\beta-m^2)A_m+\lambda A_{m-6}+\lambda A_{m+6}&=0, \\ m&=7, 11, 13, \text{ etc.} \end{aligned} \tag{6}$$

Let $v_m=A_{m+6}/A_m$, $u_0=A_5/A_1$. Then

$$\begin{aligned} \beta-1+\lambda u_0+\lambda v_1&=0, \\ (\beta-25)u_0+\lambda+\lambda v_5u_0&=0, \\ (\beta-m^2)v_{m-6}+\lambda+\lambda v_mv_{m-6}&=0, \quad m>5. \end{aligned} \tag{7}$$

To determine the value of the lowest root β of symmetry E_1 for a given value of λ, assume that $v_m=0$ for some sufficiently high value of m. Then from Eq. (7) calculate the lower ratios

[5] J. E. Rosenthal and G. M. Murphy, Rev. Mod. Phys. 8, 317 (1936).

[6] E. L. Ince, Proc. Roy. Soc. Edin. 52, 355 (1932). S. Goldstein, Trans. Camb. Phil. Soc. 23, 303 (1927).

[7] K. S. Pitzer, J. Chem. Phys. 5, 469 (1937).

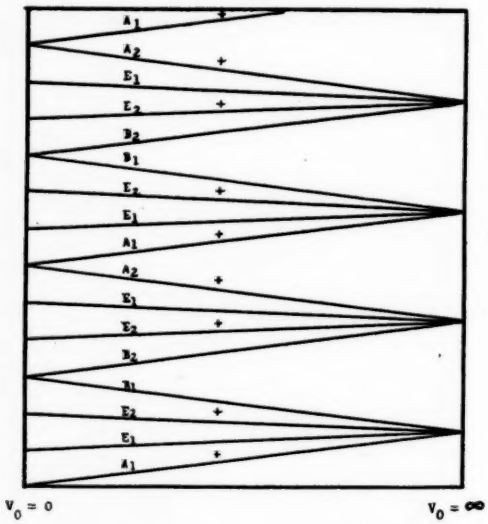

FIG. 1. Diagram showing the way in which the energy levels for free rotation connect with those for oscillation. + signs indicate levels which go with K even. Letters represent symmetry of level with respect to $\mathbf{D}_6$. This is not a plot of energy against potential.

v_{m-6}, etc., using an estimated value of β. It is necessary to come down both the $6p+1$ and the $6p-1$ series in this way until u_0 and v_1 have been calculated. Then a better approximation to β is calculated from the first equation of Eq. (7). This new value is used in repeating the process for a better approximation. To obtain higher levels, the same method is used except that the estimated value of β is substituted in all the equations except the one containing $\beta-k^2$, k^2 being the value of β for $\lambda=0$ for the level of interest. Solution of this equation for β gives the next approximation to the root. This method is quite rapid if the barrier is not too high. For high barriers the lower E_1 and E_2 levels are so narrowly limited by the other previously calculated levels above and below them, that they do not need to be computed.

Figure 1 shows the way in which the energy levels W_i for $V_0=0$ connect with those for V_0 large. It does not represent the variation of W_i with V_0. It is to be remembered that for a given rotational state only half these levels occur. Levels which go with even K values are marked +.

PERMUTATION GROUP AND STATISTICAL WEIGHTS

The permutations of the hydrogen atoms in ethane which are equivalent to rotations of the molecule (including internal rotation) form a group of 18 operations, hereafter called group **G**. This is not isomorphous with any of the standard symmetry point groups, so that it was necessary to determine its classes, irreducible representations, and their characters by the standard group theory methods.[8] The results are contained in Table II. In Table II, C_3' and C_3'' refer to rotations by $2\pi/3$ of one methyl group and the other, respectively; $C_3'^2$, $C_3''^2$ are similar

TABLE II. *Character table for pure rotation group for ethane (18 elements). Group* **G**, $\omega=exp\,(2\pi i/3)$.

	E	$C_3',C_3''^2$	$C_3'^2,C_3''$	C_3,C_3^2	$C_3'C_3$	$C_3''C_3$	$3C_2$	$3C_2C_3'$	$3C_2C_3''$
Γ_1	1	1	1	1	1	1	1	1	1
Γ_2	1	1	1	1	1	1	−1	−1	−1
Γ_3	1	ω	ω^2	1	ω	ω^2	1	ω	ω^2
Γ_4	1	ω^2	ω	1	ω^2	ω	1	ω^2	ω
Γ_5	1	ω	ω^2	1	ω	ω^2	−1	$-\omega$	$-\omega^2$
Γ_6	1	ω^2	ω	1	ω^2	ω	−1	$-\omega^2$	$-\omega$
Γ_7	2	$-\omega$	$-\omega^2$	−1	2ω	$2\omega^2$	0	0	0
Γ_8	2	$-\omega^2$	$-\omega$	−1	$2\omega^2$	2ω	0	0	0
Γ_9	2	−1	−1	−1	2	2	0	0	0
h	1	2	2	2	1	1	3	3	3

rotations by $4\pi/3$; C_3 and C_3^2 are rotations by $2\pi/3$ and $4\pi/3$ of both methyl groups simultaneously; C_2 is an end over end rotation by π. C_2C_3', for example, represents the product of C_2 and C_3', when written without a comma. Γ_i is the symbol for the ith irreducible representation and h is the number of operations in each class.

The next step is to find the number of nuclear spin wave functions in each irreducible representation. There are $2^6=64$ spin functions for C_2H_6. The methods previously described[3] quickly show that the symmetry of these spin functions is

$$10\Gamma_1+6\Gamma_2+3\Gamma_3+3\Gamma_4+\Gamma_5+\Gamma_6+8\Gamma_7+8\Gamma_8+4\Gamma_9.$$

Since Γ_7, Γ_8 and Γ_9 are each doubly degenerate, this accounts for all 64 functions. The same treatment of C_2D_6 gives

$$66\Gamma_1+55\Gamma_2+36\Gamma_3+36\Gamma_4+28\Gamma_5+28\Gamma_6+88\Gamma_7+88\Gamma_8+64\Gamma_9.$$

The effect of the symmetry operations of group **G** on ψ_i, the internal wave function, is best obtained by a consideration of the rotational subgroup $\mathbf{C}_6$ of the group $\mathbf{D}_6$. The characters for

[8] See, for example, E. Wigner, *Gruppentheorie.*

$\mathbf{C_6}$ are given in Table III. Comparing Table I and Table III, one sees that the representations of $\mathbf{D_6}$ are related to those of $\mathbf{C_6}$ as follows: $A_1, A_2 \rightarrow A$; $B_1, B_2 \rightarrow B$; $E_1 \rightarrow E_1$; $E_2 \rightarrow E_2$. Furthermore, the operations of the group **G** are related to those of $\mathbf{C_6}$ by their effect on γ as follows: $E \rightarrow E$, $C_3' \rightarrow C_6$, $C_3'^2 \rightarrow C_3$, $C_3 \rightarrow E$, $C_3'C_3 \rightarrow C_6$, $C_3''C_3 \rightarrow C_6^5$. These operations affect χ as follows: $E\chi \rightarrow \chi$, $C_3'\chi \rightarrow \chi + \pi/3$, $C_3'^2\chi \rightarrow \chi + 2\pi/3$, $C_3\chi \rightarrow \chi + 2\pi/3$, $C_3'C_3\chi \rightarrow \chi + \pi$, $C_3''C_3\chi \rightarrow \chi + \pi$. Since

TABLE III. *Character table for* $\mathbf{C_6}$.

	E	C_6	C_3	C_2	C_3^2	C_6^5
A	1	1	1	1	1	1
B	1	−1	1	−1	1	−1
E_1	1	ω	ω^2	1	ω	ω^2
	1	ω^2	ω	1	ω^2	ω
E_2	1	$-\omega^2$	ω	−1	ω^2	$-\omega$
	1	$-\omega$	ω^2	−1	ω	$-\omega^2$

$\psi_e = e^{iK\chi} f_{JK}(\theta, \varphi)$, this enables one to calculate the effect of the operations of **G** on ψ_e. Table IV contains the characters of the representations formed by $\psi_e\psi_i$ for various quantum numbers, as well as their symmetries calculated therefrom.

There now remains the problem of combining the spin and rotation functions in such a way that the whole function has the correct symmetry. For C_2H_6 this correct symmetry is Γ_2 of **G**, since this is the antisymmetric representation. For C_2D_6, it is Γ_1, the symmetric representation. Table V gives the necessary multiplication relations between the representations of **G**. The use of these, together with the symmetries of the rotational and spin functions previously obtained, yields the statistical weights of the rotational levels given in Table VI. The assumption has been made that the electronic and vibrational wave functions are completely symmetrical. This is not always true for excited vibrational states, but they do not contribute appreciably to the thermodynamic properties at low temperatures; also, since it will be found that spin effects are negligible, the general conclusions will hold even with vibrational excitation. Table VI, however, will be different for states with ψ_v not completely symmetrical.

TABLE V. *Multiplication table for group* **G**.

$\Gamma_1\times\Gamma_2=\Gamma_3\times\Gamma_6=\Gamma_4\times\Gamma_5=\Gamma_2$;
$\Gamma_1\times\Gamma_1=\Gamma_2\times\Gamma_2=\Gamma_3\times\Gamma_4=\Gamma_5\times\Gamma_6=\Gamma_1$;
$\Gamma_7\times\Gamma_8=\Gamma_1+\Gamma_2+\Gamma_9$; $\Gamma_9\times\Gamma_9=\Gamma_1+\Gamma_2+\Gamma_9$

NONCOMBINING SPECIES

The group **G** has 9 irreducible representations but Γ_3 and Γ_4, Γ_5 and Γ_6, and Γ_7 and Γ_8 are complex conjugate pairs. Consequently, states with spin symmetry Γ_3 have the same rotational weights as those with spin symmetry Γ_4, etc. Therefore there can be only 6 species of ethane whose proportions could be altered in the same way as is done with ortho- and parahydrogen. Later it will be shown that these species divide into two sets such that only at very low temperatures could there be any possible segregation of members of the same set. Finally it will be shown that there is no change in the proportions of even the two sets of species at temperatures as high as 90°K.

PARTITION FUNCTIONS

The partition functions for each of the six noncombining species of C_2H_6 are given below.

TABLE IV. *Characters for the representations formed by* $\psi_e\psi_i$ *and their symmetries.* p *= integer.*

K	J	ψ_i	E	$C_3', C_3''^2$	$C_3'^2, C_3''$	C_3, C_3^2	$C_3'C_3$	$C_3''C_3$	$3C_2$	$3C_2C_3'$	$3C_2C_3''$	SYM.
0	even	A	1	1	1	1	1	1	1	1	1	Γ_1
0	odd	A	1	1	1	1	1	1	−1	−1	−1	Γ_2
0	even	E_1	2	−1	−1	2	−1	−1	2	−1	−1	$\Gamma_3+\Gamma_4$
0	odd	E_1	2	−1	−1	2	−1	−1	−2	1	1	$\Gamma_5+\Gamma_6$
$6p$		A	2	2	2	2	2	2	0	0	0	$\Gamma_1+\Gamma_2$
$6p$		E_1	4	−2	−2	4	−2	−2	0	0	0	$\Gamma_3+\Gamma_4+\Gamma_5+\Gamma_6$
$6p\pm1$		B	2	−1	−1	−1	2	2	0	0	0	Γ_9
$6p\pm1$		E_2	4	1	1	−2	−2	−2	0	0	0	$\Gamma_7+\Gamma_8$
$6p\pm2$		A	2	−1	−1	−1	2	2	0	0	0	Γ_9
$6p\pm2$		E_1	4	1	1	−2	−2	−2	0	0	0	$\Gamma_7+\Gamma_8$
$6p+3$		B	2	2	2	2	2	2	0	0	0	$\Gamma_1+\Gamma_2$
$6p+3$		E_2	4	−2	−2	4	−2	−2	0	0	0	$\Gamma_3+\Gamma_4+\Gamma_5+\Gamma_6$

TABLE VI. *Statistical weights and symmetries of rotational levels (not including factor 2J+1 in weights) for symmetrical vibrational states.*

			C_2H_2		C_2D_6	
K	J	ψ_i	ψ_s	Wt.	ψ_s	Wt.
0	even	A	Γ_2	6	Γ_1	66
0	odd	A	Γ_1	10	Γ_2	55
0	even	E_1	$\Gamma_5+\Gamma_6$	2	$\Gamma_3+\Gamma_4$	72
0	odd	E_1	$\Gamma_3+\Gamma_4$	6	$\Gamma_5+\Gamma_6$	56
$6p$		A	$\Gamma_1+\Gamma_2$	16	$\Gamma_1+\Gamma_2$	121
$6p+3$		B	$\Gamma_1+\Gamma_2$	16	$\Gamma_1+\Gamma_2$	121
$6p$		E_1	$\Gamma_3+\Gamma_4+\Gamma_5+\Gamma_6$	8	$\Gamma_3+\Gamma_4+\Gamma_5+\Gamma_6$	128
$6p+3$		E_2	$\Gamma_3+\Gamma_4+\Gamma_5+\Gamma_6$	8	$\Gamma_3+\Gamma_4+\Gamma_5+\Gamma_6$	128
$6p\pm1$		B	Γ_9	4	Γ_9	64
$6p\pm2$		A	Γ_9	4	Γ_9	64
$6p\pm1$		E_2	$\Gamma_7+\Gamma_8$	16	$\Gamma_7+\Gamma_8$	176
$6p\pm2$		E_1	$\Gamma_7+\Gamma_8$	16	$\Gamma_7+\Gamma_8$	176

The nuclear spin symmetries are enclosed in parentheses.

$$Q_a=10R_A(P_1+S_0)+10R_BS_3,\ (\Gamma_1)$$

$$Q_b=6R_A(P_2+S_0)+6R_BS_3,\ (\Gamma_2)$$

$$Q_c=6R_{E_1}(P_1+S_0)+6R_{E_2}S_3,\ (\Gamma_3+\Gamma_4)$$

$$Q_d=2R_{E_1}(P_2+S_0)+2R_{E_2}S_3,\ (\Gamma_5+\Gamma_6)$$

$$Q_e=16R_{E_1}(S_2+S_4)+16R_{E_2}(S_1+S_5),\ (\Gamma_7+\Gamma_8)$$

$$Q_f=4R_A(S_2+S_4)+4R_B(S_1+S_5),\ (\Gamma_9)$$

in which the symbols have the following meaning.

$R_x=\Sigma e^{-W_i/kT}$, summed over all the internal energy levels of symmetry $x=A$, B, E_1 or E_2. E_1 and E_2 levels are to be counted once each in these sums.

$$P_1=\sum_J(2J+1)\exp\left[-J(J+1)h^2/8\pi^2AkT\right],$$

summed over all odd values of J from 1 to ∞. A is the moment of inertia about an axis perpendicular to the C−C axis. P_2 is the similar sum over the even values of J from zero to ∞.

$$S_n=\sum_{J,\,K}(2J+1)\exp\left[-(h^2/8\pi^2AkT)\times\{J(J+1)+K^2[(A/C)-1]\}\right],$$

where J runs from zero to ∞, and $K=6p+n$ with $p=0, 1, 2, \cdots$, etc., but $K\leq J$ and $K>0$.

The sums P_1, P_2 and S_n have been evaluated with the aid of their Euler-MacLaurin expansions,[9] the first terms of which are given below.

$$P_1=\frac{1}{2\sigma}\left\{1+\frac{1}{3}\sigma+\frac{1}{15}\sigma^2+\frac{4}{315}\sigma^3+\cdots\right\},$$

$P_2=P_1$ to terms in σ^3,

$$S_n=\frac{1}{12\sigma}(\pi/\nu)^{\frac{1}{2}}\left\{1+\frac{1}{3}\sigma-\frac{1}{12}(\sigma^2/\nu)+\cdots\right\}-(\alpha/\sigma),$$

with $\alpha=\frac{1}{2}$ for $n=0$, $\frac{1}{3}$ for $n=1$, $\frac{1}{6}$ for $n=2$, 0 for $n=3$, $-\frac{1}{6}$ for $n=4$, $-\frac{1}{3}$ for $n=5$. Here

$$\sigma=(h^2/8\pi^2AkT),\quad \nu=(h^2/8\pi^2CkT).$$

At 90°K or higher, it is sufficient to take the first term of P_1 and P_2. To this order of accuracy, P_1+S_0, P_2+S_0, S_2+S_4, S_1+S_5, and S_3 are all equal so that Q_a, Q_b, Q_f are proportional to each other as are Q_c, Q_d and Q_e. There can be no shift in relative proportions, therefore, inside these groups, but there might be a change in the relative proportions of the two groups, depending on whether or not R_A+R_B is always proportional to $R_{E_1}+R_{E_2}$.

The evaluation of R_A+R_B and $R_{E_1}+R_{E_2}$ was carried out for barriers of height zero, 300 and about 3000 cals. For zero barrier, the functions are theta-functions[10] so that

$$R_A+R_B=\tfrac{1}{3}(\pi/\nu)^{\frac{1}{2}}\{1+2\exp(-\pi^2/9\nu)+\cdots\},$$

$$R_{E_1}+R_{E_2}=\tfrac{1}{3}(\pi/\nu)^{\frac{1}{2}}\{1-2\exp(-\pi^2/9\nu)-\cdots\}.$$

Since $\nu\leqq0.043$ at 100°K, these functions differ by less than 1 in 10^9.

For a barrier of 300 cal., R_A+R_B and $R_E+R_{E_2}$ were obtained by actual summation over the energy levels and were found to be the same, at least to 1 part in a thousand, even at 50°K. For this barrier the heat capacity was calculated for several temperatures above 90°K and no difference was found between the two species.

For high barriers the two types of energy levels (A, B and E_1, E_2) coincide so closely that it is not necessary to carry out the numerical calculations to see that there can be no difference in the partition functions and heat capacities of the two species above 90°K.

Where comparisons were made, it was found that the values for the thermodynamic quantities which were obtained agreed with those tabulated by Pitzer.[7]

[9] L. S. Kassel, Chem. Rev. **18**, 277 (1936). Whittaker and Watson, *Modern Analysis*, Sec. 7.21.

[10] Whittaker and Watson, *Modern Analysis*, Sec. 21.51.

Discussion

These calculations show that no appreciable change in the equilibrium proportions of the several species of ethane can take place unless the temperature is reduced considerably below 50°K. It is therefore impossible to account for the low value of the observed heat capacity of C_2H_6 at 94°K by postulating such spin effects. Since C_2D_6 is heavier, spin effects will not occur in this molecule until still lower temperatures are considered. The only other explanation which has been proposed for the low temperature heat capacity is the existence of a barrier of about 3000 cal., an explanation which is compatible with all the known experimental data on ethane, including the heat capacity, Raman and infra-red vibrational spectra, infra-red rotational spectrum, entropy from the third law and from equilibrium measurements, etc. Some of these data are also compatible with the low value of the barrier, but not all of them, so that the evidence at present seems quite strong for the high barrier.

It should be emphasized, however, that this "barrier height" is a rather arbitrary quantity, being the value of the parameter V_0 in the function $V=\frac{1}{2}V_0(1-\cos 3\chi')$ chosen so as to give the best fit with certain observed thermodynamic properties. If a different shape for the potential barrier is assumed, the "height" may need to be changed considerably in order to obtain agreement with experiment. For example, rough calculations with a square shape of barrier in which the width of the "valleys" is equal to the width of the "hills" shows that in order to fit the heat capacity at 100° a very high "barrier" is needed—over ten thousand calories. Such a calculation means very little, however, because at 100°K, even the second level above the ground level contributes but slightly to the heat capacity (assuming roughly equal spacing), so that this experimental value can give very little information about the nature of the barrier except that it must yield no level nearer than about 280 wave numbers or 800 cal. from the ground state. Heat capacity data at higher temperatures would yield information about higher levels but there is the difficulty that the importance of these higher levels is possibly of the same order of magnitude as that of the unknown, low lying fundamental frequency of vibration. Until this frequency is definitely located from spectroscopic arguments it is not safe to draw too refined conclusions from the heat capacity data at higher temperatures.

Nevertheless, whatever the shape, it seems evident that the barrier must be fairly high in order that the lowest excited state may be as high as 280 cm.*

* *Note added in proof:* Since the above was submitted, a paper by K. Schäfer, Zeits. f. physik. Chemie **40**, 357 (1938), has been received, belonging to the same series as that of Hunsmann, ref. 1. In it methods similar to those used above lead to the same conclusion, and as a consequence, Schäfer accepts the high value of the barrier.

The Relative Adsorbabilities of Hydrogen and Deuterium

A. WHEELER*
Frick Chemical Laboratory, Princeton University, Princeton, New Jersey
(Received July 19, 1938)

The unexpected results of Beebe, Klar and others on the relative adsorbabilities of H_2 and D_2 on metal surfaces are explained by a statistical-mechanical treatment. By constructing simple partition functions for the adsorbed molecules and atoms, equal adsorption at low temperatures and an inversion temperature at higher temperatures are predicted. Both predictions are fulfilled by the experimental results.

THE experiments of Beebe *et al.*[1] and Klar[2] on the relative adsorbabilities of hydrogen and deuterium have brought forward the interesting fact that there exists an inversion temperature below which hydrogen is more strongly absorbed and above which deuterium is more strongly absorbed. The catalysts employed were copper (Beebe) and nickel (Klar). Considerably below the inversion temperature in the region −80°C, Beebe finds both isotopes equally absorbed. (Here more "strongly absorbed," "equally absorbed," etc., apply to the equilibrium amount taken up by the metal surface.) In the following it will be shown that these experimental results are in strict conformity with the theoretical predictions of statistical mechanics. Using a form of the Langmuir isotherm due to Fowler,[3] simple partition functions will be constructed for the adsorbed molecules, and from this the relative adsorbability of the two hydrogen isotopes will be deduced.

In terms of statistical mechanics, the Langmuir isotherm is:

$$p=\frac{\theta}{1-\theta}(kT)\frac{F_g}{F_a}\exp -\frac{E_0}{kT}, \tag{1}$$

where p is the equilibrium pressure in the gas phase, θ is the fraction of the surface covered, F_g is the partition function for a gas molecule, and F_a is the partition function for an adsorbed molecule. T is the absolute temperature and k the Boltzmann constant. E_0 is the difference in energy at the absolute zero between a gas molecule in its lowest state and an adsorbed molecule in its lowest state. If adsorption results in the dissociation of the adsorbed molecule into two atoms, the isotherm is:

$$p=\left(\frac{\theta}{1-\theta}\right)^2(kT)\frac{F_g}{F_a^2}\exp -\frac{E_0}{kT}. \tag{2}$$

For molecular adsorption we then have for the ratio of pressures of D_2 and H_2 in the gas phase necessary to produce an amount of adsorption θ:

$$\frac{p}{p'}=\frac{F_g}{F_g'}\frac{F_a'}{F_a}\exp -\left(\frac{E_g-E_a}{kT}\right), \tag{3}$$

where a primed quantity refers to H_2 and an unprimed quantity to D_2. E_g is the difference in zero-point energy between gaseous D_2 and H_2 and E_a is the same quantity for adsorbed H_2 and D_2. For atomic adsorption we have:

$$\frac{p}{p'}=\frac{F_g}{F_g'}\frac{F_a'^2}{F_a^2}\exp -\frac{E_g-2E_a}{kT}. \tag{4}$$

The quantities F_g and F_g' are well known, and since the vibrational partition functions in each are contributing a factor very nearly unity, we may write for the ratio:

$$\frac{F_g}{F_g'}=\left(\frac{m(D_2)}{m(H_2)}\right)^{3/2}\frac{I(D_2)}{I(H_2)}=(2)^{5/2}. \tag{5}$$

Here the I's are moments of inertia, and the m's are masses of H_2 and D_2. Eq. (5) will be an excellent approximation at ordinary temperatures (0–500°C) and at lower temperatures where the rotations cannot be treated classically, the deviations will tend to cancel each other.

* Now member of the Research Staff, Shell Development Co., Emeryville, California.
[1] Beebe, Low, Wildner, and Goldwasser, J. Am. Chem. Soc. **57**, 12 (1935).
[2] Klar, Naturwiss. **22**, 822 (1934).
[3] R. H. Fowler, Proc. Camb. Phil. Soc. **31**, 260 (1935).

For temperatures at which a loose molecular adsorption predominates, we may evaluate F_a and F_a' as follows. It is logical to assume that the molecule is held to the metallic surface by five loose vibrations, these having replaced the three translational and two rotational degrees of freedom in the gas phase. The sixth degree of freedom, namely the internal vibration of the two hydrogen atoms, will remain virtually unperturbed. (The fact that liquefaction scarcely changes the fundamental frequencies of a molecule insures the truth of the last sentence.) The five loose vibrations may be treated classically so that:

$$\frac{F_a'}{F_a}=\frac{\Pi^5_{i=1}\,kT/h\nu_i'}{\Pi^5_{i=1}\,kT/h\nu_i}=\frac{\Pi^5_{i=1}\,\nu_i}{\Pi^5_{i=1}\,\nu_i'}. \tag{6}$$

The ν_i and ν_i' are the five loose vibrational frequencies for the adsorbed deuterium and hydrogen molecules, respectively. The Π's are symbols for continued products. Since identical forces are involved in the vibrations of the two isotopic molecules, we have

$$\nu_i=\frac{1}{2\pi}\left[\frac{f_i}{m(D_2)}\right]^{\frac{1}{2}} \quad \text{and} \quad \nu_i'=\frac{1}{2\pi}\left[\frac{f_i}{m(H_2)}\right]^{\frac{1}{2}}, \tag{7}$$

where f_i is the force constant for ith normal mode of vibration. Substituting in Eq. (5) we have:

$$\frac{F_a'}{F_a}=\frac{\Pi^5_{i=1}\dfrac{1}{2\pi}\left[\dfrac{f_i}{m(D_2)}\right]^{\frac{1}{2}}}{\Pi^5_{i=1}\dfrac{1}{2\pi}\left[\dfrac{f_i}{m(H_2)}\right]^{\frac{1}{2}}}=(\tfrac{1}{2})^{5/2}. \tag{8}$$

Further, since the internal mode of vibration of the hydrogen molecule is practically unchanged, E_g-E_a (of Eq. (3)) is to a first approximation zero. Substituting this result, along with (5) and (8), in Eq. (3) we obtain:

$$p/p'=1 \tag{9}$$

or namely that hydrogen and deuterium are equally absorbed at temperatures for which molecular adsorption predominates. This result is confirmed experimentally by Beebe and his co-workers.

At higher temperatures where atomic adsorption is important, we must use Eq. (4). For the case in which each atom is held to the absorbing surface by three loose vibrations which may be treated classically, we find:

$$\frac{F_a'^2}{F_a^2}=\frac{\Pi^3_{i=1}\left(\dfrac{1}{2\pi}\right)^2\dfrac{f_i}{m_D}}{\Pi^3_{i=1}\left(\dfrac{1}{2\pi}\right)^2\dfrac{f_i}{m_H}}=(\tfrac{1}{2})^3. \tag{10}$$

Substituting (10) and (5) in (4), there results

$$\frac{p}{p'}=(\tfrac{1}{2})^{\frac{1}{2}}\exp-\left[\frac{E_g-2E_a}{kT}\right]. \tag{11}$$

This result predicts that at low temperatures H_2 will be more strongly absorbed, but that at a temperature:

$$T=\frac{2E_a-E_g}{k}\,\frac{2}{\log 2} \tag{12}$$

an inversion will occur, with D_2 being more strongly absorbed.

For the general case where the three vibrations cannot be treated classically we still have the result that the inversion will take place at a temperature

$$T=\frac{2(E_a'-E_a)-1800}{\left[\dfrac{5}{2}\log 2+2\log\dfrac{F_a'}{F_a}\right]R}, \tag{13}$$

where E_a' and E_a are, respectively, the zero-point energies in calories of an absorbed H or D atom, and 1800 is $-E_g$ (the difference in zero-point energy between gaseous D_2 and H_2). Eq. (13) shows the inversion should take place at ordinary temperatures providing the three vibration frequencies for the absorbed H atom are around 1000 cm^{-1}, and $(\frac{1}{2})^{\frac{1}{2}}$ times this for D. The approximations (uniform surface etc.) involved in the derivation of Eq. (4) make any quantitative predictions of Eq. (13) of doubtful value, but the prediction of an experimentally observed inversion temperature show that the approach is essentially correct. Eq. (13) also shows that not every absorbing surface will exhibit an inversion

temperature, as certain sets of vibrational frequencies will make T negative or experimentally out of reach.

The parallelism between the absorbability of the hydrogen isotopes and the rate with which they hydrogenate ethylene has been pointed out by Beebe and Klar.[1, 2] On nickel the ratio α of the rate of the light hydrogen reaction to the heavy hydrogen reaction actually "turns over" in the region of the inversion temperature, while on copper[4] between 0°C and 300°C α falls from 2.07 to approximately unity.

[4] Wheeler and Pease, J. Am. Chem. Soc. **58**, 1665 (1936); **57**, 1144 (1935).

LETTERS TO THE EDITOR

This section will accept reports of new work, provided these are terse and contain few figures, and especially few halftone cuts. The Editorial Board will not hold itself responsible for opinions expressed by the correspondents. Contributions to this section should not exceed 600 words in length and must reach the office of the Managing Editor not later than the 15th of the month preceding that of the issue in which the letter is to appear. No proof will be sent to the authors. The usual publication charge ($3.00 per page) will not be made and no reprints will be furnished free.

Raman Spectrum of Thiophosgene

In an analysis of the ultraviolet absorption spectrum of thiophosgene it became desirable to know the vibration frequencies of the molecule. Each of the six normal vibrations should be excited in the Raman spectrum, which was accordingly measured, using the liquid substance. The exciting frequency was the 5876A line of a specially constructed helium discharge lamp, though a few lines scattered from the 6678A helium line gave corroborative data. The spectrograph was a large aperture glass prism instrument giving a dispersion of about 100A/mm in the region involved. The Hα and neon lines were used as standards. The following frequencies, (cm^{-1}) with rough relative intensities, were found: 200 (1), 287 (3), 363 (1), 496 (5), 660 (0), 1121 (10), 1388 (2). Using the same nomenclature as has been given for the case of phosgene,* the three relatively intense symmetric vibrations are assigned as follows: $\nu_1=1121$, $\nu_2=496$, $\nu_3=287$. The two antisymmetric planar vibrations will probably be $\nu_4=660$, $\nu_5=363$, and the nonplanar oscillation $\nu_6=200$. It seems probable that the Raman interval 1388 is to be interpreted as due to the excitation of the combination $(\nu_1+\nu_3)$. A preliminary survey of the infra-red spectrum of thiophosgene vapor confirms the above values both as regards magnitude and assignment. The analysis of the ultraviolet absorption band system reveals that the most prominently excited vibrations are the symmetrical ones. The details of the ultraviolet and infra-red data will shortly be published, as well as a comparison with the corresponding data for formaldehyde and phosgene, and a discussion of the force constants in these molecules.

H. W. THOMPSON

Old Chemistry Department,
Oxford, England,
September 28, 1938.

* Bailey and Hale, Phil. Mag. **25**, 98 (1938).

Statistical Mechanics of Mobile Monolayers

Following a suggestion to the writer by Professor R. H. Fowler, the methods of Mayer and Ackermann[1, 2] giving the saturated vapor pressure curves for condensing systems have been adapted to the problem of mobile monolayers. The problem is simplified as an example in the theory of dissociating (clustering) assemblies,[3] and the equation giving the saturated vapor tension F_c and the critical area A_c for a monolayer of X molecules is easily found to be of the form

$$F_cA_c/XkT=(1+\nu)/(1+\sigma),$$

where ν and σ are sums which can be evaluated in terms of the molecular fields. For the latter, point functions of the radius alone are useless, but it is found sufficient to specify only the number of bonds with nearest neighbors and the mean energy per bond. Good agreement is obtained with the data of Adam and Jessop on the fatty acids[4] by assuming six bonds with mean energy 3.8×10^{-14} erg per bond, for the vapor-duplex change at large molecular areas. And in myristic acid for the duplex-liquid change at small molecular areas good agreement is found with the modified duplex equation

$$(F_c-F_0)(A_c-A_0)/XkT=(1+\nu)/(1+\sigma)$$

with six bonds of mean energy 5.6×10^{-14} erg per bond, provided the spreading effect of the liquid surface is

$$F_0=-11.2 \text{ dynes/cm}$$

and the area occupied by the clustered molecules is

$$A_0=(14+0.2t)X,$$

where t is the temperature in degrees Centigrade. This last agreement is supporting evidence for Langmuir's duplex theory of the expanded film.[6]

WILLIAM BAND

Department of Physics,
Yenching University,
Peiping, China,
August 8, 1938.

[1] Joseph E. Mayer, J. Chem. Phys. **5**, 67 (1937).
[2] Mayer and Ackermann, J. Chem. Phys. **5**, 74 (1937).
[3] W. Band, J. Chem. Phys. **6**, 654 (1938).
[4] Adam and Jessop, Proc. Roy. Soc. **A110**, 423 (1926).
[5] Adam and Jessop, Proc. Roy. Soc. **A112**, 362 (1926).
[6] Langmuir, J. Chem. Phys. **1**, 769 (1933).